UNIVERSITY OF BIRMINGHAM

Science and Technology Facilities Council
Rutherford Appleton Laboratory

The MIGDAL experiment:

Measuring a rare atomic process to aid the search for dark matter

Lex Millins
University of Birmingham & STFC Rutherford Appleton Laboratory

QMUL, Particle Physics Seminar
18th March 2026

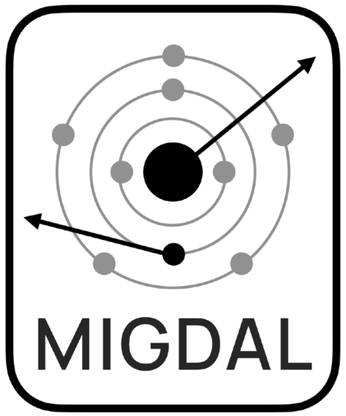

lkm892@student.bham.ac.uk

Evidence for Dark Matter

- Wealth of astrophysical evidence for existence of DM
- Inferred through it's gravitational effects
- Makes up 27% of the mass-energy content of the universe

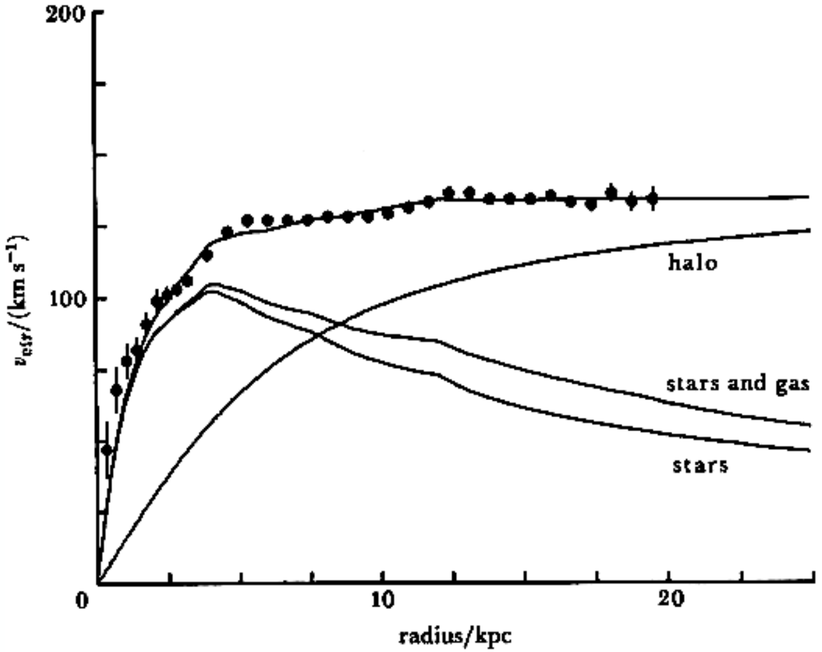

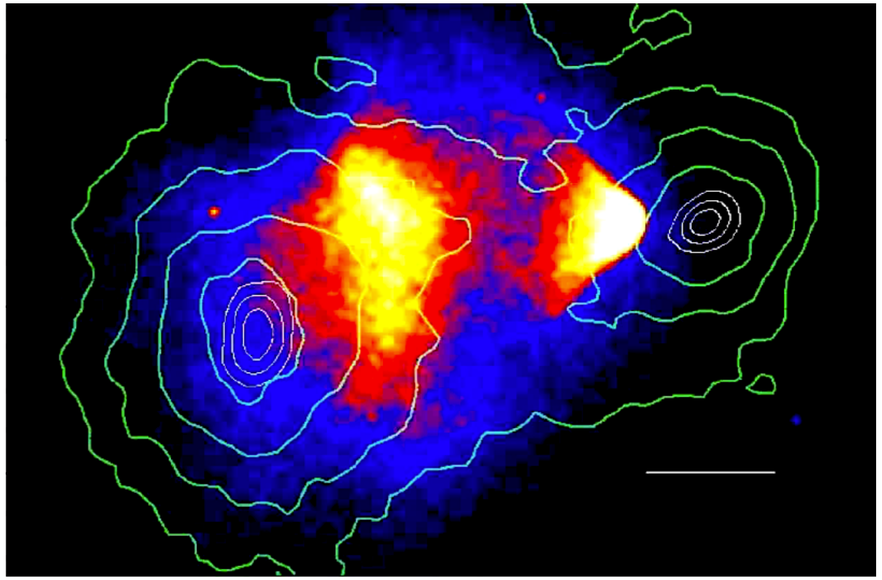

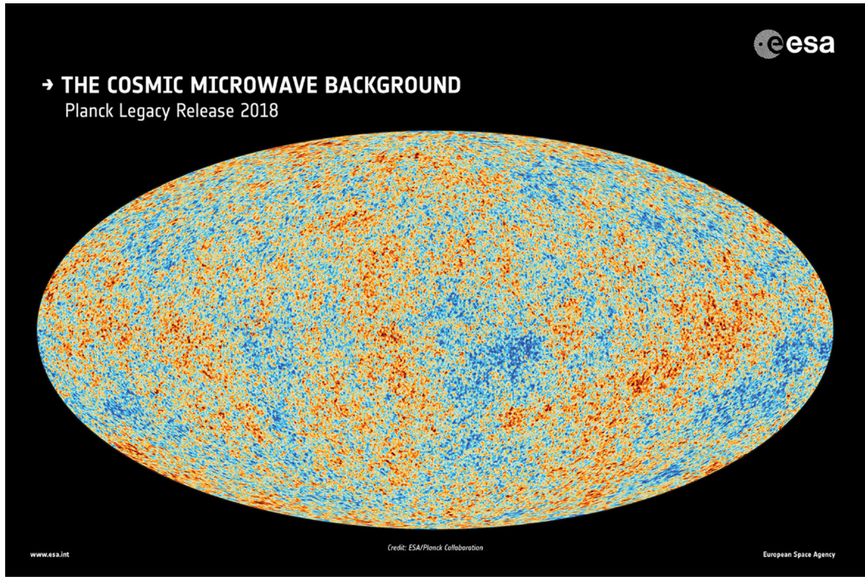

Phil. Trans. Roy. Soc. Lond. A 320.1156 (1986)

Astrophys. J. Lett. 648 (2006)

Astron.Astrophys. 641 (2020) A6

Expected Properties of DM

- 85% of the total mass of the universe
- A typical candidate may be
  - No (or very small) electric charge
  - Non-baryonic
  - Non-relativistic at freeze-out
  - Stable on scale of age of universe
  - No/little interaction with ordinary matter
- No standard model particle fits the bill!

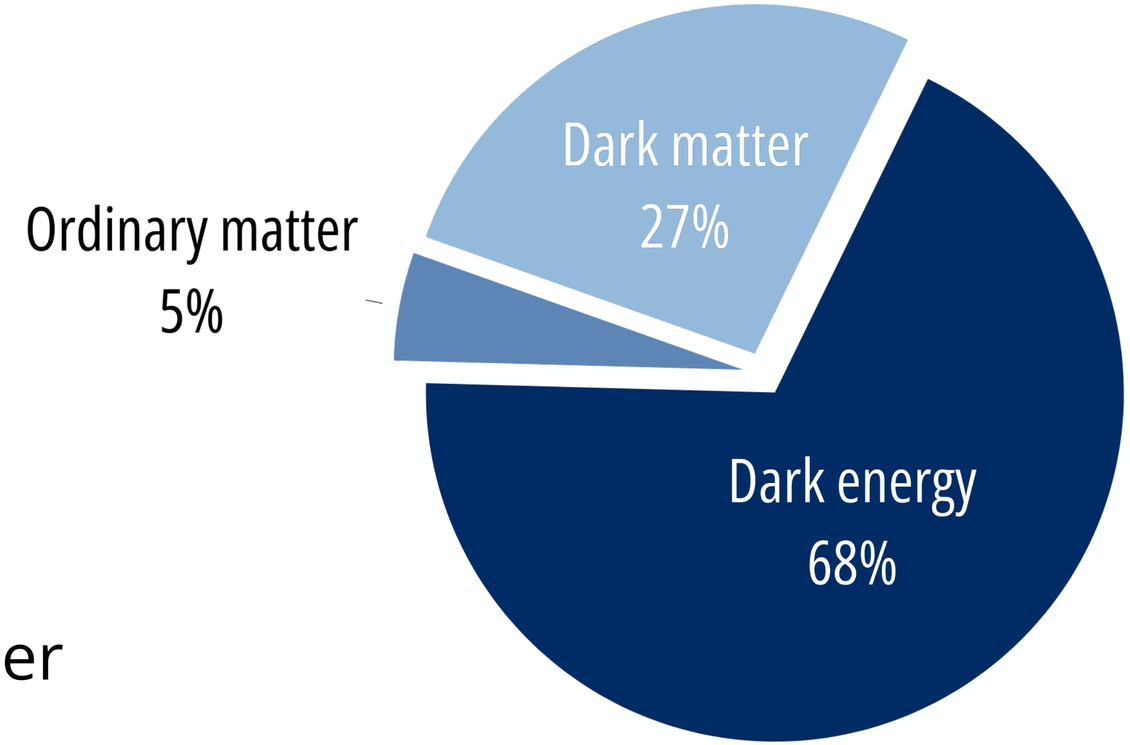

DM Candidates

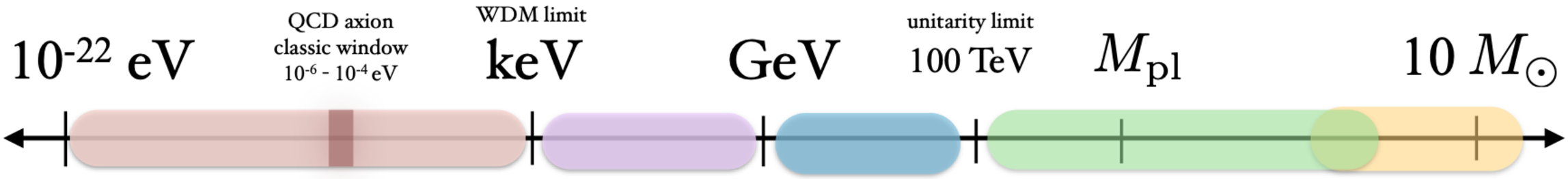

``Ultralight" DM
non-thermal
bosonic fields

``Light" DM
dark sectors
sterile ν
can be thermal

WIMP

Composite DM
(Q-balls, nuggets, etc)

Primordial black holes

T.lin 1904.07915

Wave-like | Particle-like

DM Detection

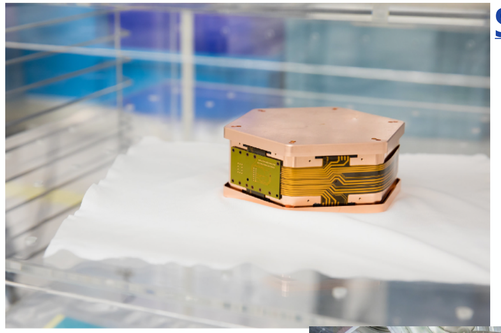

SuperCDMS

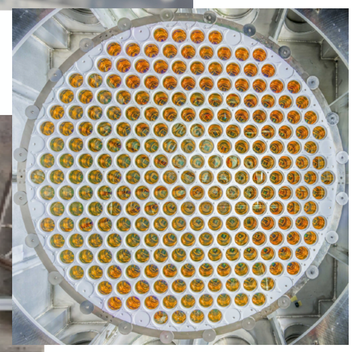

LZ

NEWS-G

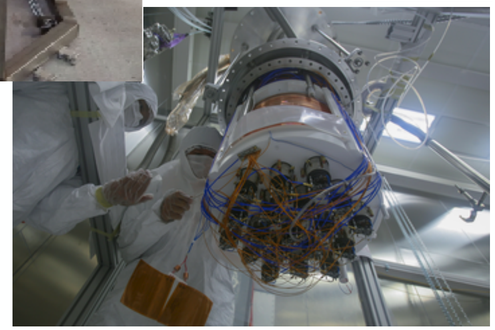

DarkSide

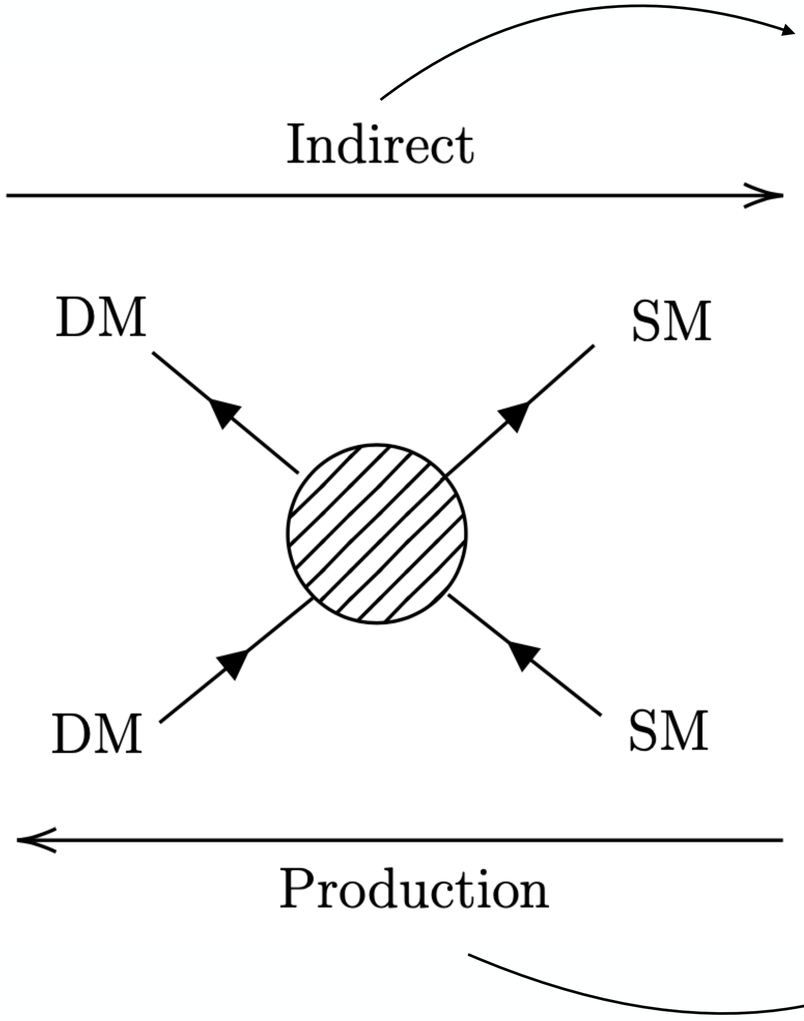

Fermi

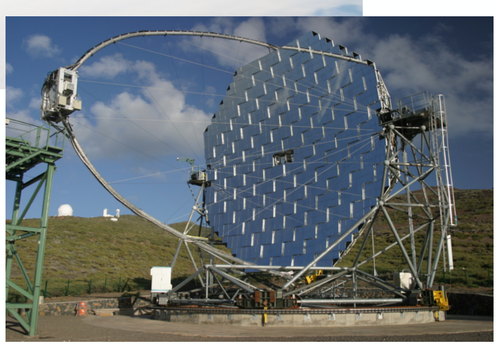

MAGIC

LHC - CERN

DM Detection

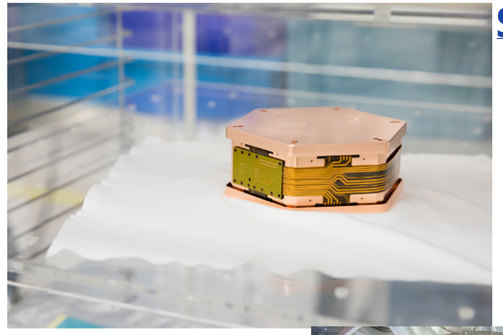

SuperCDMS

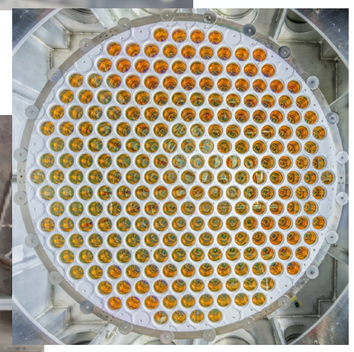

LZ

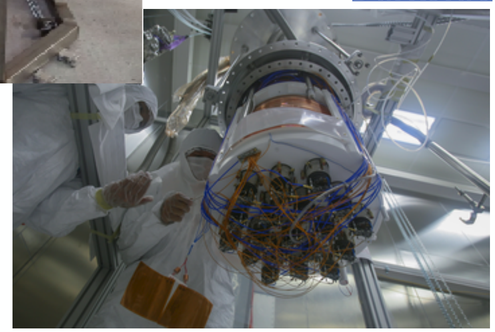

DarkSide

NEWS-G

Direct

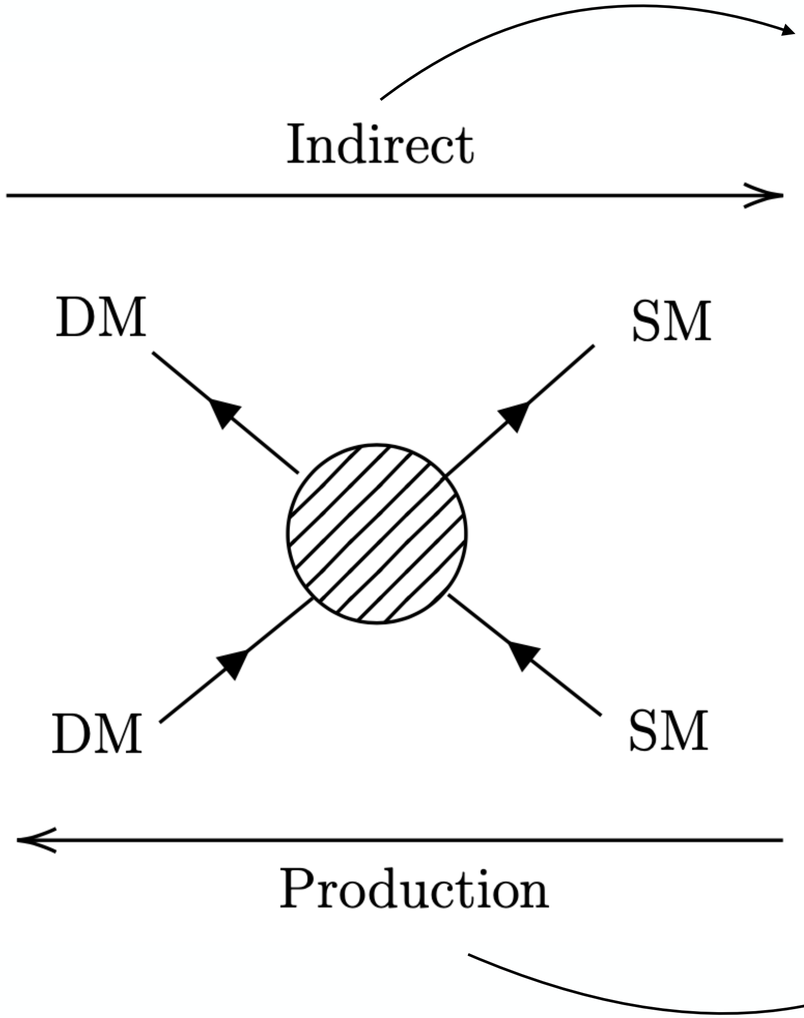

Fermi

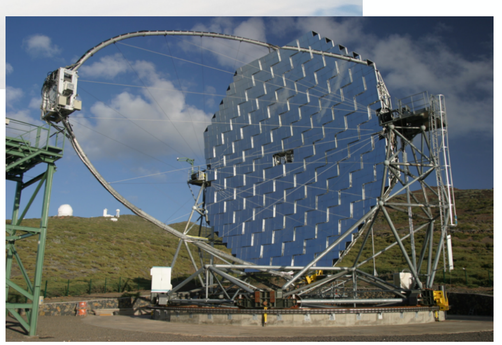

MAGIC

LHC - CERN

Direct Detection

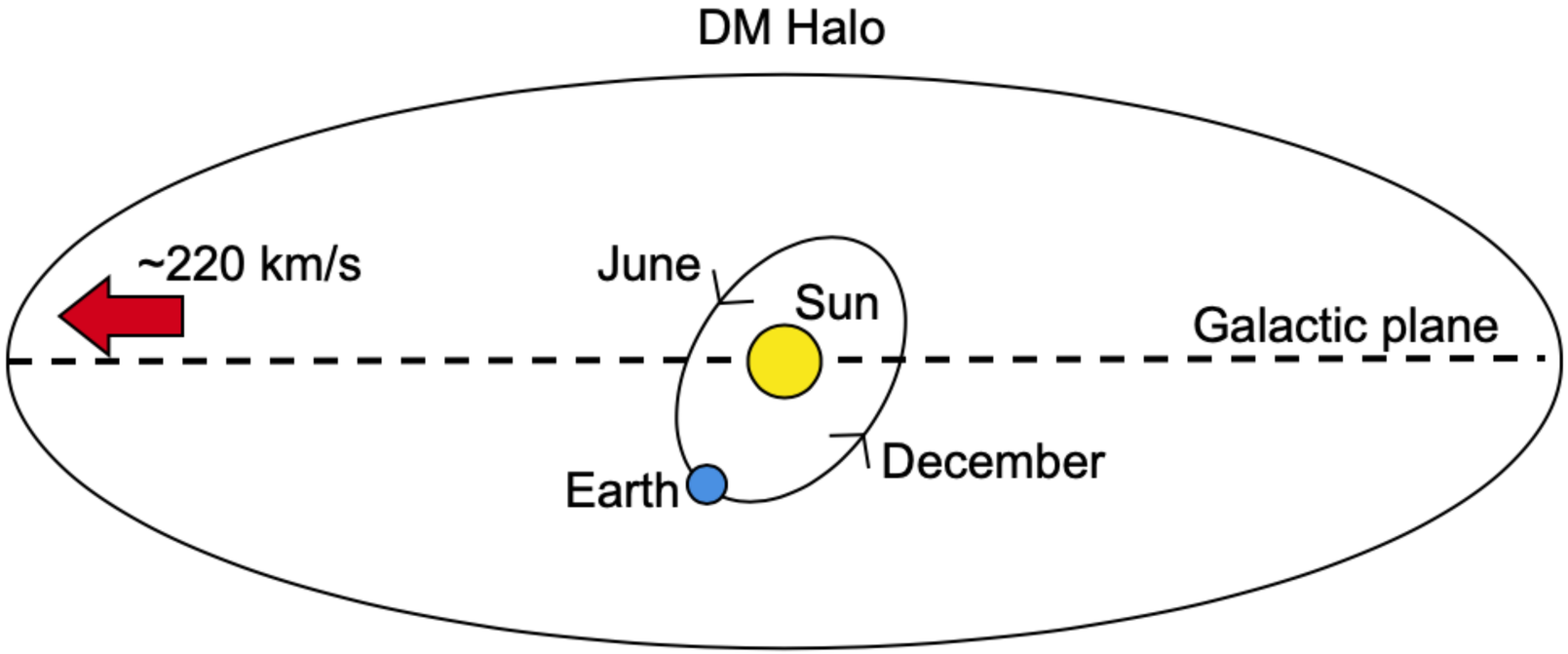

- Moving through DM halo with a velocity of ~220 km/s
- Local DM density ~ 0.3 GeV/cm^3
- Model as collisionless gas - from Maxwell-Boltzmann velocity distribution local flux of ~ $(10^7/m_\chi)$ GeV/cm^{2}s
- Motion of Earth induces annual signal modulation

Direct Detection

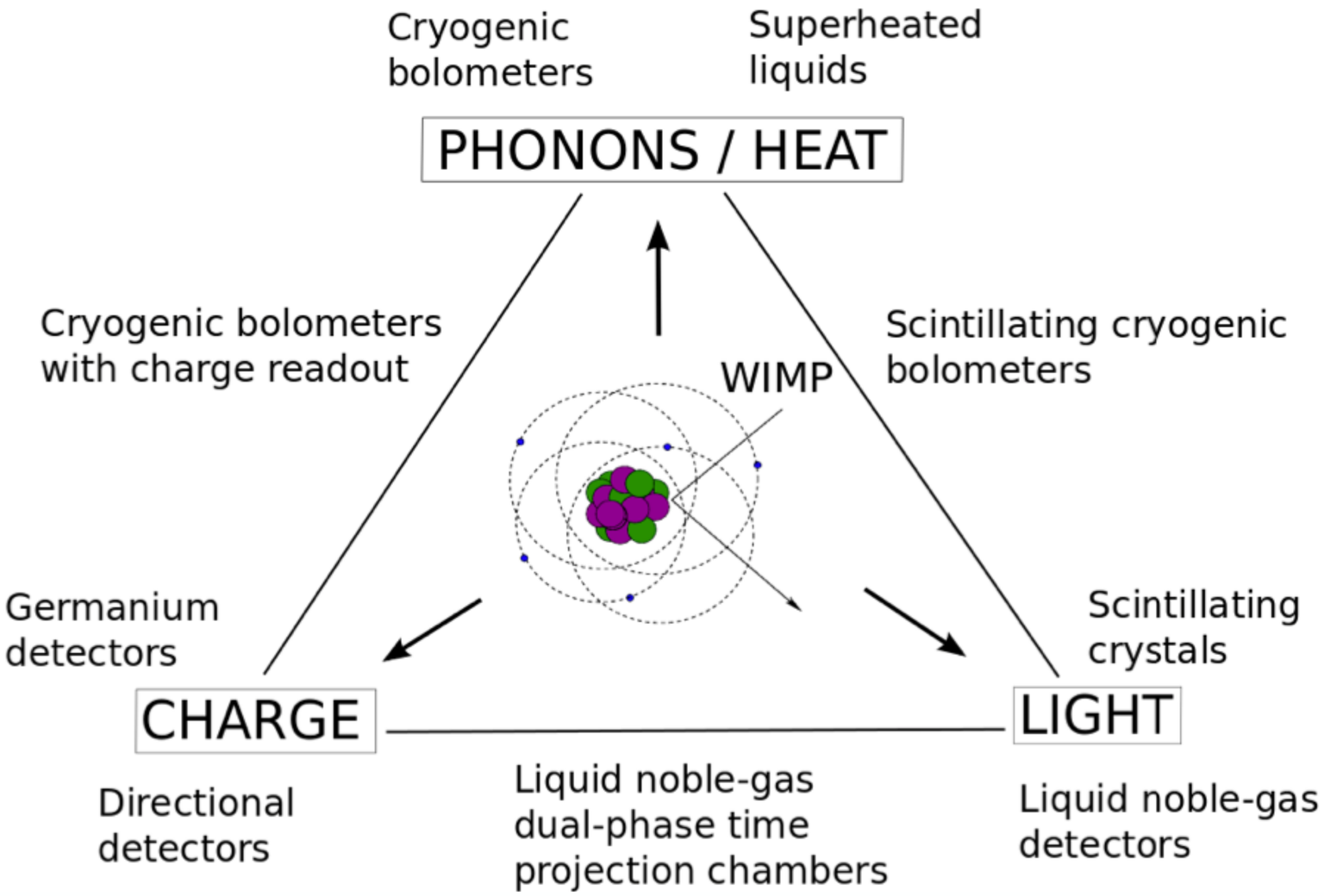

J.Phys.G 43 (2016) 1, 013001

Current Landscape

- Much progress made in search for WIMP-like DM
- Sub-GeV less explored as experimentally more challenging
- Can exploit the Migdal effect which leads to additional energy above threshold

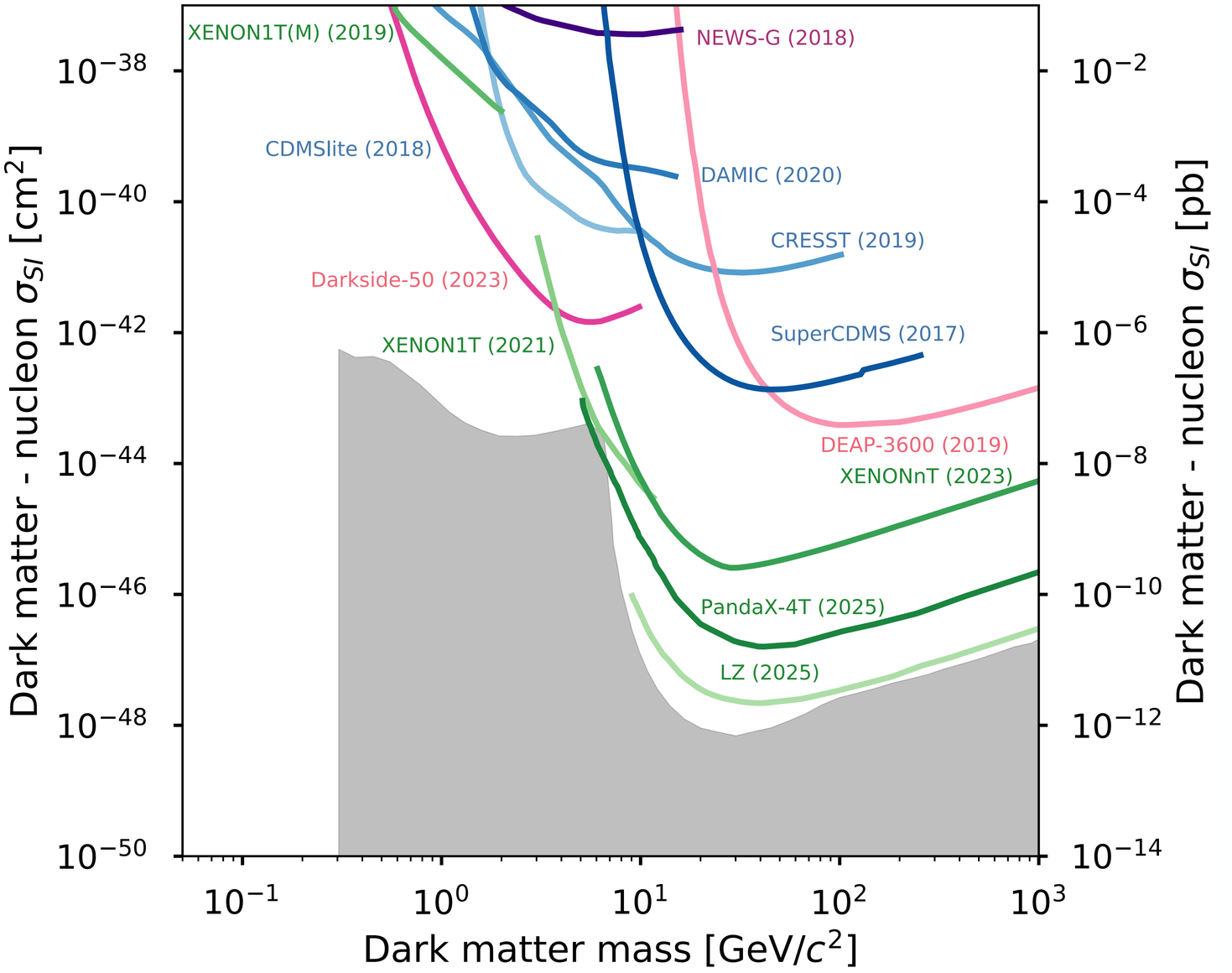

Low mass particle DM

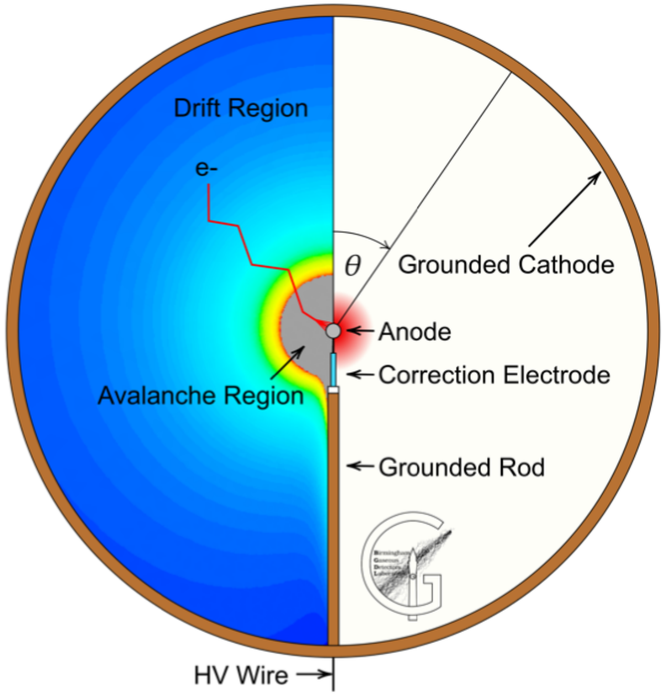

NEWS-G arxiv:2407.12769

Light gaseous target

Choice of target and pressure

Low capacitance

- Single electron detection

Low mass particle DM

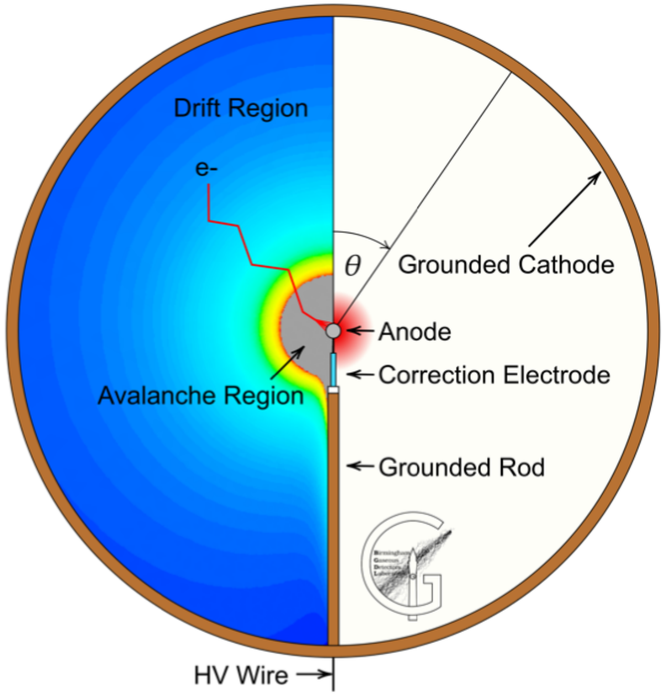

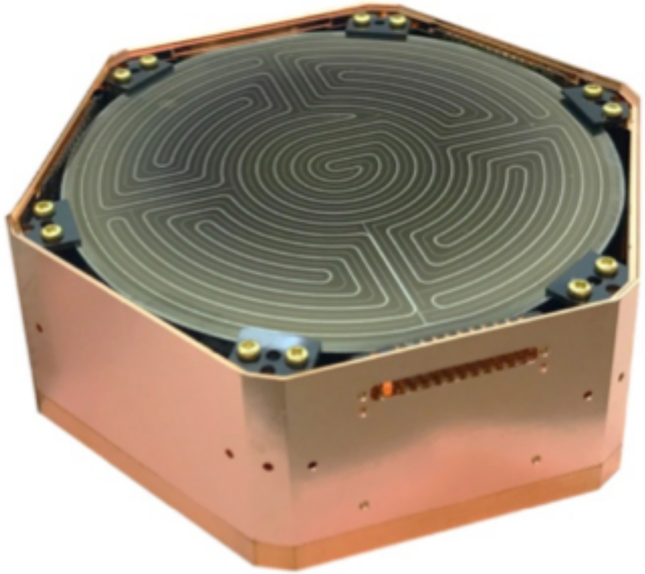

NEWS-G arxiv:2407.12769

Light gaseous target

Choice of target and pressure

Low capacitance

- Single electron detection

SuperCDMS arxiv:2302.09115

Semiconducting calorimeter

Phonon and ionisation detection

- Low energy thresholds

Low mass particle DM

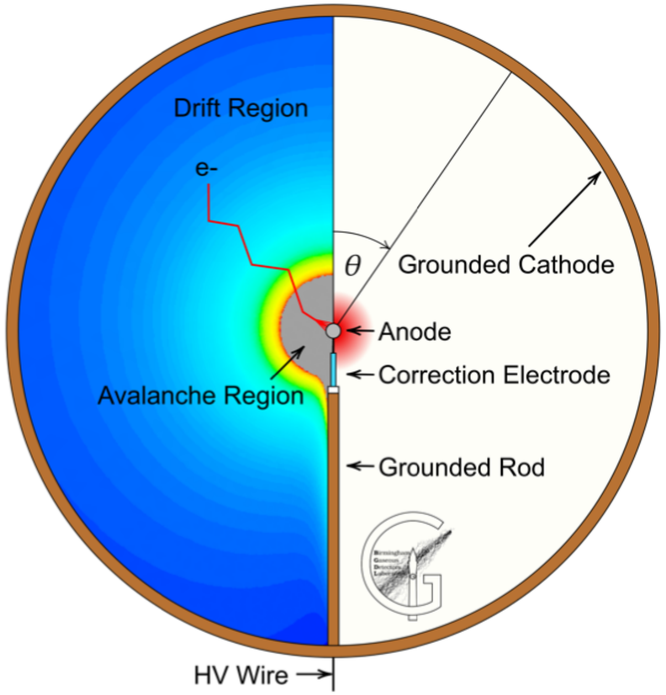

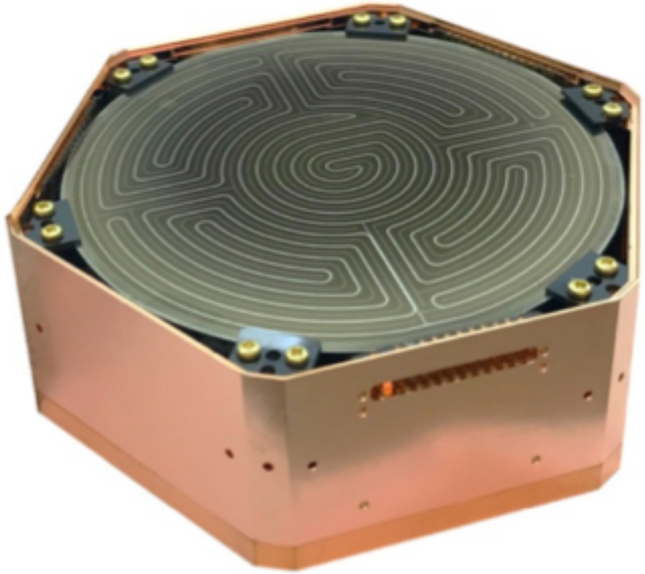

Image: VA Kudryavtsev ICNFP 2018

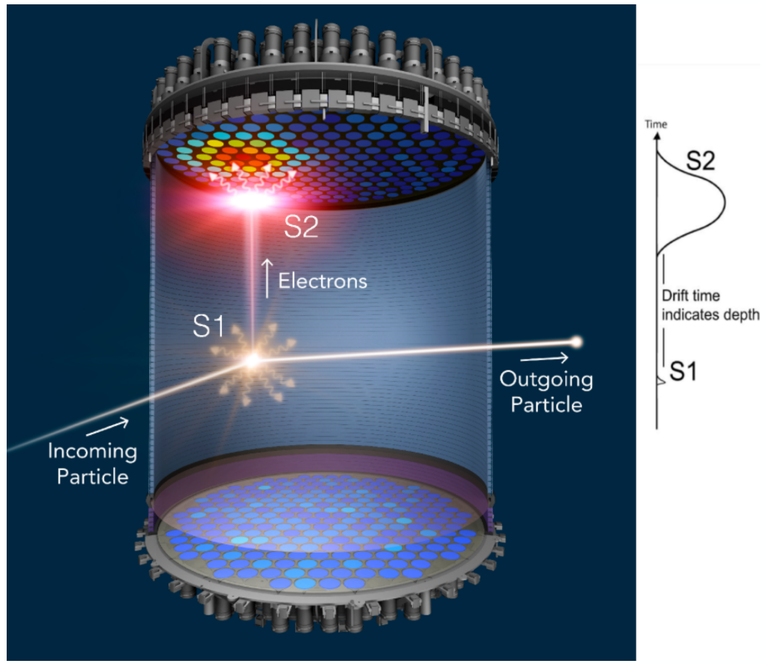

NEWS-G arxiv:2407.12769

Light gaseous target

Choice of target and pressure

Low capacitance

- Single electron detection

SuperCDMS arxiv:2302.09115

Semiconducting calorimeter

Phonon and ionisation detection

- Low energy thresholds

Liquid noble element TPCs

S2 only searches (lower threshold) PhysRevD.106.022001

H doped Xe HydroX

The Migdal Effect

- During nuclear recoil sudden displacement of nucleus with respect to atomic electron cloud excites the atom
- De-excitation can result in emission of one or more Migdal electrons (with low probability)
- Observed in α, β decay (Phys. Rev. C 11 (1975), 1740-1745 & 1746-1754, Phys. Rev. 93 (1954), 518-523, Phys. Rev. A 97 (2018), 023402)
- For low mass WIMP-like DM energy deposited by electron can exceed *O*(keV) nuclear recoil
- Recently observed for the first time in nuclear scattering (Nature 649, 580–583 (2026))

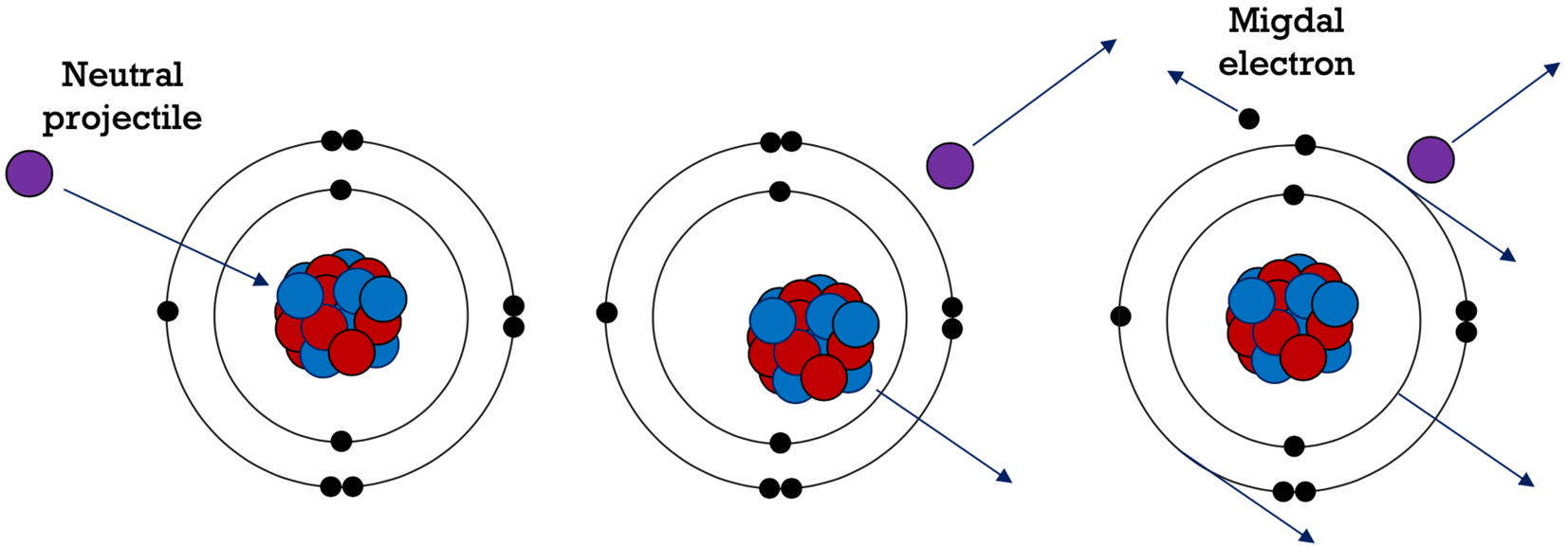

Migdal experimental efforts

- Searches for Migdal in nuclear scattering induced by neutrons
- Detect nuclear recoil and simultaneously Migdal electron or associated de-excitation x-ray

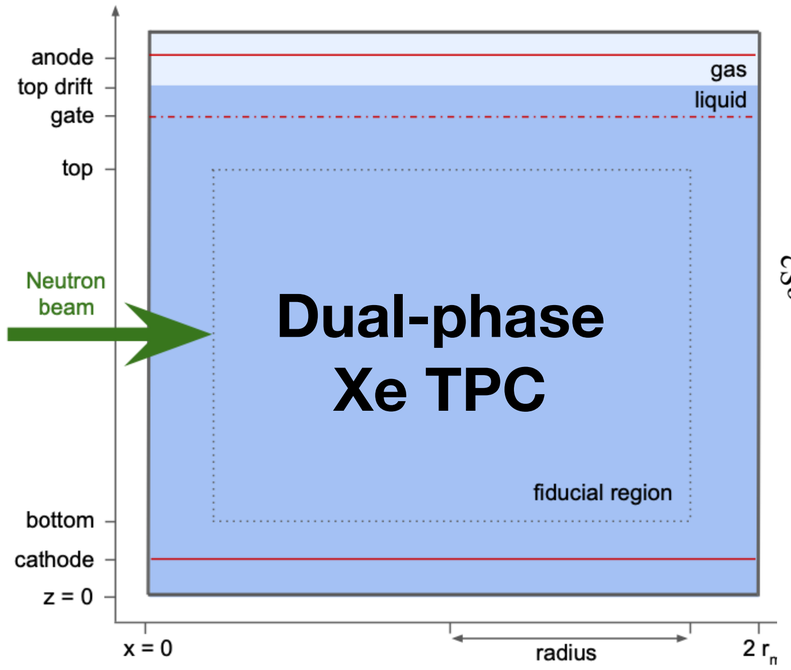

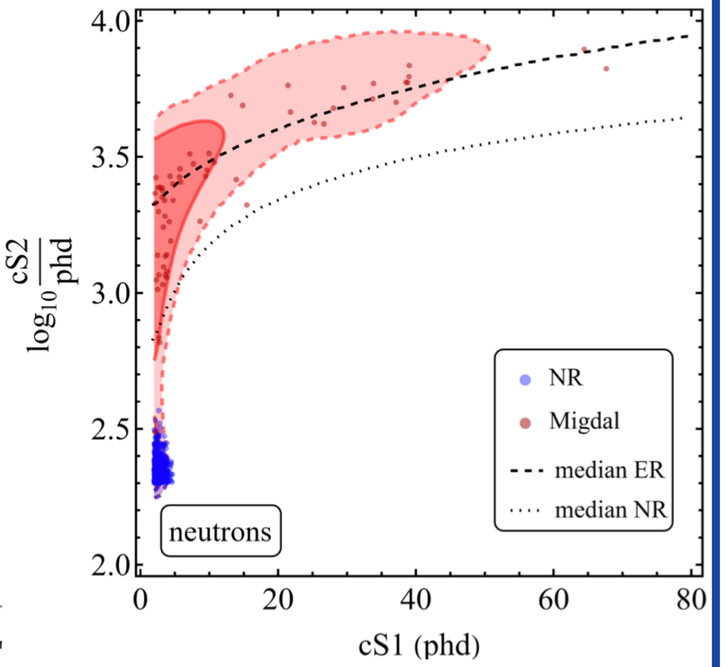

[Bell et al, arxiv:2112.08514]

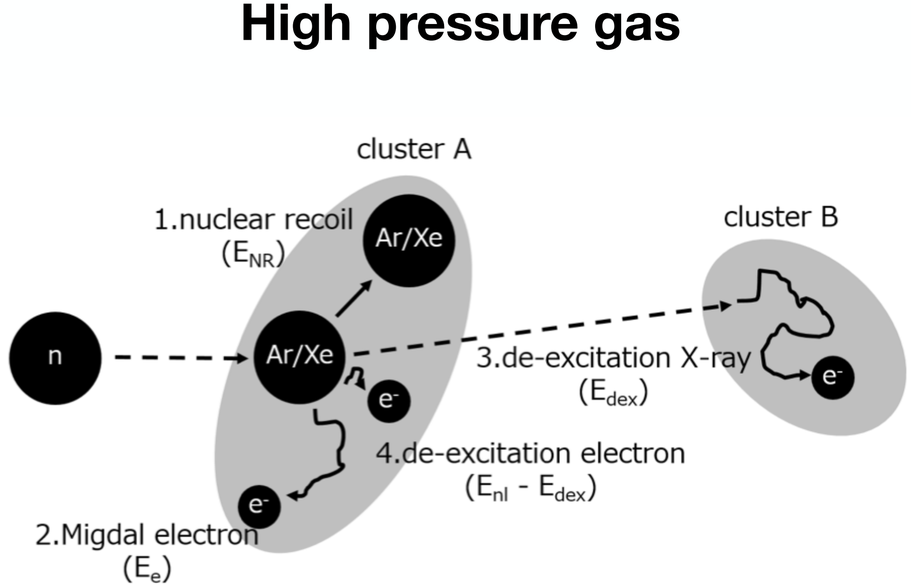

[Nakamura et al, arxiv:2009.05939]

Migdal Experimental Results

- Dual-phase Xe TPC results

LZ: Observe excess in high S2 region consistent with Migdal
Analysis to be finalised

J.Bang, UCLA Dark Matter 2023

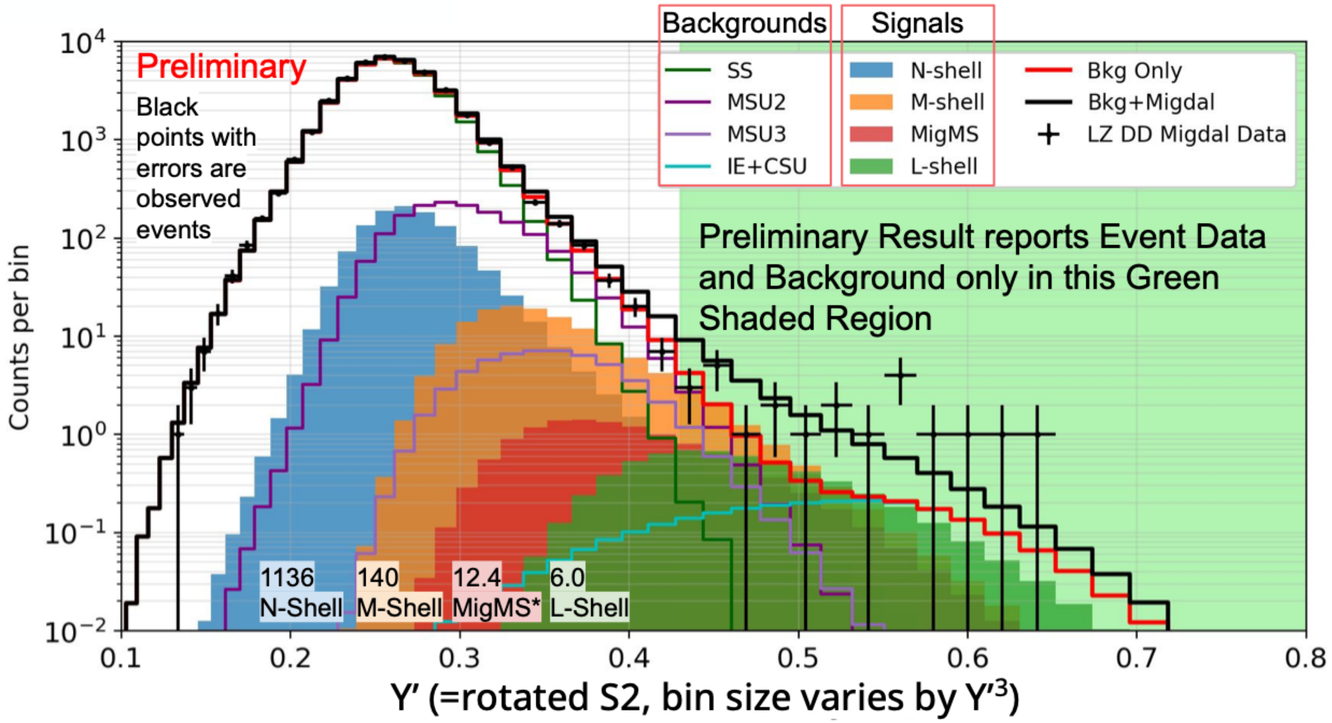

Xu et al: Signal suppressed due to recombination

Phys.Rev.D 109 (2024) 5, L051101 arXiv 2503.07562

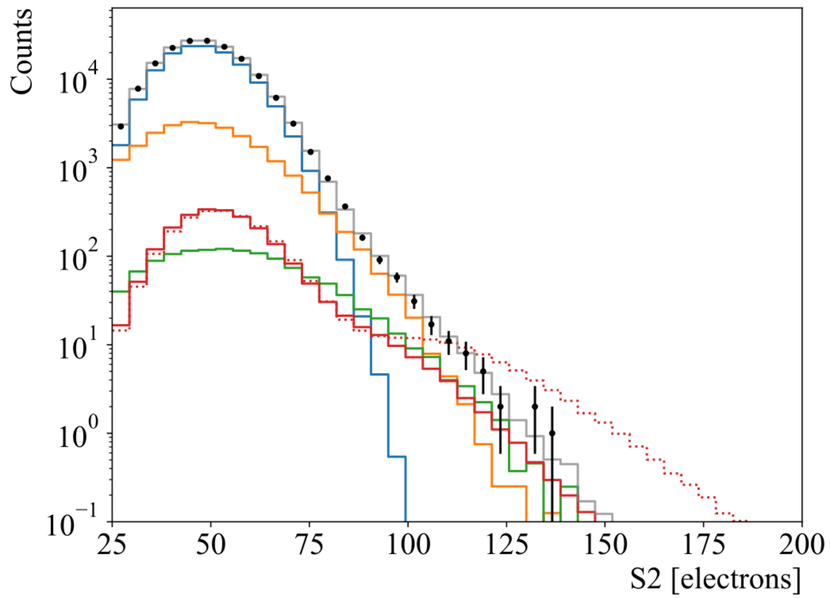

FIG. 5. Reanalysis of Migdal search data in [28] using a Migdal signal yield from this work. The electron spectrum with scintillation signals between 4 and 10 photoelectrons is compared with the best-fit signal and background models: Migdal signal at the nominal strength (solid red), single-scatter NR (blue), neutron multi-scatters in xenon (green) and in passive materials (orange), and the sum of all components (grey); the Migdal signal model that simply adds the NR and ER yields without considering recombination enhancement is also shown (dotted red).

First observation of the Migdal effect in nuclear scattering

- First observation of the Migdal Effect in nuclear scattering by MARVEL (Nature 649, 580–583 (2026))
- Using a gas pixel detector with He:CH30CH3 (40:60)
- 2.45 MeV neutrons from a D-D generator
- Signal is primarily from He and H
- In agreement with theoretical predictions

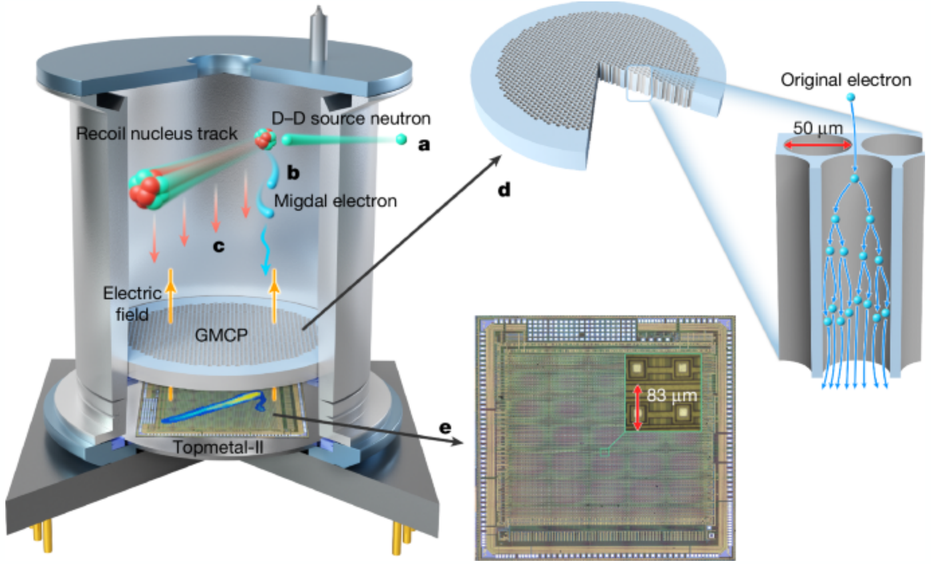

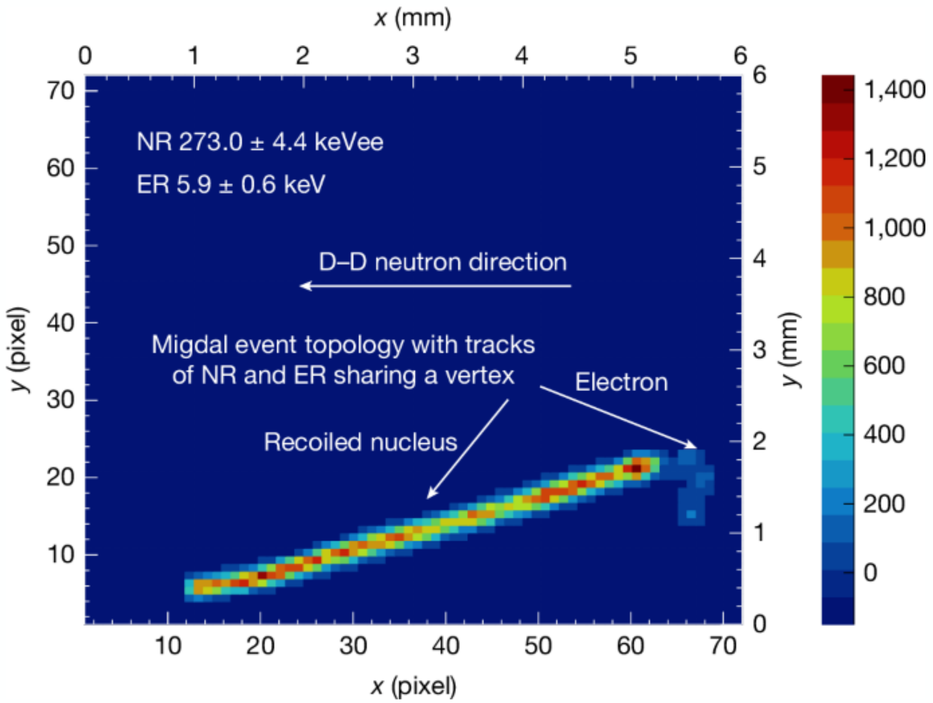

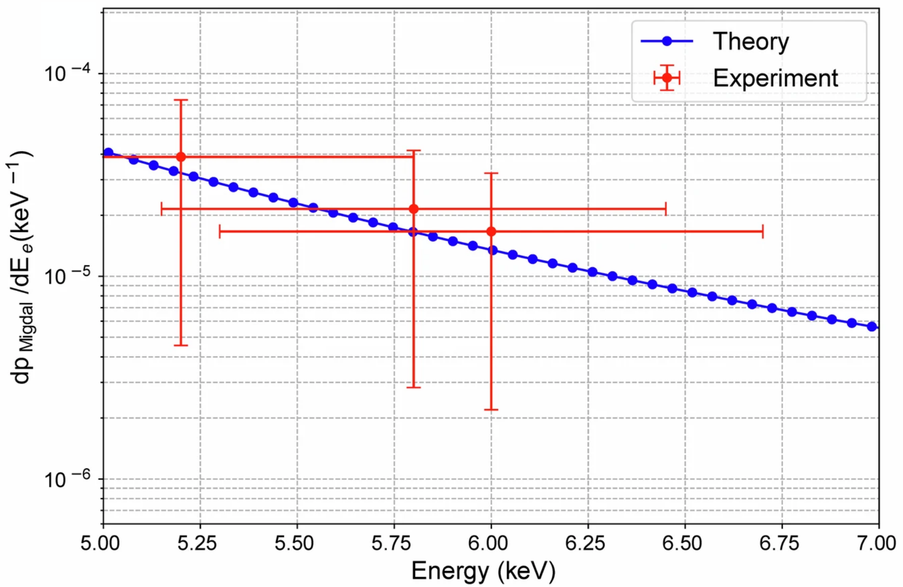

The MIGDAL Collaboration

- Aim to characterise the Migdal Effect in CF_4 + noble gas mixtures
- Use a low pressure Optical Time Projection Chamber to image electron and nuclear recoil in three-dimensions
- Over 35 physicists and engineers from 14 institutions and 8 countries

Science and Technology Facilities Council

U.S. DEPARTMENT OF ENERGY

Horizon 2020 European Union Funding for Research & Innovation

FCT Fundação para a Ciência e a Tecnologia

MARIE CURIE ACTIONS

NSF National Science Foundation

The MIGDAL experiment

- Aim to characterise the Migdal Effect in a range of species
- Low pressure Optical Time Projection Chamber (OTPC) with **50 Torr CF_4**
- Unambiguous measurement of electron and nuclear recoil from common vertex

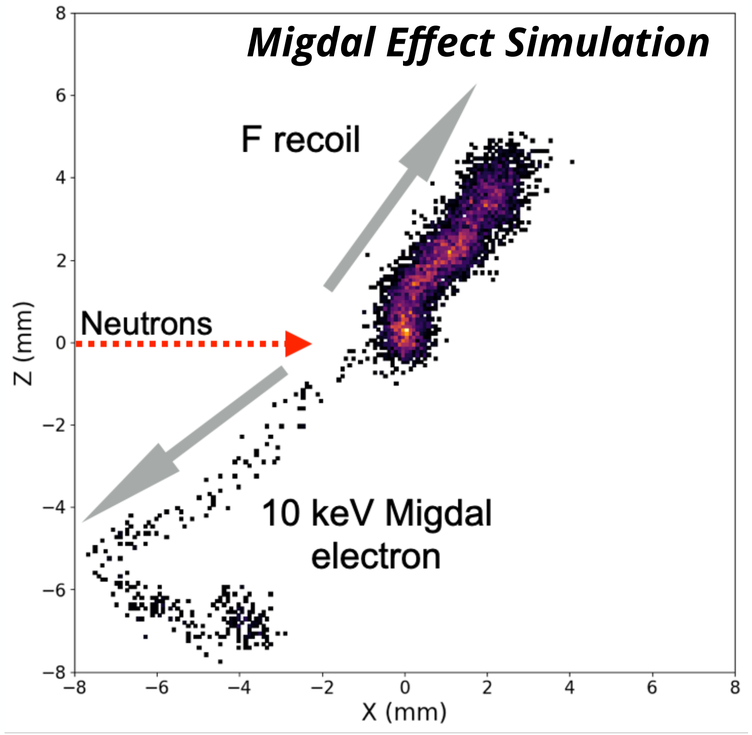

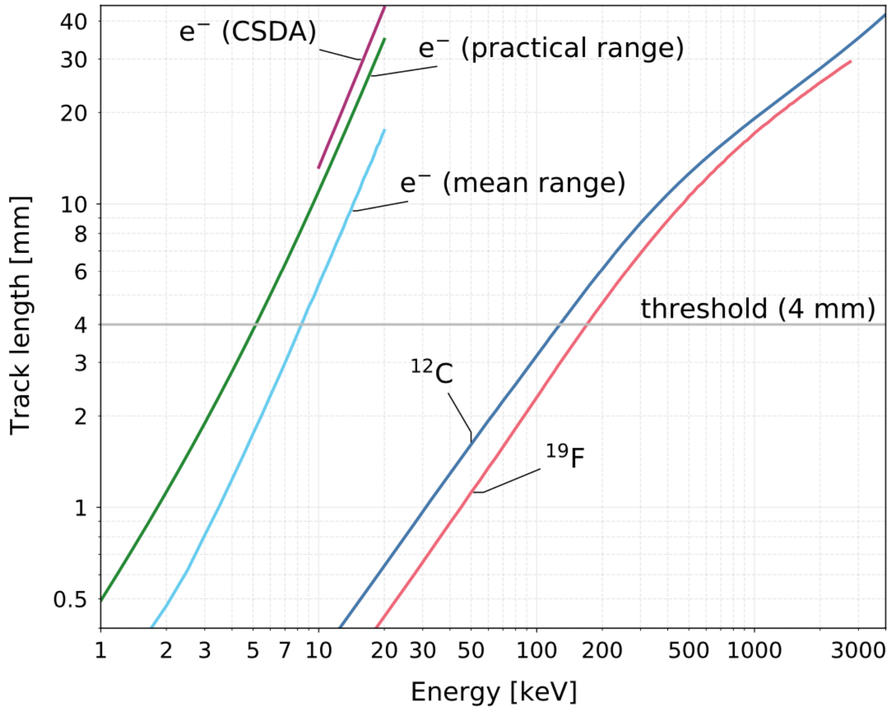

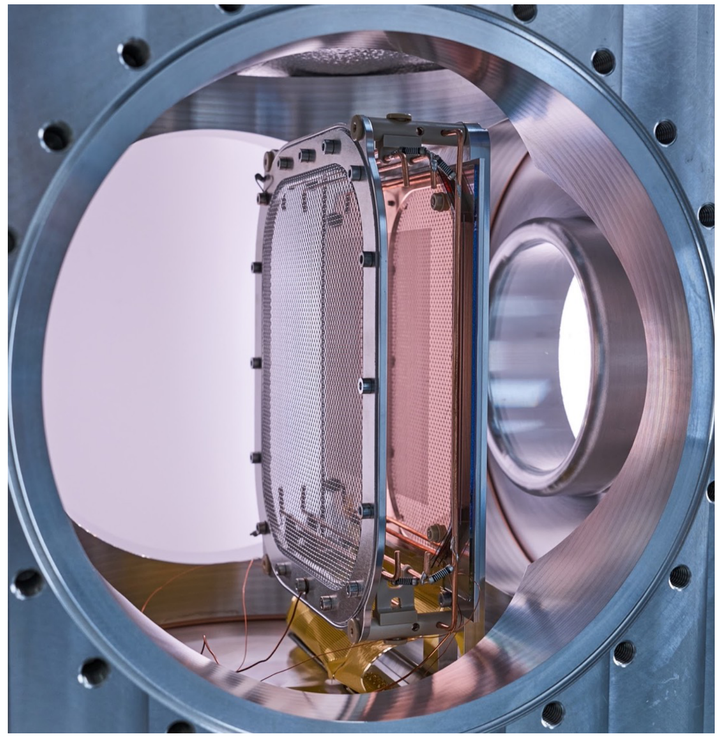

The MIGDAL Experiment

- Event signature is nuclear recoil and an electron sharing a common vertex
- Nuclear scattering induced by 2.47 MeV neutrons from a D-D generator

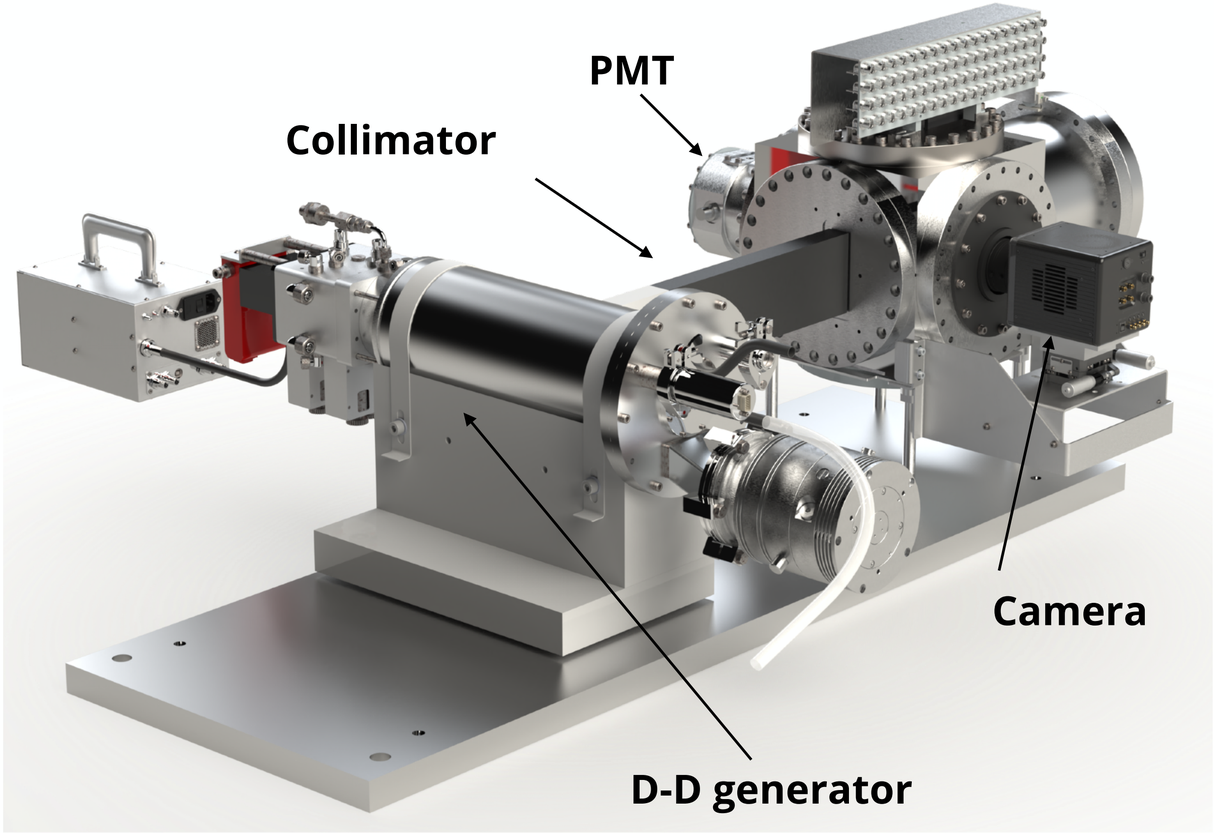

The MIGDAL Detector

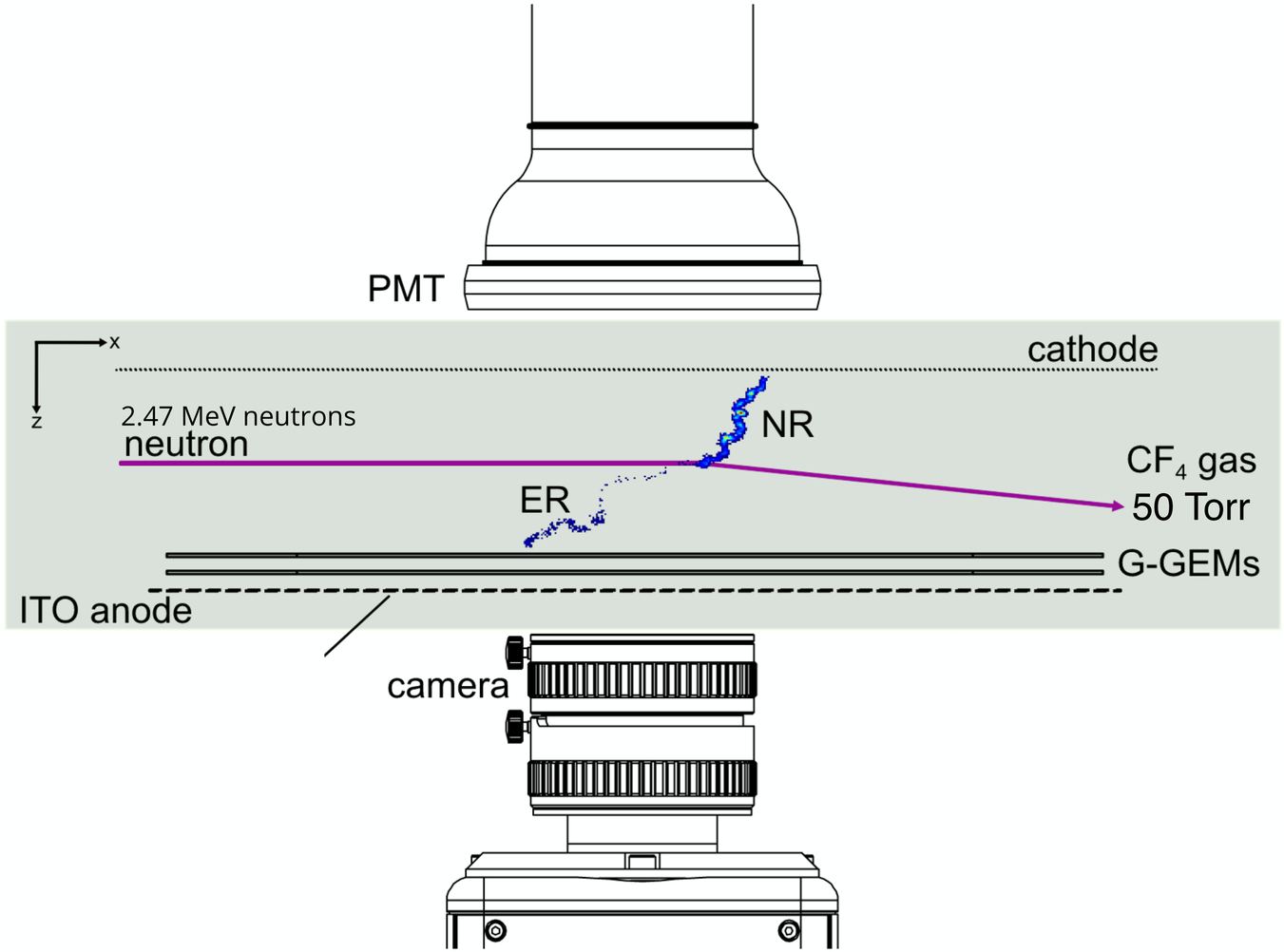

Astropart.Phys. 151 (2023) 102853

The MIGDAL Detector

Charge Amplification

Two glass GEMs

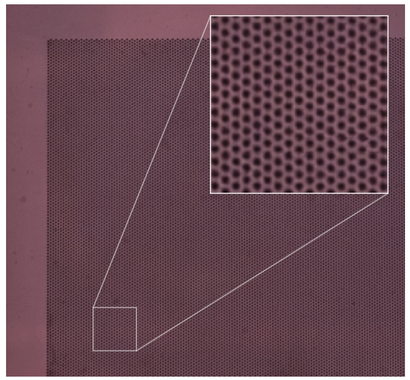

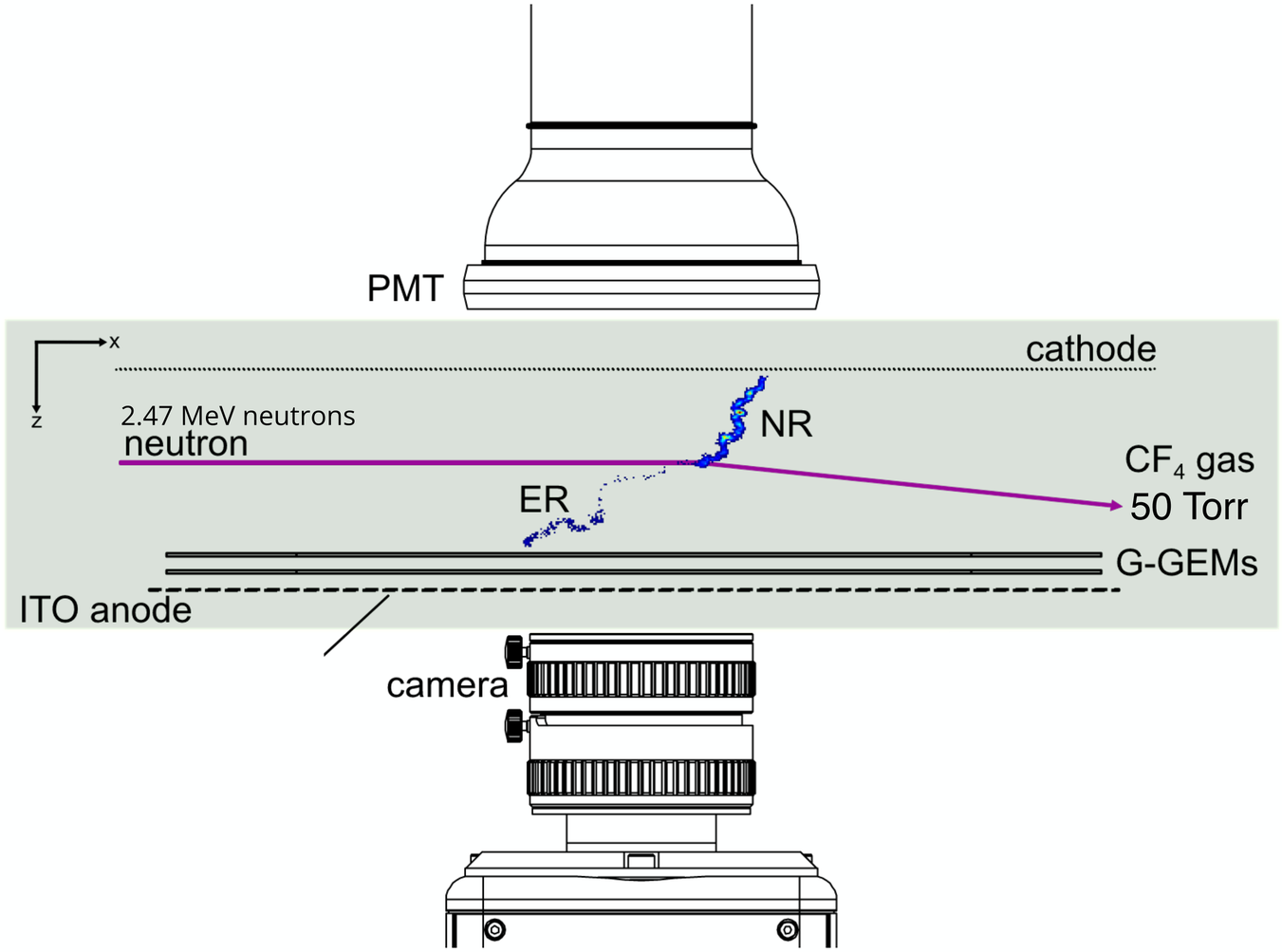

Astropart.Phys. 151 (2023) 102853

The MIGDAL Detector

Charge Amplification
Two glass GEMs

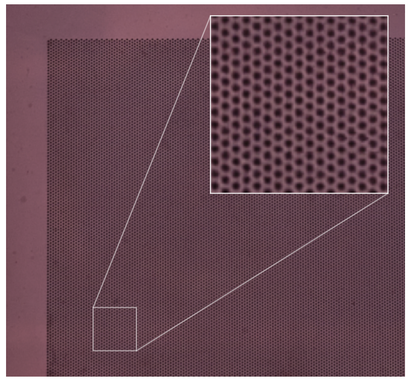

Charge read-out
anode segmented into 120 strips

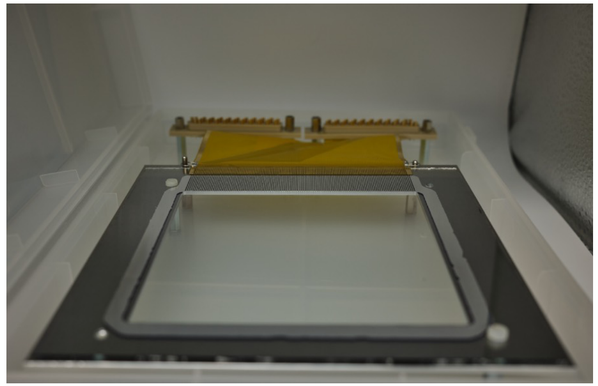

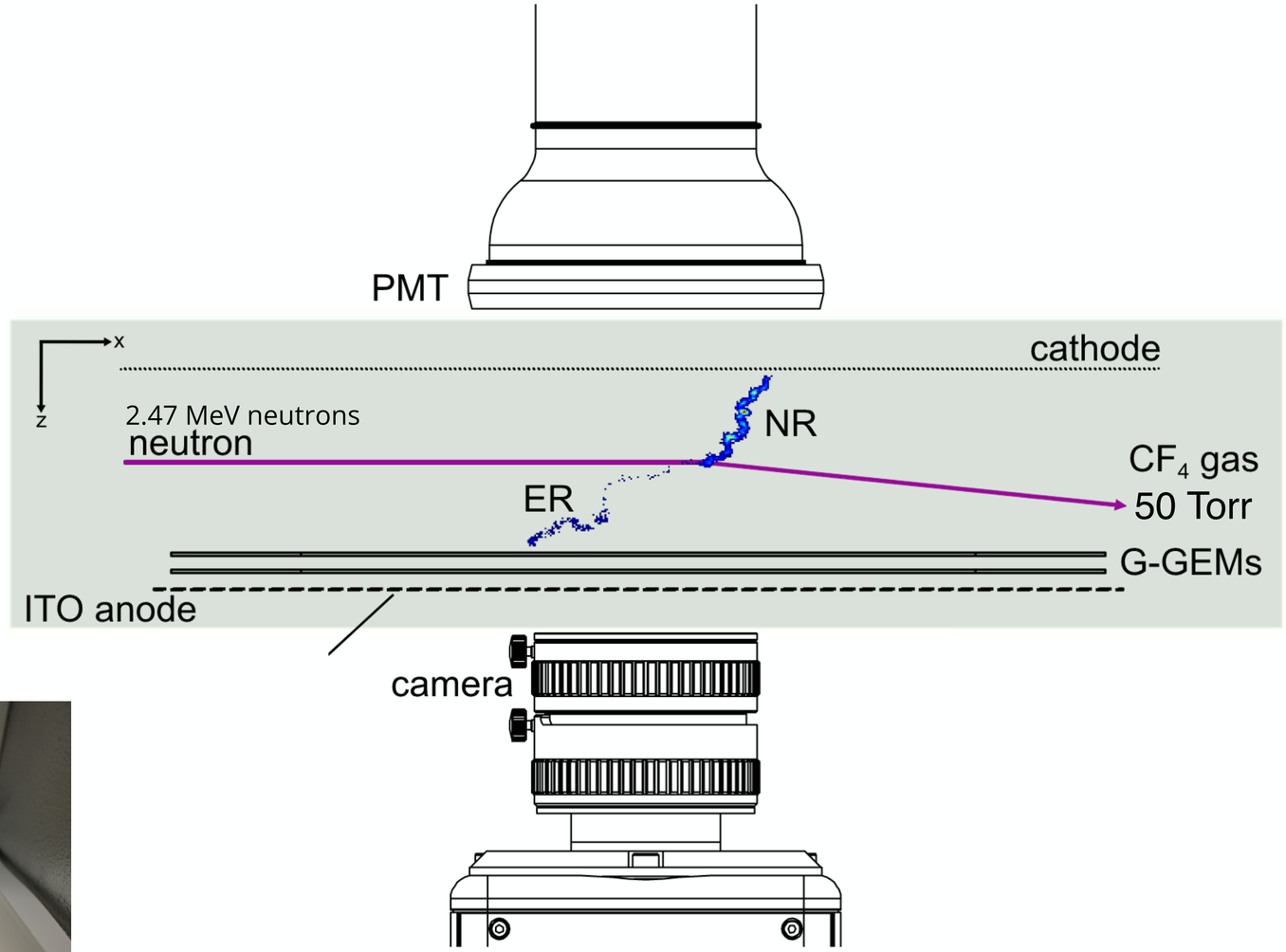

Astropart.Phys. 151 (2023) 102853

The MIGDAL Detector

Charge Amplification
Two glass GEMs

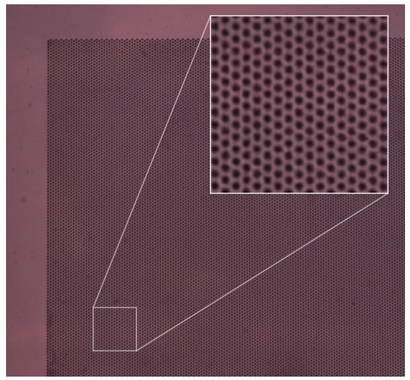

Charge read-out
anode segmented into 120 strips

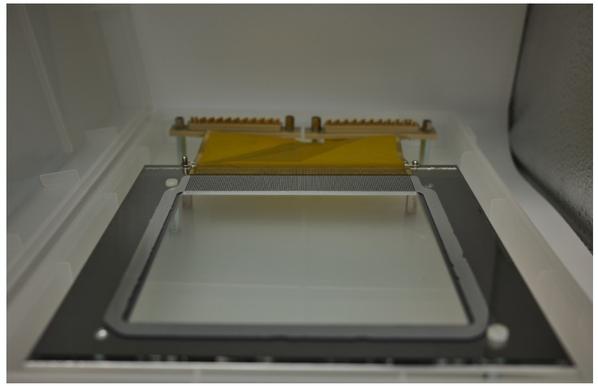

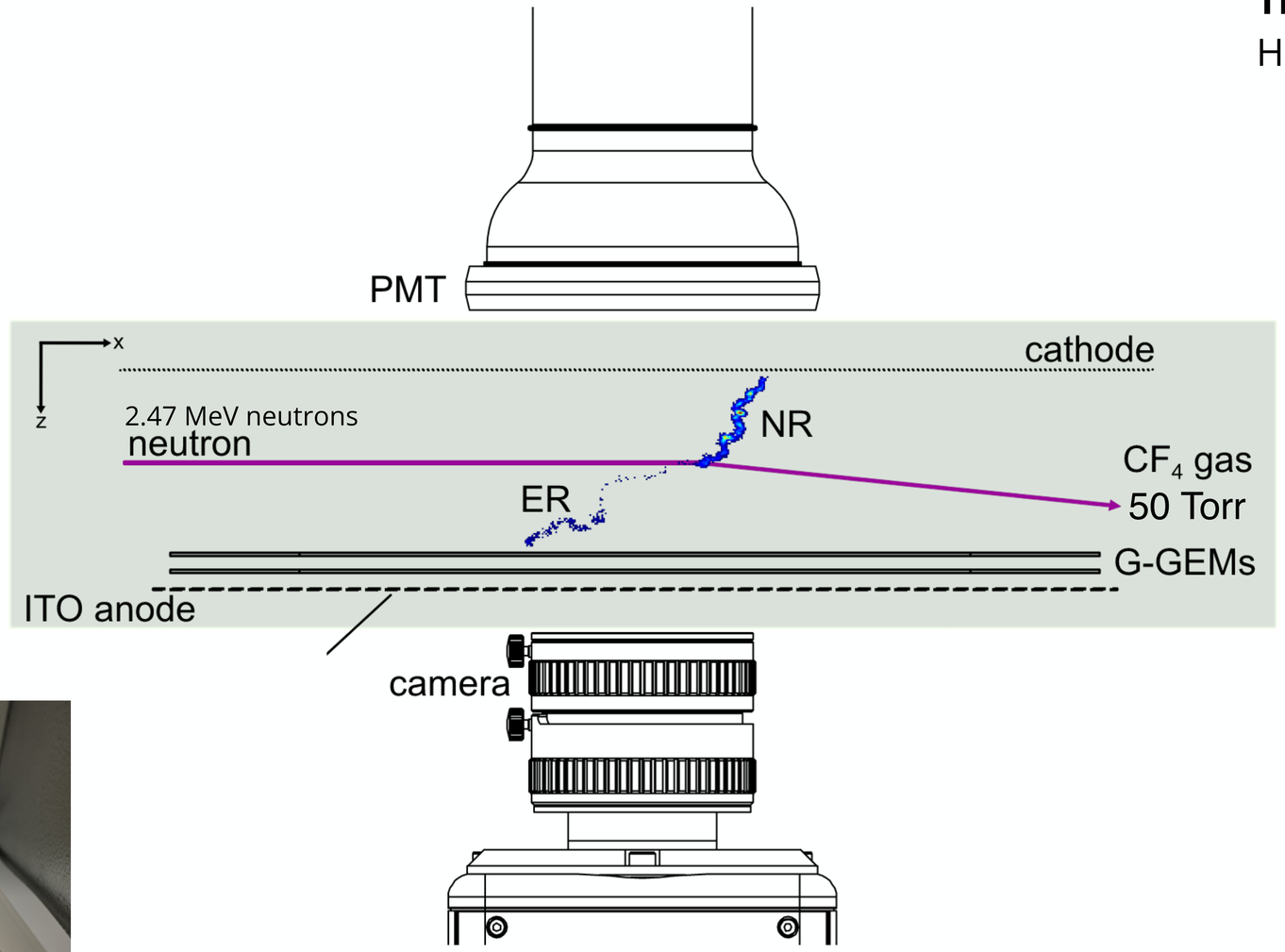

Trigger and timing
Hamamatsu R11410 VUV PMT

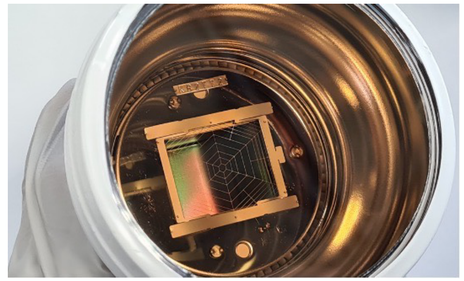

Astropart.Phys. 151 (2023) 102853

The MIGDAL Detector

Charge Amplification
Two glass GEMs

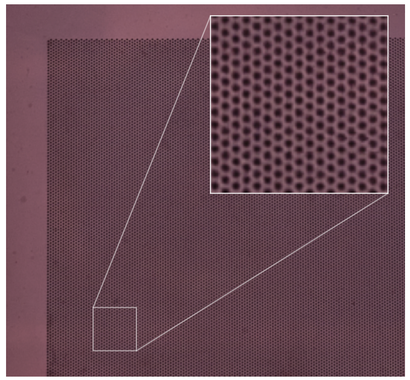

Charge read-out
anode segmented into 120 strips

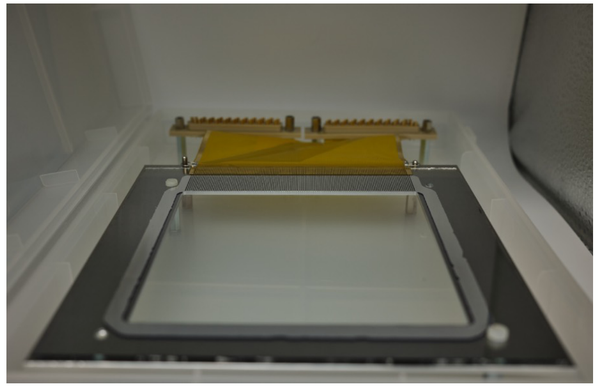

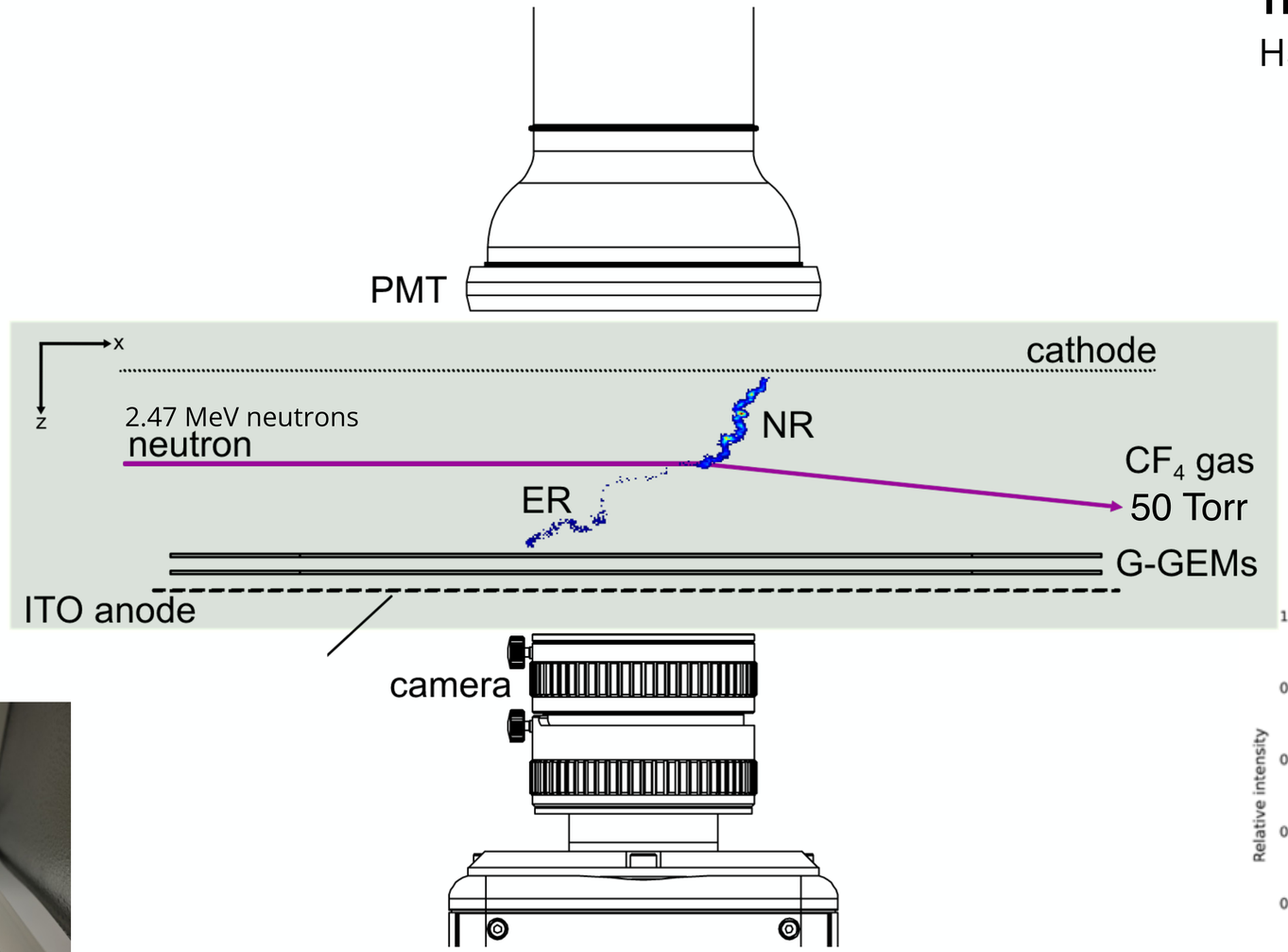

[Astropart.Phys. 151 (2023) 102853]

Trigger and timing
Hamamatsu R11410 VUV PMT

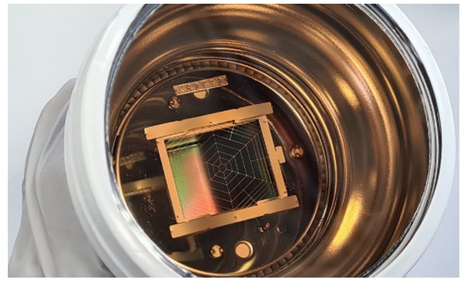

Light read-out
Orca Quest qCMOS camera
8.3 ms exposure

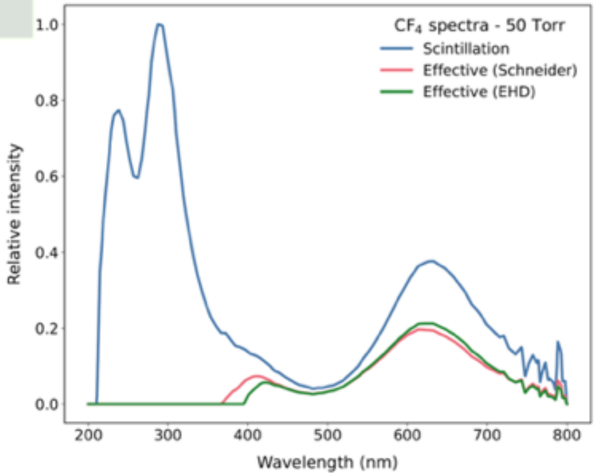

Gas Electron Multipliers

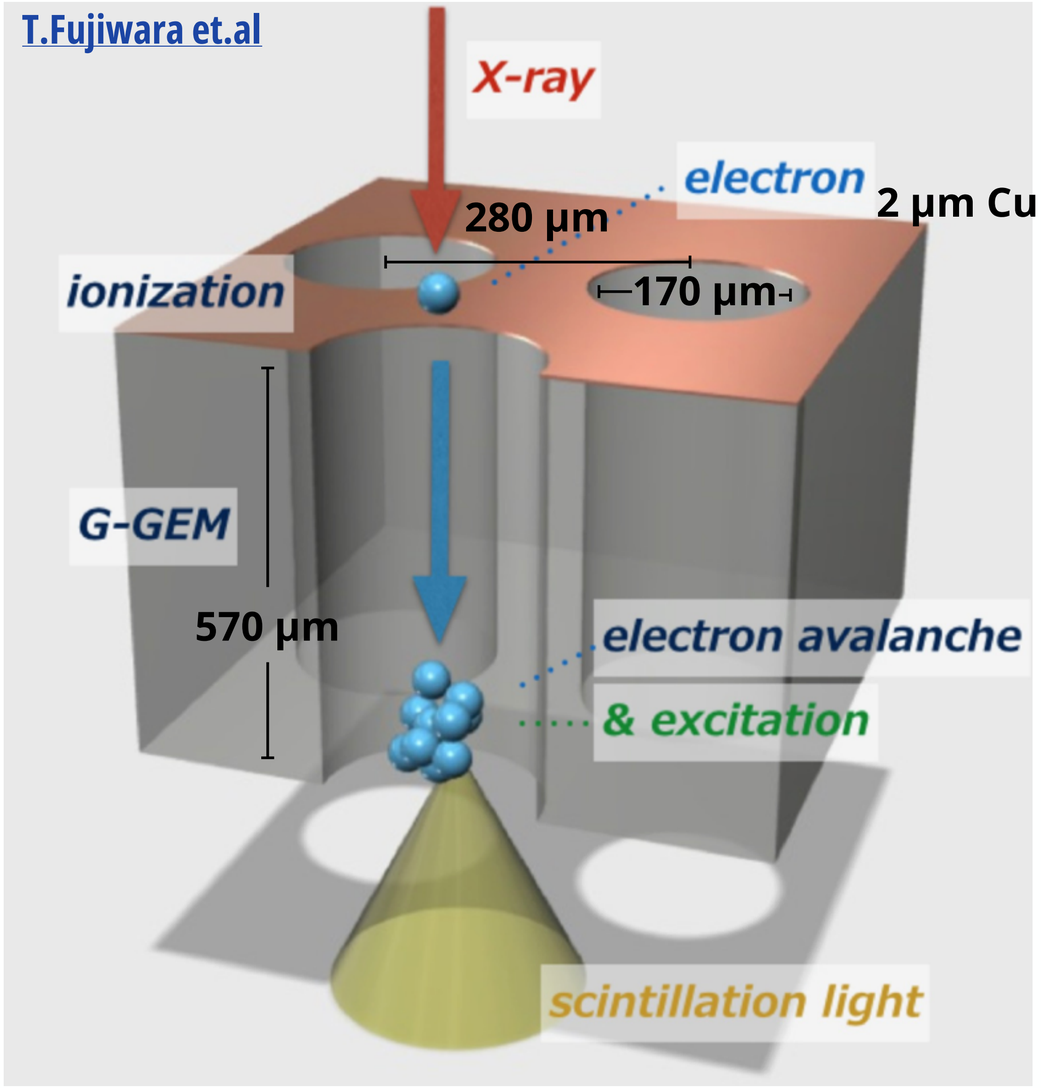

- Voltage applied across dielectric
- Electrons funnelled through holes
- Strong field results in avalanche
- Charge multiplication and scintillation
- Use two glass GEMs for gas gains ~ 10^5

MIGDAL@NILE

- Installed summer 2023

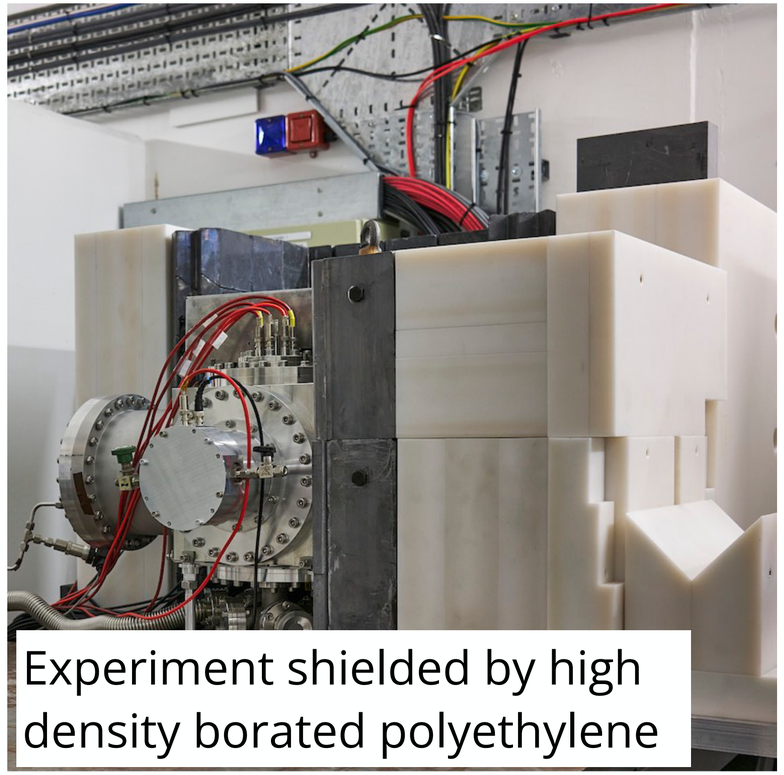

Experiment shielded by high density borated polyethylene

Detector with lead shielding

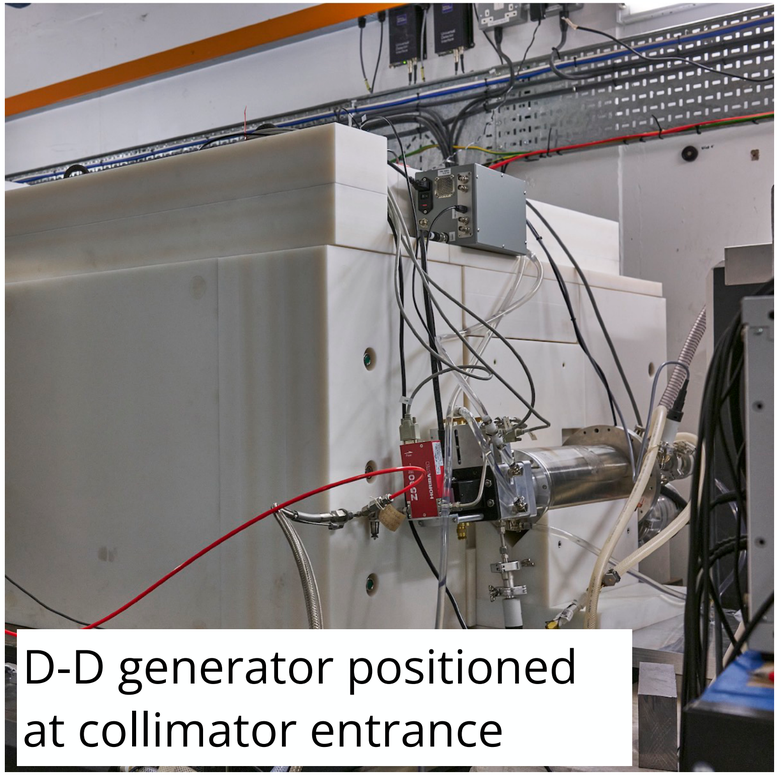

D-D generator positioned at collimator entrance

- Science run data collected from 15/01/2024 - 06/02/2024
- Gas replaced ~ every 3 days and calibration with ^{55}Fe every 3 hours
- Total exposure of 85.3 hours with ~3.6×10^5 nuclear recoils
- Initial selection criteria defined on 49% of the data

Calibration

- Calibration with ^{55}Fe source
- Operate near threshold for large stable dynamic range
- Energy resolution of ~20% in all sub-systems
- Gain and resolution monitored in all sub-systems
- GEM voltages increased ~2V per day to maintain gain

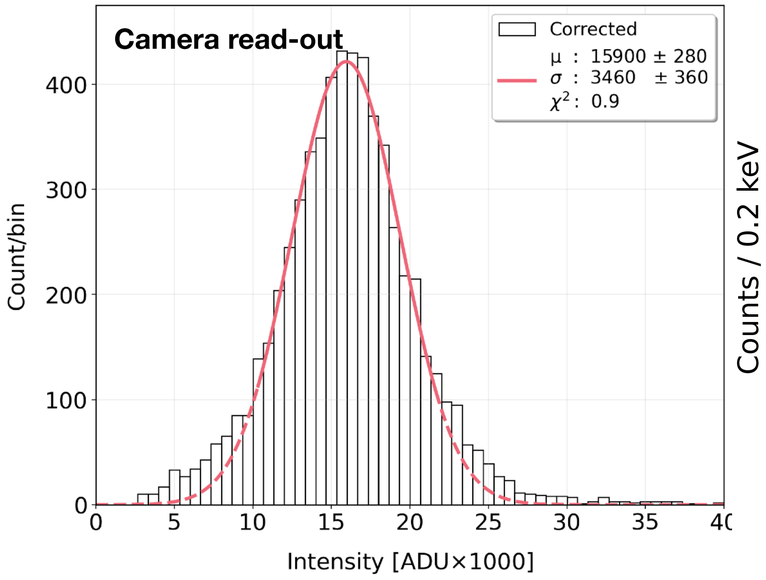

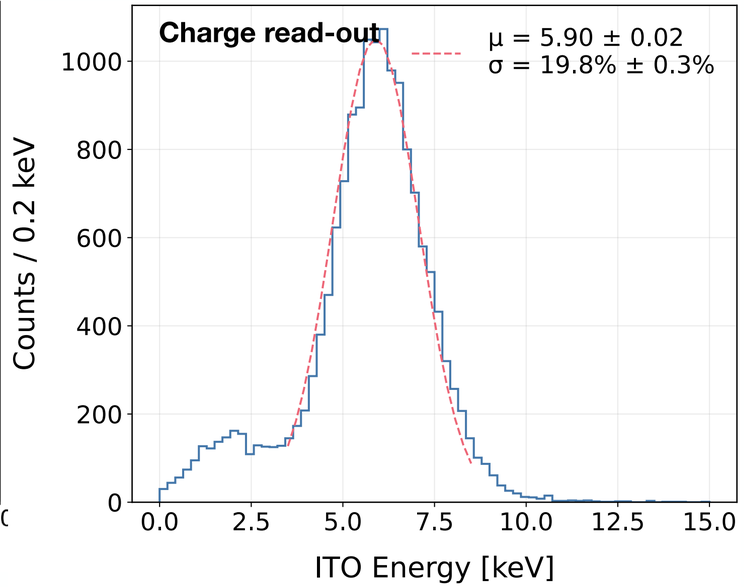

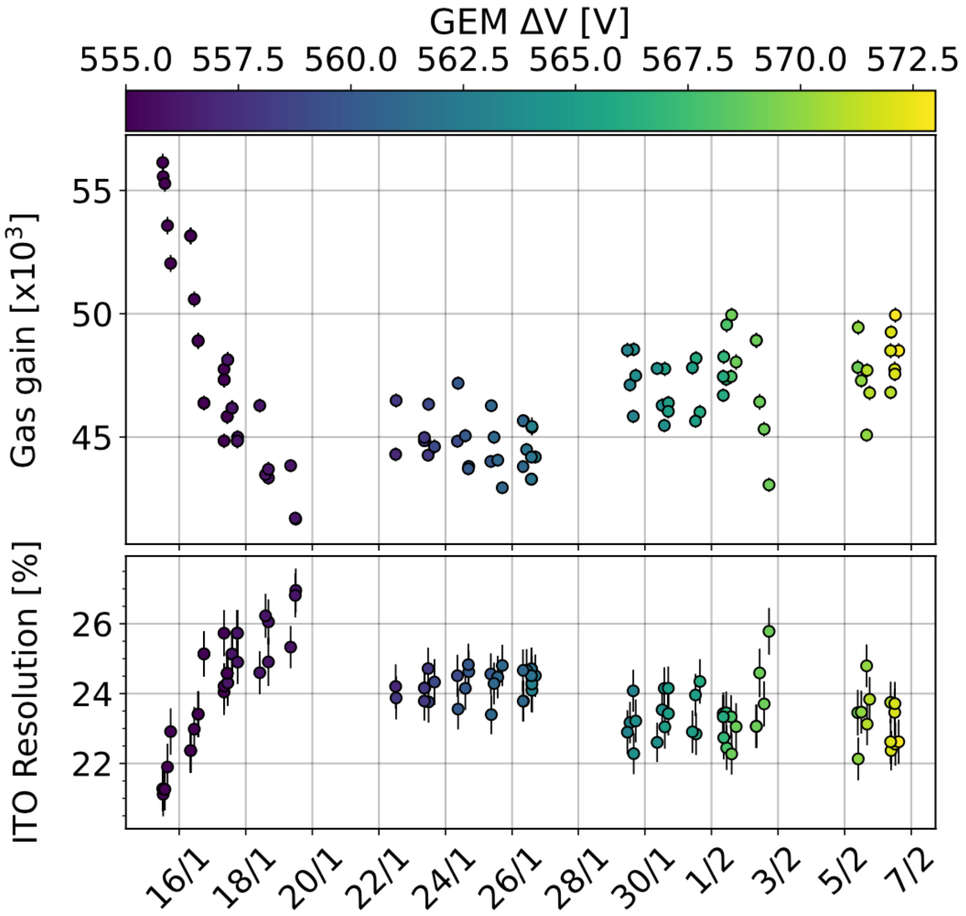

Signal and Backgrounds

- Backgrounds suppressed through energy thresholds and timing resolution
- Main source of background from gammas produced in inelastic scattering with fluorine Compton scattering near track vertex

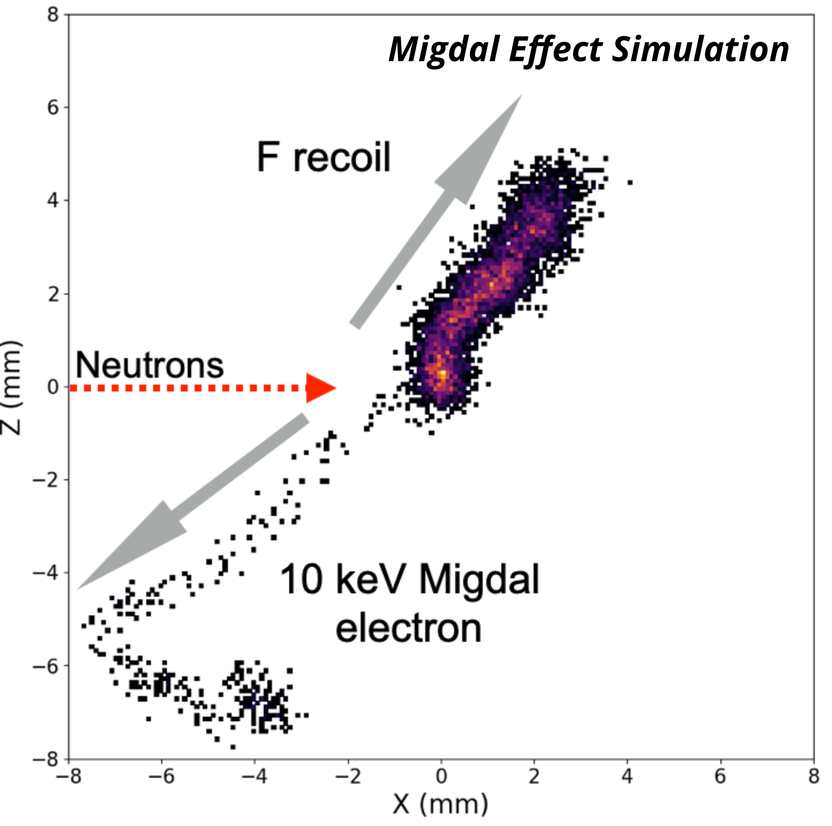

Component	Topology	D-D neutrons >0.5	D-D neutrons 5–15 keV
Recoil-induced δ-rays	Delta electron from NR track origin	≈0	0
Particle-Induced X-ray Emission (PIXE)			
X-ray emission	Photoelectron near NR track origin	1.8	0
Auger electrons	Auger electron from NR track origin	19.6	0
Bremsstrahlung processes[†]			
Quasi-Free Electron Br. (QFEB)	Photoelectron near NR track origin	112	≈0
Secondary Electron Br. (SEB)	Photoelectron near NR track origin	115	≈0
Atomic Br. (AB)	Photoelectron near NR track origin	70	≈0
Nuclear Br. (NB)	Photoelectron near NR track origin	≈0	≈0
Neutron inelastic γ-rays	Compton electron near NR track origin	1.6	0.47
Random track coincidences			
External γ- and X-rays	Photo-/Compton electron near NR track	≈0	≈0
Trace radioisotopes (gas)	Electron from decay near NR track origin	0.2	0.01
Neutron activation (gas)	Electron from decay near NR track origin	0	0
Muon-induced δ-rays	Delta electron near NR track origin	≈0	≈0
Secondary nuclear recoil fork	NR track fork near track origin	–	≈1
Total background	Sum of the above components		1.5
Migdal signal	Migdal electron from NR track origin		32.6

[Astropart. Phys. 151 (2023) 102853]

Signal and Backgrounds

- Backgrounds suppressed through energy thresholds and timing resolution
- Main source of background from gammas produced in inelastic scattering with fluorine Compton scattering near track vertex

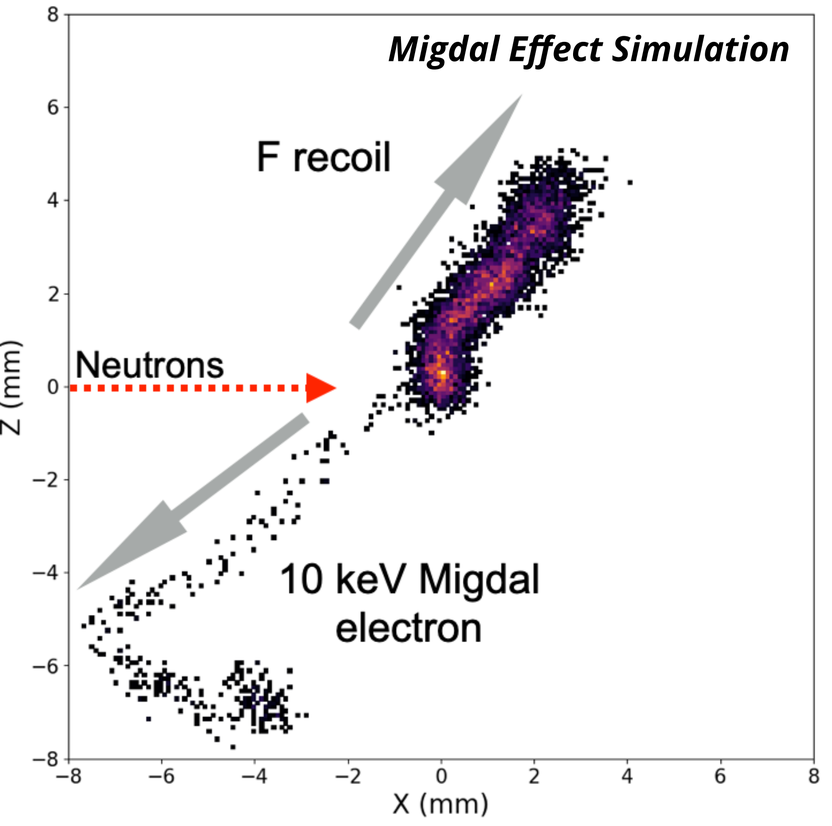

Component	Topology	D-D neutrons >0.5	D-D neutrons 5–15 keV
Recoil-induced δ-rays	Delta electron from NR track origin	≈0	0
Particle-Induced X-ray Emission (PIXE)			
X-ray emission	Photoelectron near NR track origin	1.8	0
Auger electrons	Auger electron from NR track origin	19.6	0
Bremsstrahlung processes[†]			
Quasi-Free Electron Br. (QFEB)	Photoelectron near NR track origin	112	≈0
Secondary Electron Br. (SEB)	Photoelectron near NR track origin	115	≈0
Atomic Br. (AB)	Photoelectron near NR track origin	70	≈0
Nuclear Br. (NB)	Photoelectron near NR track origin	≈0	≈0
Neutron inelastic γ-rays	Compton electron near NR track origin	1.6	0.47
Random track coincidences			
External γ- and X-rays	Photo-/Compton electron near NR track	≈0	≈0
Trace radioisotopes (gas)	Electron from decay near NR track origin	0.2	0.01
Neutron activation (gas)	Electron from decay near NR track origin	0	0
Muon-induced δ-rays	Delta electron near NR track origin	≈0	≈0
Secondary nuclear recoil fork	NR track fork near track origin	–	≈1
Total background	Sum of the above components		1.5
Migdal signal	Migdal electron from NR track origin		32.6

[Astropart. Phys. 151 (2023) 102853]

Signal and Backgrounds

- Backgrounds suppressed through energy thresholds and timing resolution
- Main source of background from gammas produced in inelastic scattering with fluorine Compton scattering near track vertex

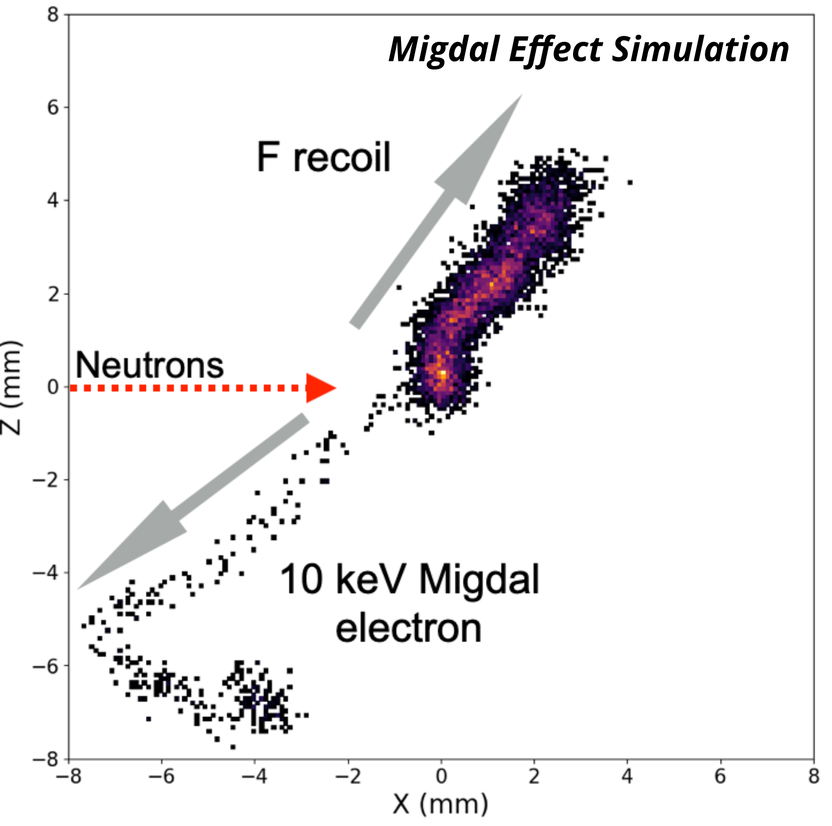

Component	Topology	D-D neutrons >0.5	D-D neutrons 5–15 keV
Recoil-induced δ-rays	Delta electron from NR track origin	≈0	0
Particle-Induced X-ray Emission (PIXE)			
X-ray emission	Photoelectron near NR track origin	1.8	0
Auger electrons	Auger electron from NR track origin	19.6	0
Bremsstrahlung processes†			
Quasi-Free Electron Br. (QFEB)	Photoelectron near NR track origin	112	≈0
Secondary Electron Br. (SEB)	Photoelectron near NR track origin	115	≈0
Atomic Br. (AB)	Photoelectron near NR track origin	70	≈0
Nuclear Br. (NB)	Photoelectron near NR track origin	≈0	≈0
Neutron inelastic γ-rays	Compton electron near NR track origin	1.6	0.47
Random track coincidences			
External γ- and X-rays	Photo-/Compton electron near NR track	≈0	≈0
Trace radioisotopes (gas)	Electron from decay near NR track origin	0.2	0.01
Neutron activation (gas)	Electron from decay near NR track origin	0	0
Muon-induced δ-rays	Delta electron near NR track origin	≈0	≈0
Secondary nuclear recoil fork	NR track fork near track origin	–	≈1
Total background	Sum of the above components		1.5
Migdal signal	Migdal electron from NR track origin		32.6

[Astropart. Phys. 151 (2023) 102853]

Signal and Backgrounds

- Backgrounds suppressed through energy thresholds and timing resolution
- Main source of background from gammas produced in inelastic scattering with fluorine Compton scattering near track vertex

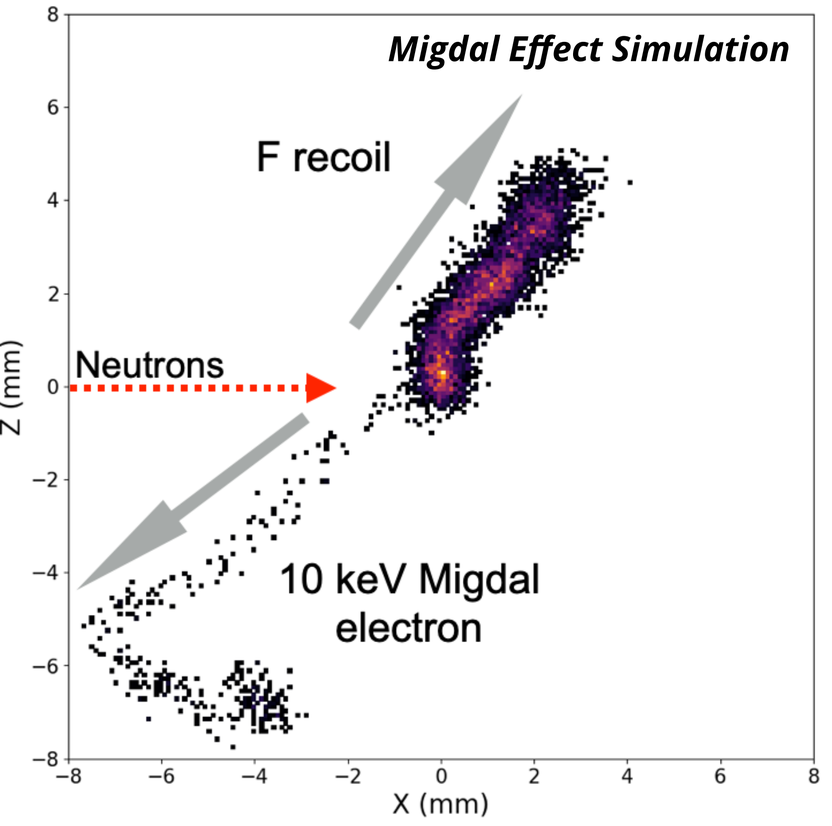

Component	Topology	D-D neutrons >0.5	D-D neutrons 5–15 keV
Recoil-induced δ-rays	Delta electron from NR track origin	≈0	0
Particle-Induced X-ray Emission (PIXE)			
X-ray emission	Photoelectron near NR track origin	1.8	0
Auger electrons	Auger electron from NR track origin	19.6	0
Bremsstrahlung processes†			
Quasi-Free Electron Br. (QFEB)	Photoelectron near NR track origin	112	≈0
Secondary Electron Br. (SEB)	Photoelectron near NR track origin	115	≈0
Atomic Br. (AB)	Photoelectron near NR track origin	70	≈0
Nuclear Br. (NB)	Photoelectron near NR track origin	≈0	≈0
Neutron inelastic γ-rays	Compton electron near NR track origin	1.6	0.47
Random track coincidences			
External γ- and X-rays	Photo-/Compton electron near NR track	≈0	≈0
Trace radioisotopes (gas)	Electron from decay near NR track origin	0.2	0.01
Neutron activation (gas)	Electron from decay near NR track origin	0	0
Muon-induced δ-rays	Delta electron near NR track origin	≈0	≈0
Secondary nuclear recoil fork	NR track fork near track origin	–	≈1
Total background	Sum of the above components		1.5
Migdal signal	Migdal electron from NR track origin		32.6

[Astropart. Phys. 151 (2023) 102853]

YOLOv8 for track identification

Phys.Rev.D 111 (2025) 7

- YOLOv8 is a state-of-the-art object detection algorithm
- Localises and classifies objects within images
- Trained on real data with hand-labelled bounding boxes
  - Search for overlapping electron and nuclear recoil rather than a simulated signal topology
- Runs in real time providing mixed-field particle ID and detector performance feedback

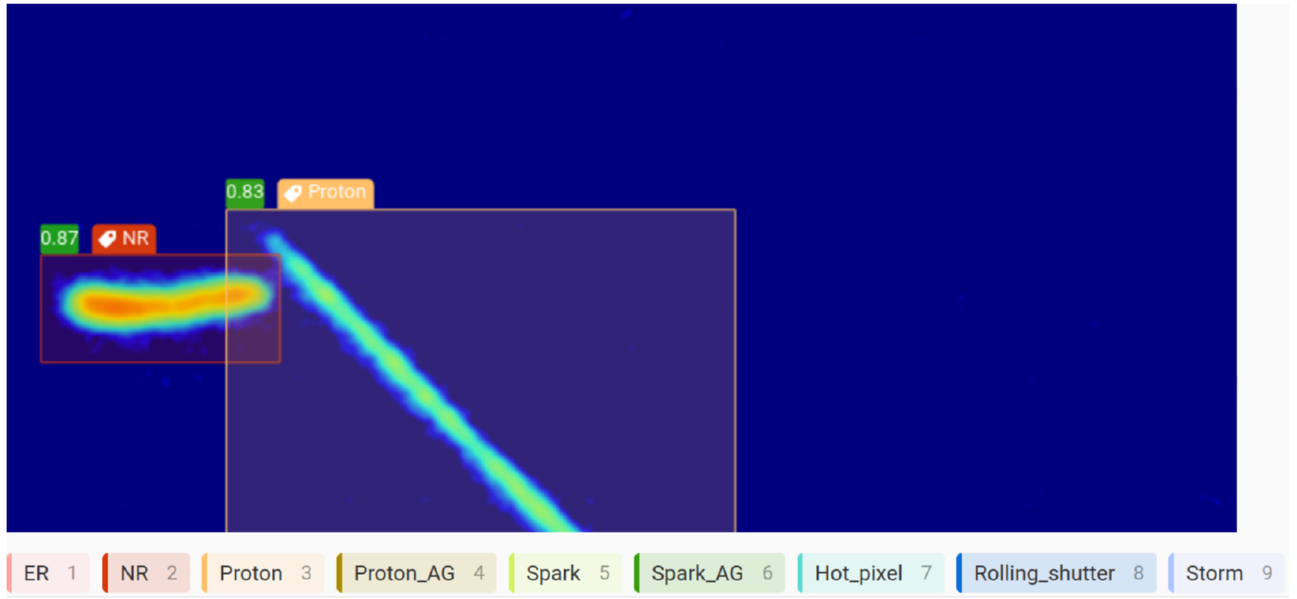

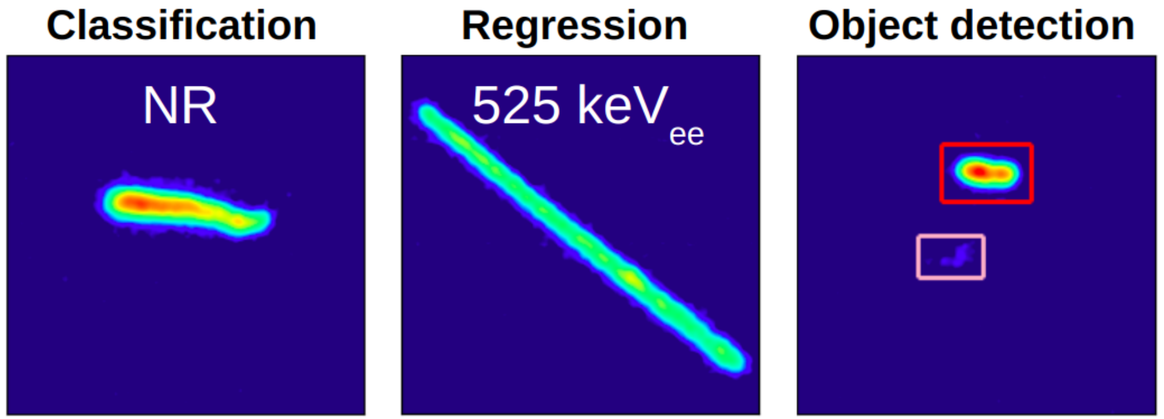

3D Reconstruction

- Tracks in the ITO anode are identified using **DBSCAN**
- Camera and DAQ events synchronised offline using timestamp information from an FPGA counter
- Timing between S1 and S2 in the PMT gives absolute depth

Nucl.Instrum.Meth.A 1069 (2024)

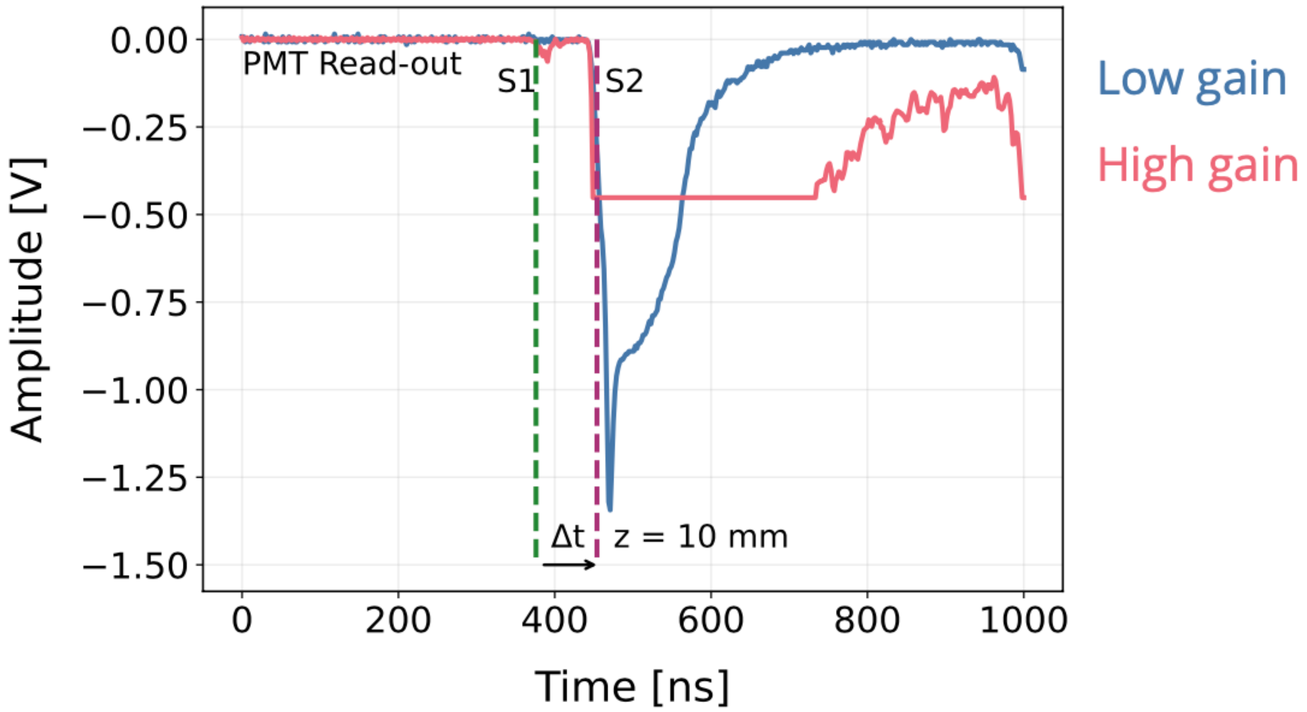

3D Reconstruction: JINST 18 C07013

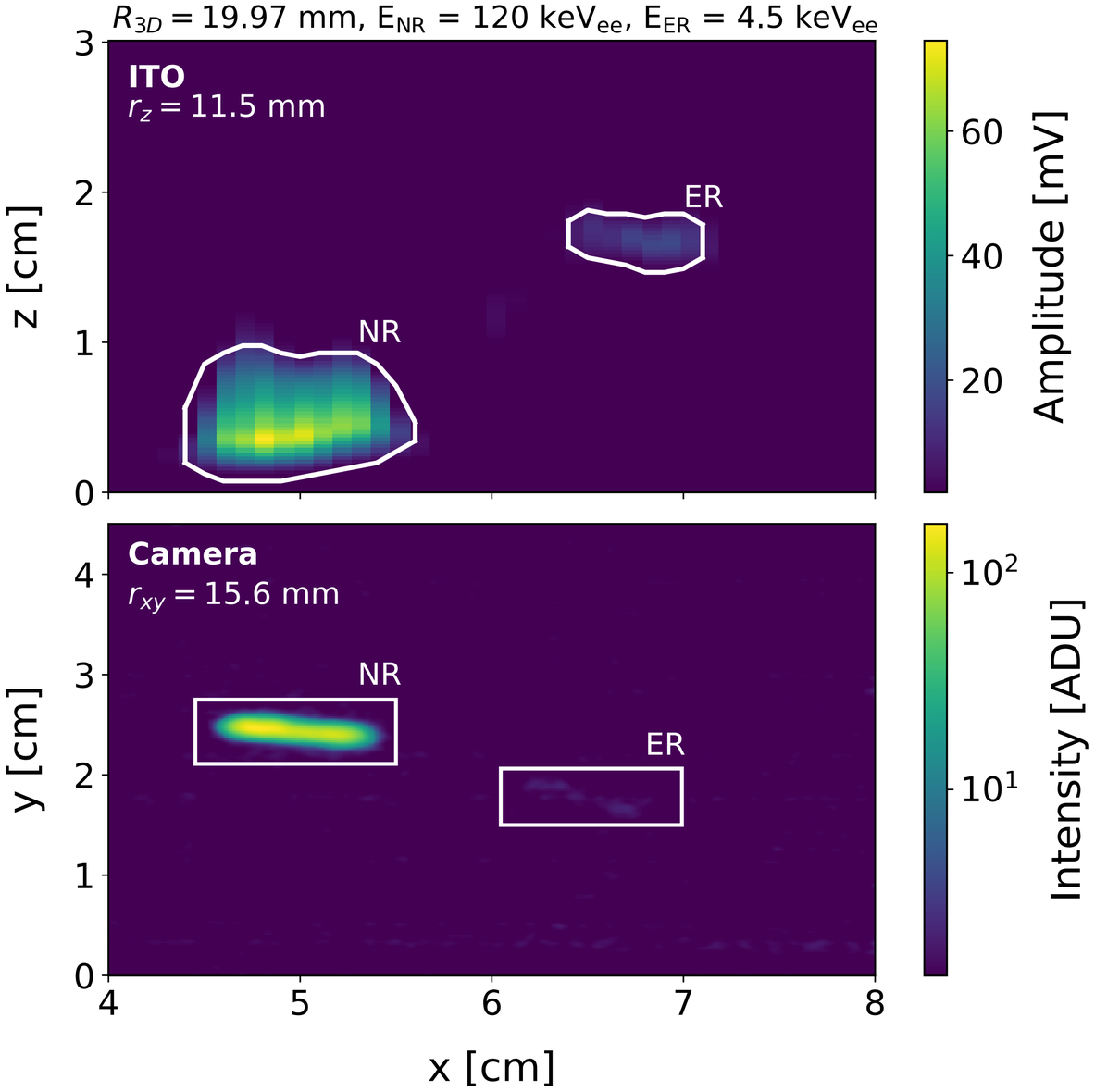

Event Selection

- Nuclear recoil energy in the ITO > 50 keV_{ee}, corresponding to ~150 keV (F)
- Electron energy 3 < E_{ER} < 15 keV in the ITO
- Electron and nuclear recoil both identified in image by YOLO
- Define a control region and a signal region:
  - Signal region: ER-NR separation ≤ 10mm
  - Control region: ER-NR separation 10 - 70 mm

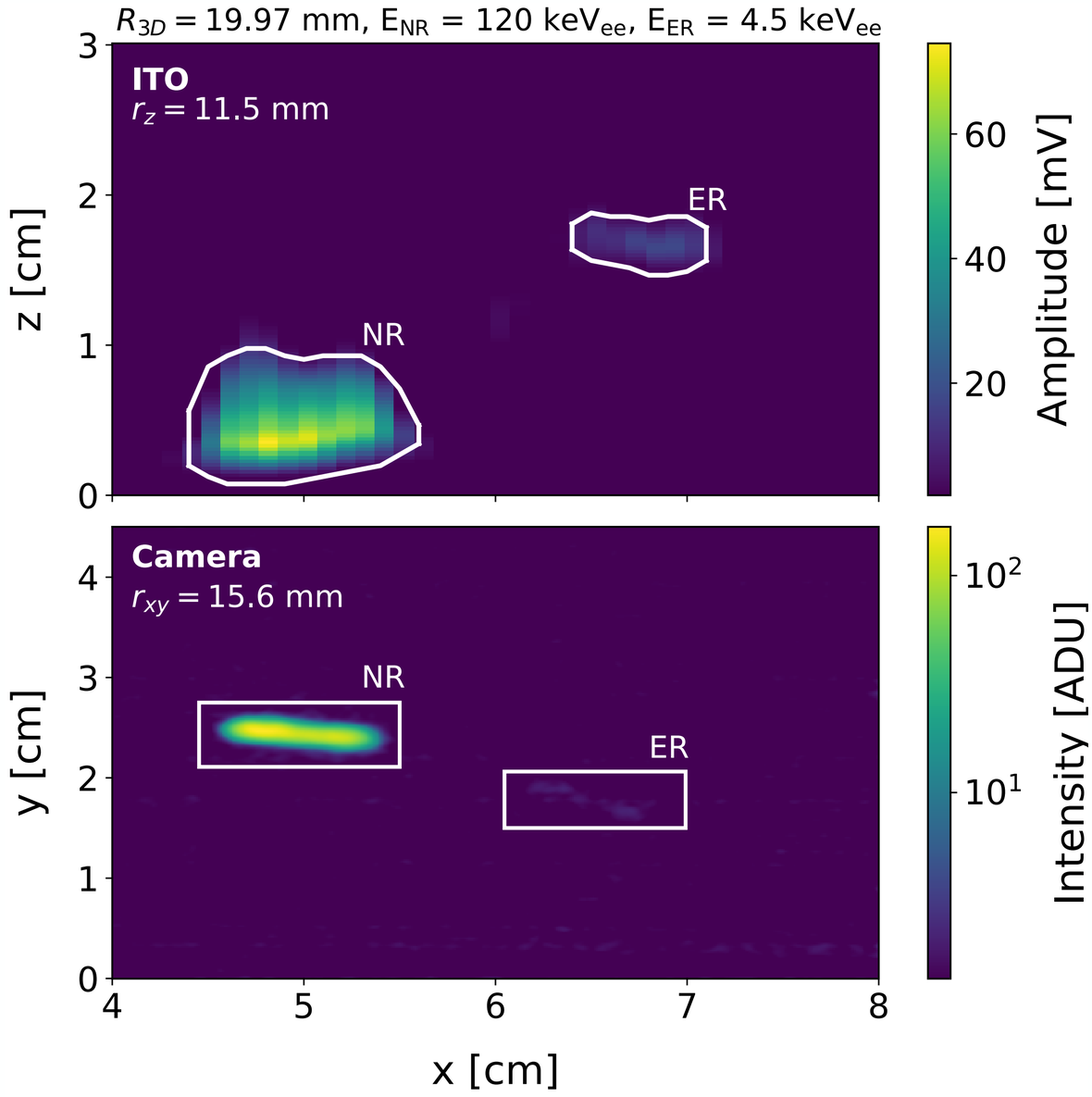

Additional Event Selection Requirements

- After unblinding, two pathological classes of events were observed and the selection criteria were updated to target these classes of events
- Signal efficiency was reevaluated to reflect this and reduced by 1.5%

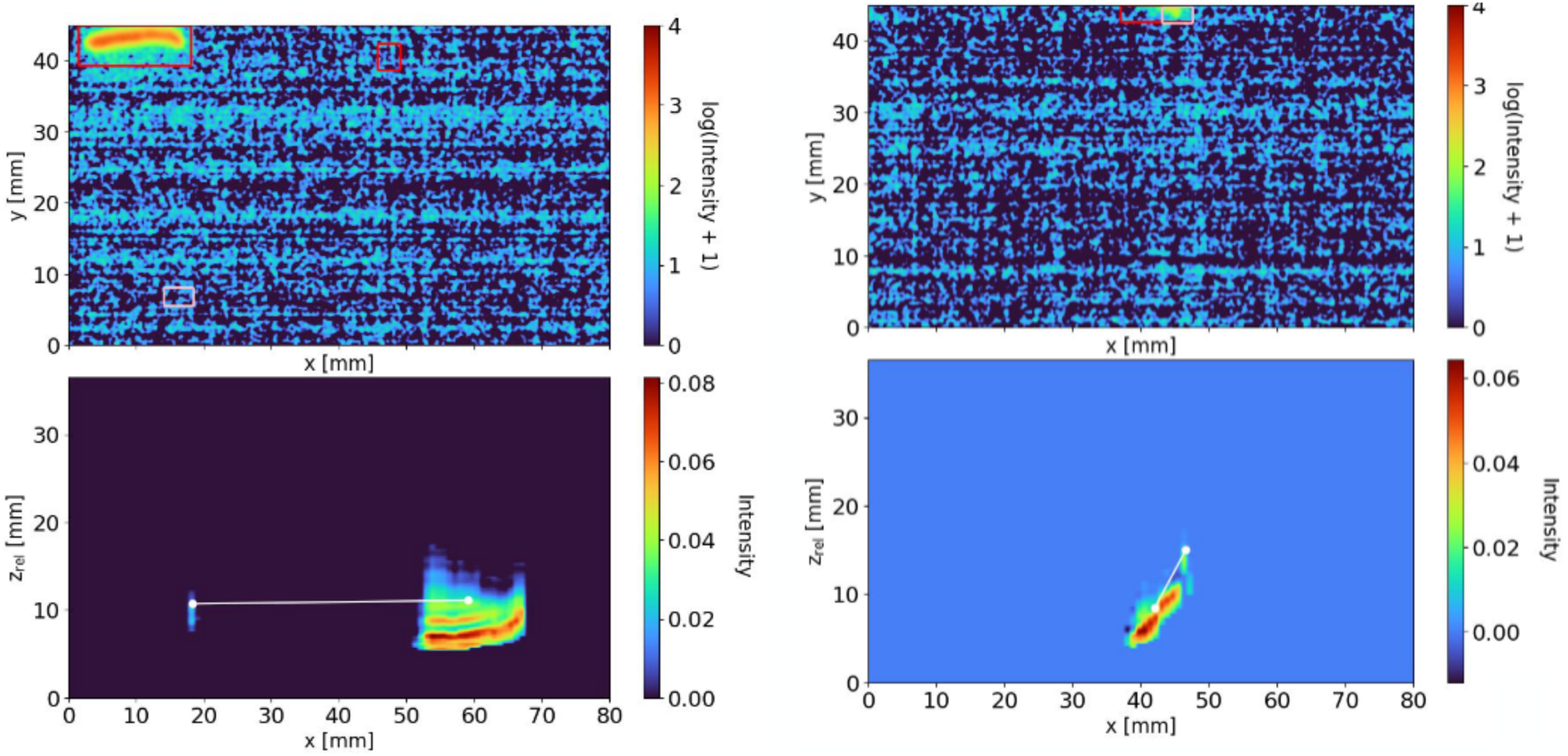

Additional Event Selection Requirements

- Strips are read-out in pairs. When event crosses channel 0 and 59 a wrap around correction applied
- Implementation insufficient in cases where ITO signal oscillated
  - Small probability for additional cluster to be identified in the ITO
  - Requirement added to reject such clusters
- This impacts only events in the control region

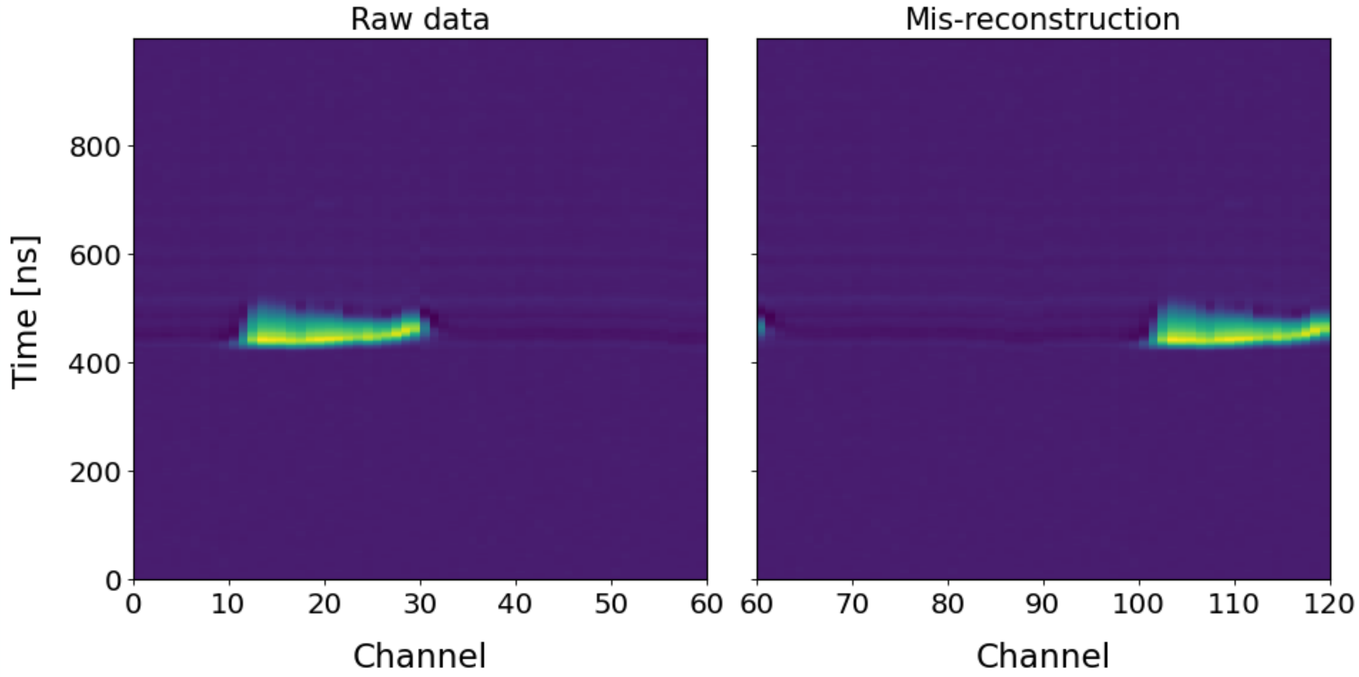

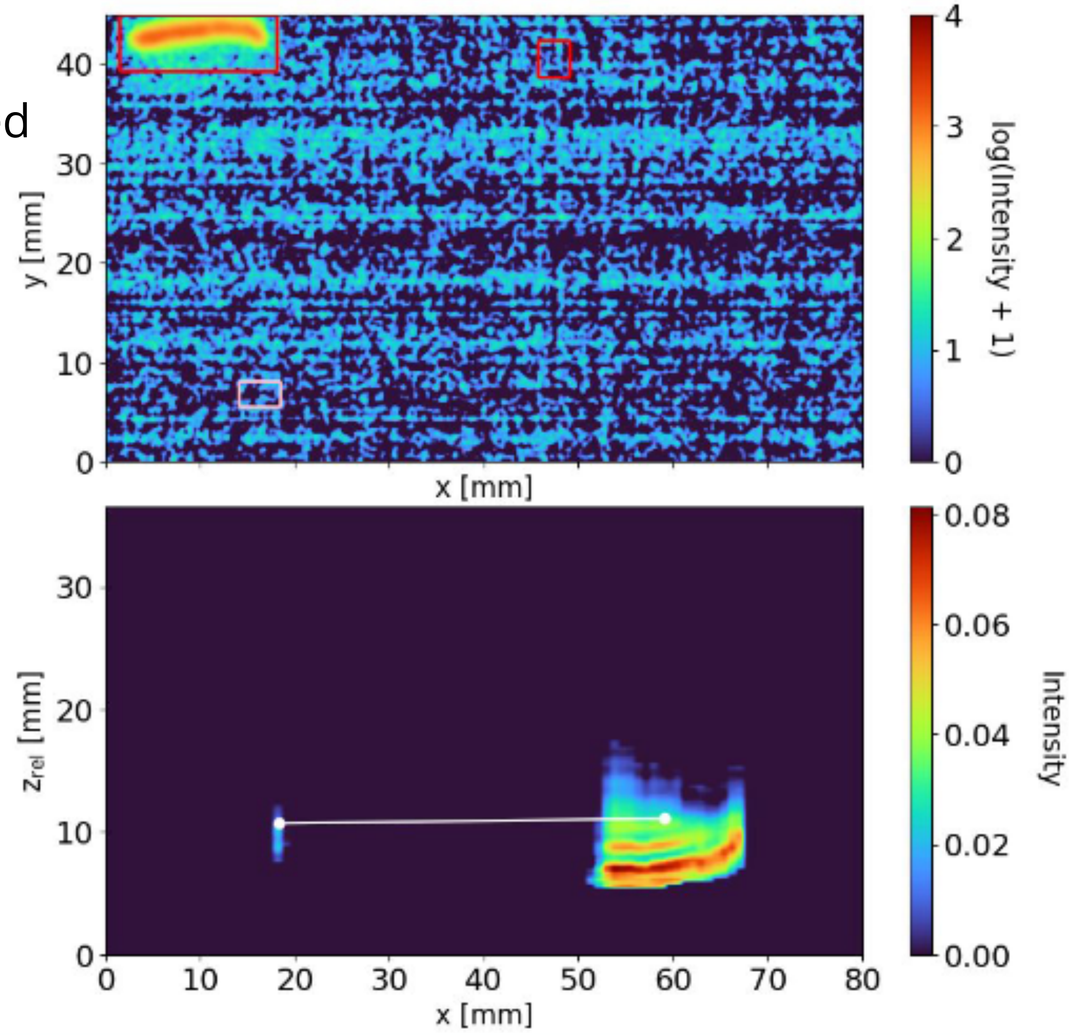

Additional Event Selection Requirements

- After unblinding issue with DAQ identified
  - Affects <1% of events where single strip misaligned in time
  - Relevant for 4 specific read-out channels (out of 60)
- Additional requirement applied to reject events with non-physical dE/dx profile

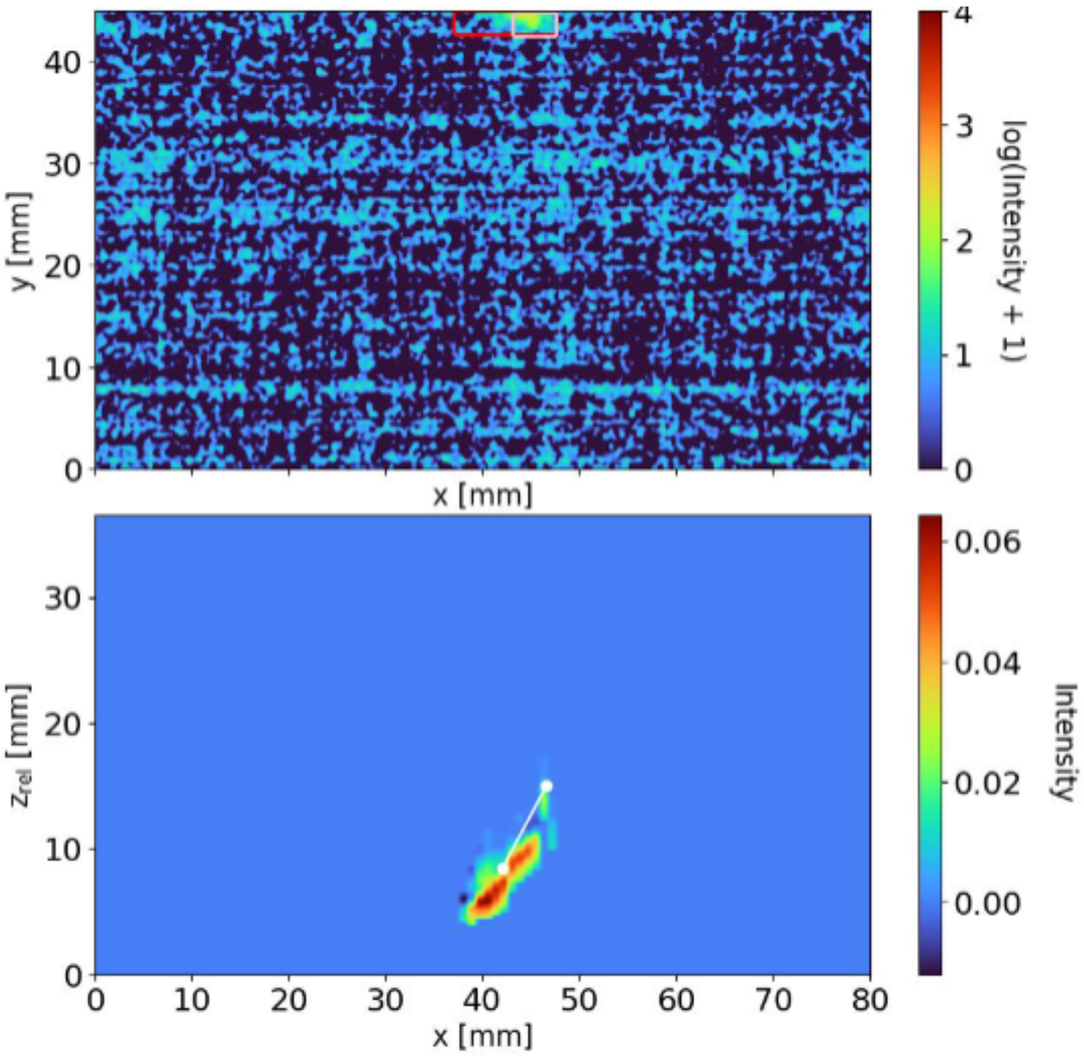

Background: Random Track Coincidences

- Estimate random coincidences from spatially coinciding out-of-time events
- For each NR:
  - Look for ERs 3-8 ms following NR
  - Split remaining time into 250 ns windows and count any electrons that would be spatially coincident
- Probability of random coincidence per NR = Number of spatial coincidences / Number of trials
- Random coincidence probability per NR is **$(1.8 \pm 0.1) \times 10^{-8}$**
- Negligible background

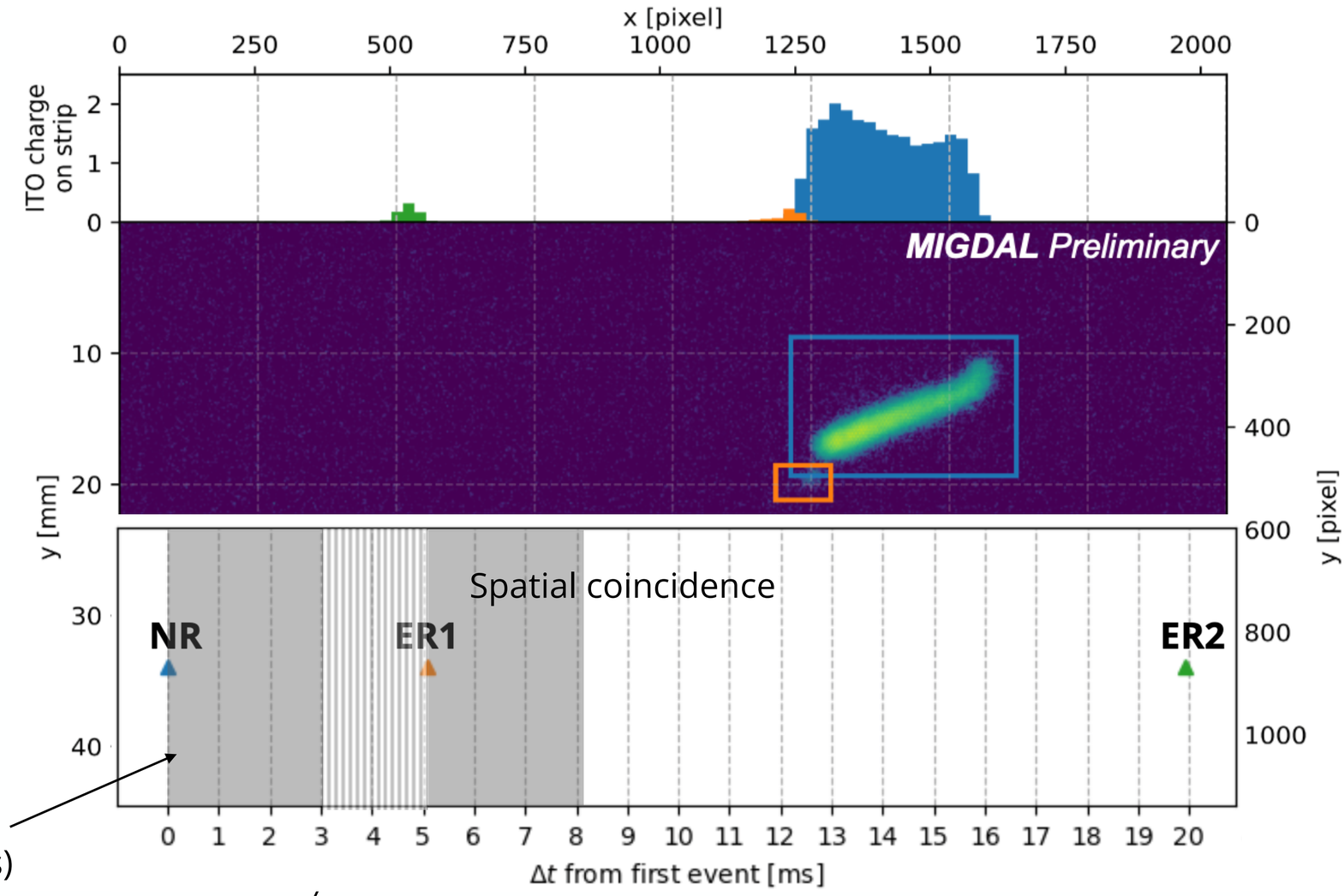

Background: Secondary Nuclear Recoils

- 7% of NRs will have secondary that is:
  - < 1mm from vertex
  - Reconstructed energy 5-15 keV_{ee}
- By requiring a track length > 3 mm expect 1 in 10^6 will mimic signal
- As the clustering is sensitive to dE/dx, expect < 0.1 events in our dataset - assume to be negligible

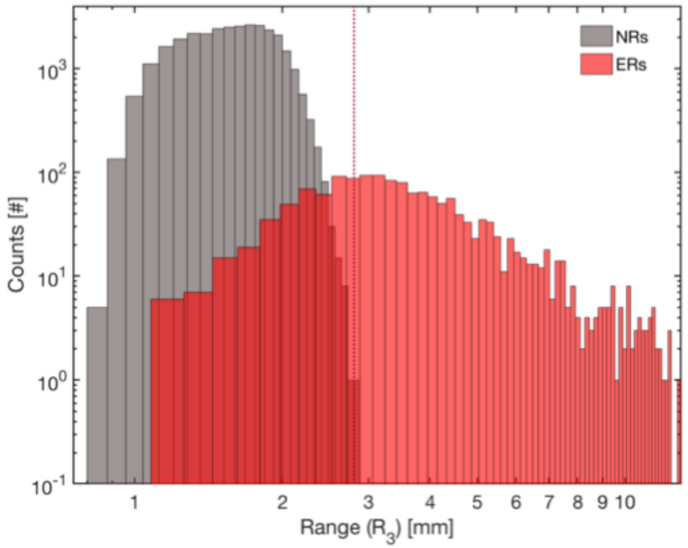

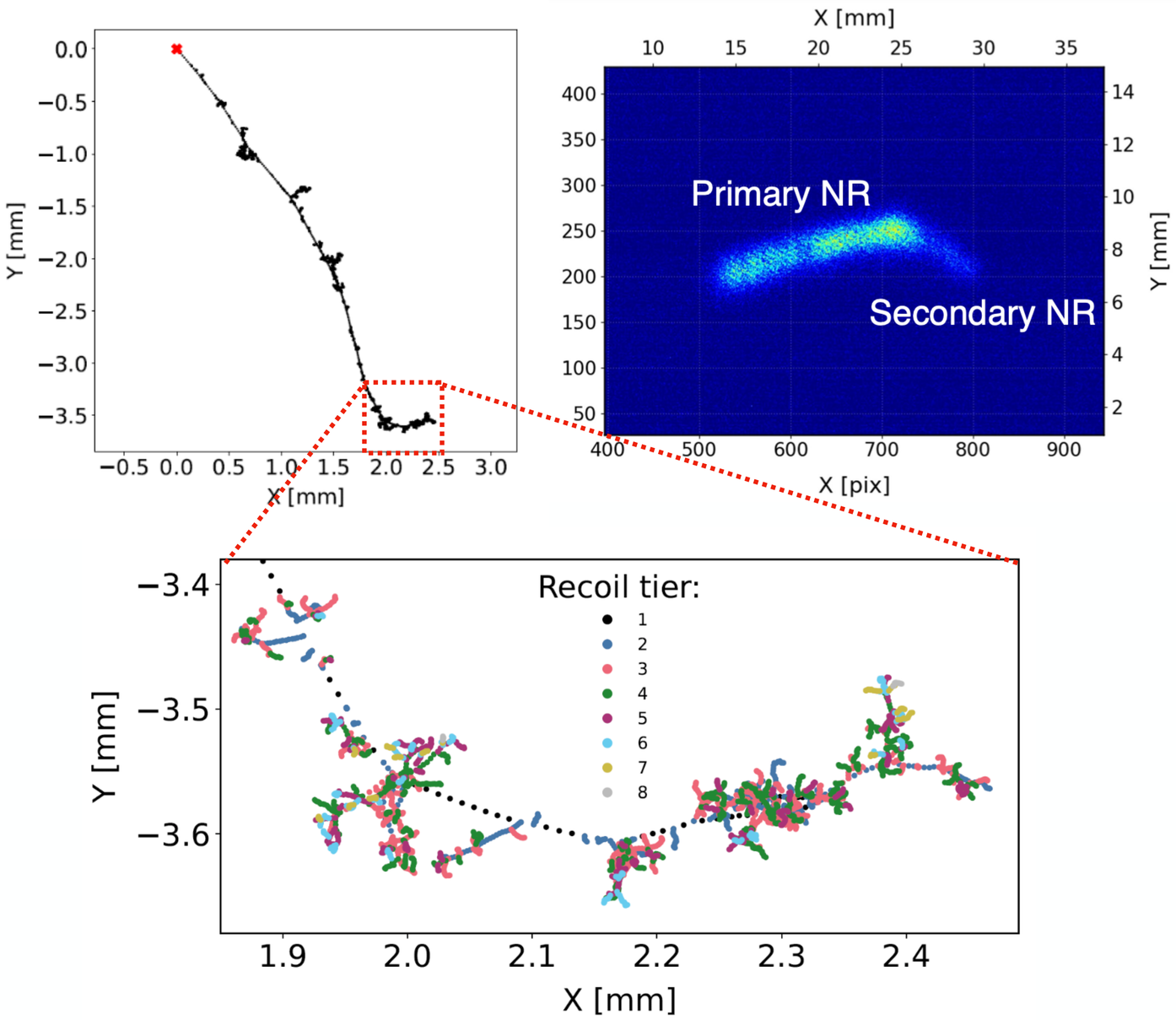

Background: Fluorine Inelastic Scattering

- Inelastic scattering prediction from Geant4 simulations of neutron interactions
- Validate the rate with control region
- Observe 3 events
  - Expected from simulation 5.7 ± 0.6 events
- Gives an expectation of 0.45 ± 0.05 events in the signal region

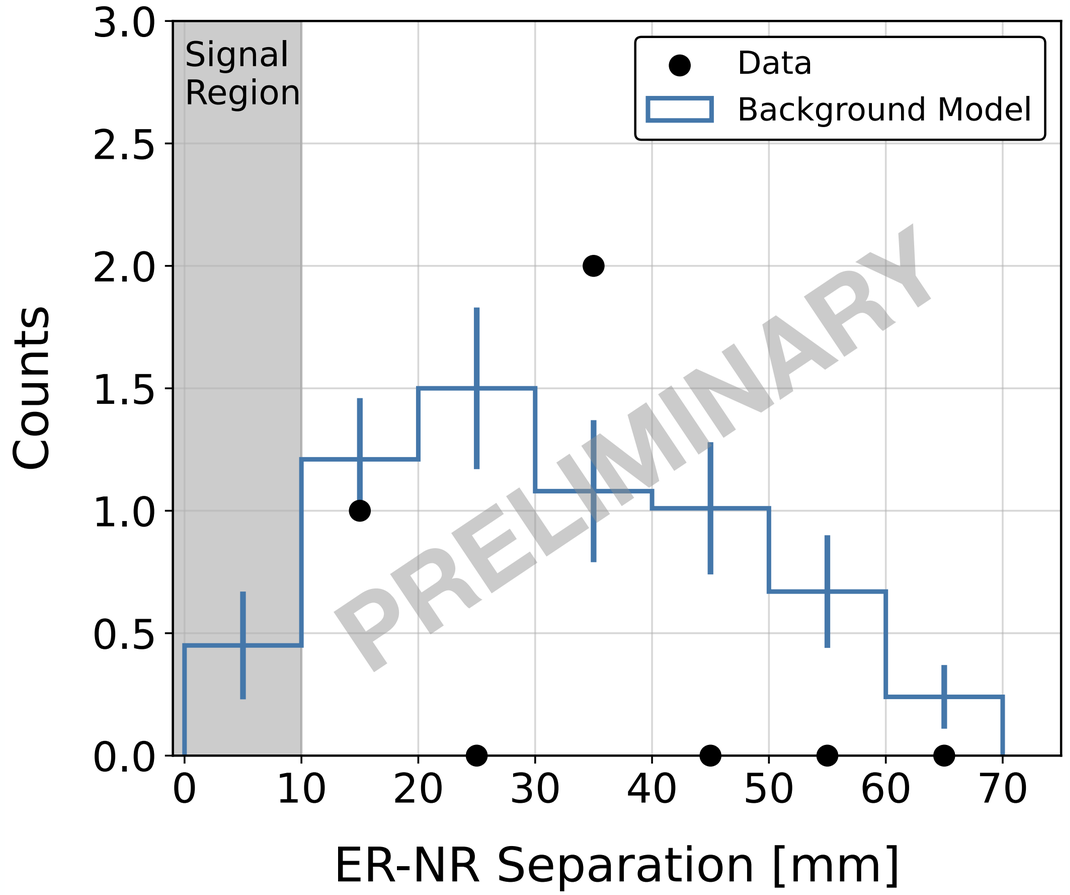

Hybrid Signal Simulations

- Migdal events are simulated by stitching nuclear recoils from data with simulated electrons
- Vertex is estimated in nuclear recoils using the Bragg intensity curve along the ridge of the track for *(x, y)*
- Use absolute depth and track extent to reconstruct z vertex

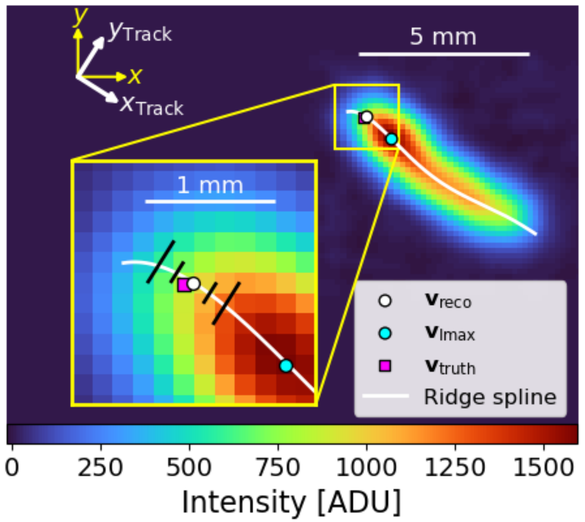

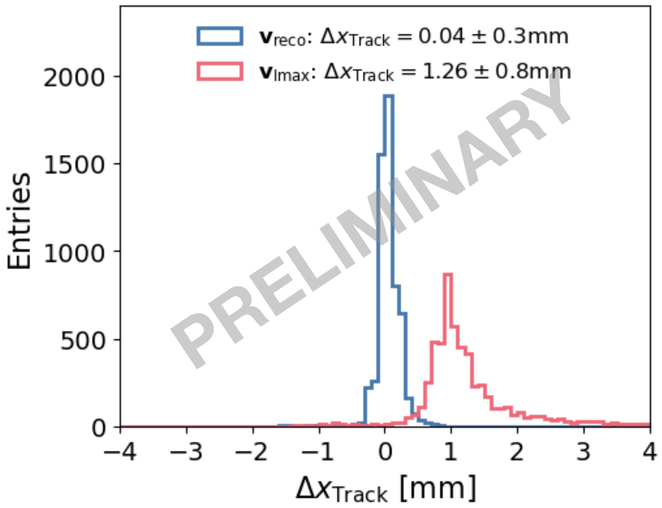

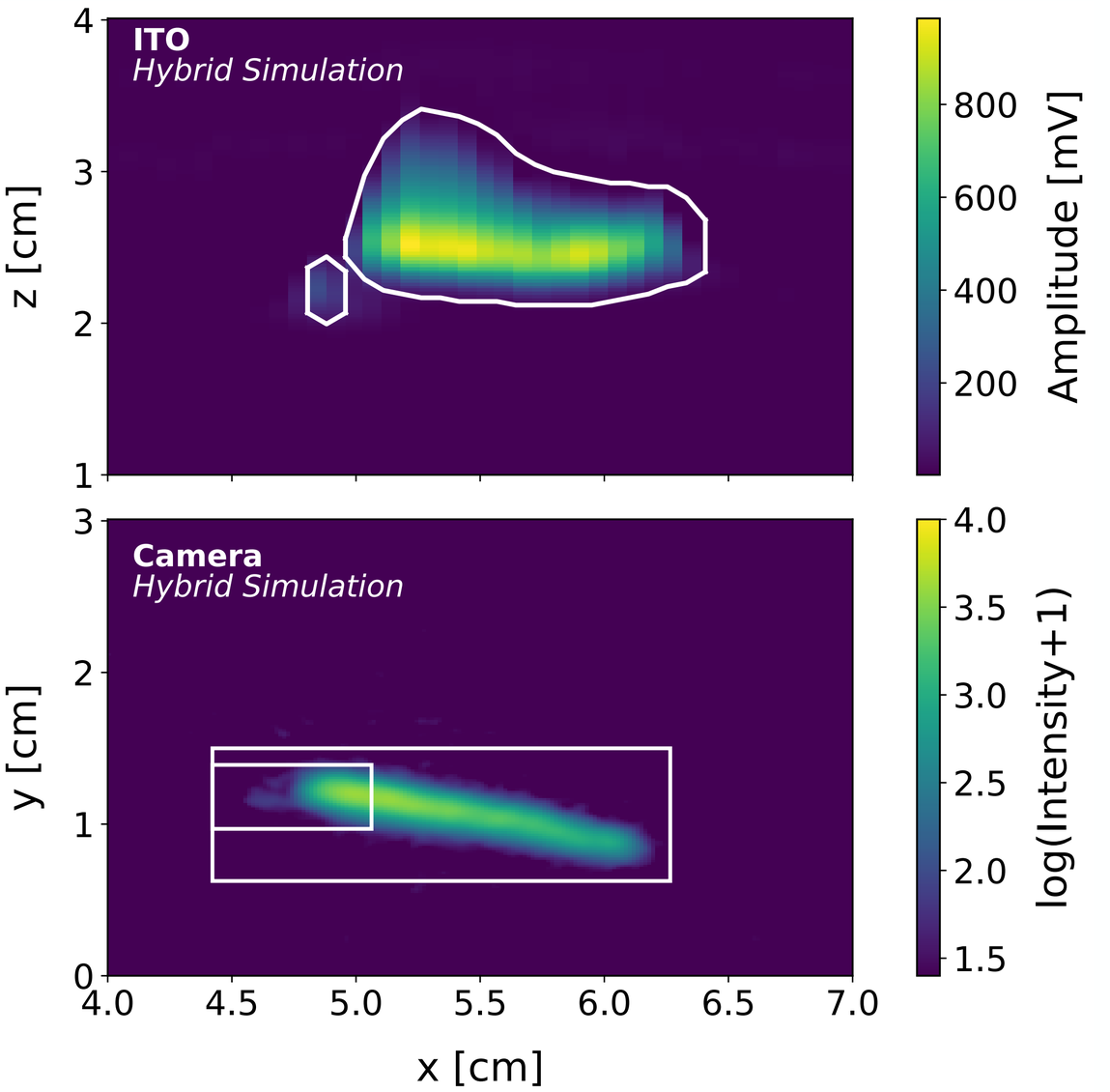

Efficiency

- Efficiencies are estimated by passing hybrid events through analysis chain
- Dominant source of systematic uncertainty comes from uncertainty in vertex position of nuclear recoil
- Estimate systematic uncertainty by shifting vertex in hybrids by the uncertainty in the *(x, y)* position and the expected diffusion length in *z*
- Overall efficiency is:

$$\epsilon = 14.9 \pm (1.0)_{stat.} \pm \binom{+0.1}{-0.9}_{xy,syst} \pm \binom{+1.9}{-0.4}_{z,syst}$$

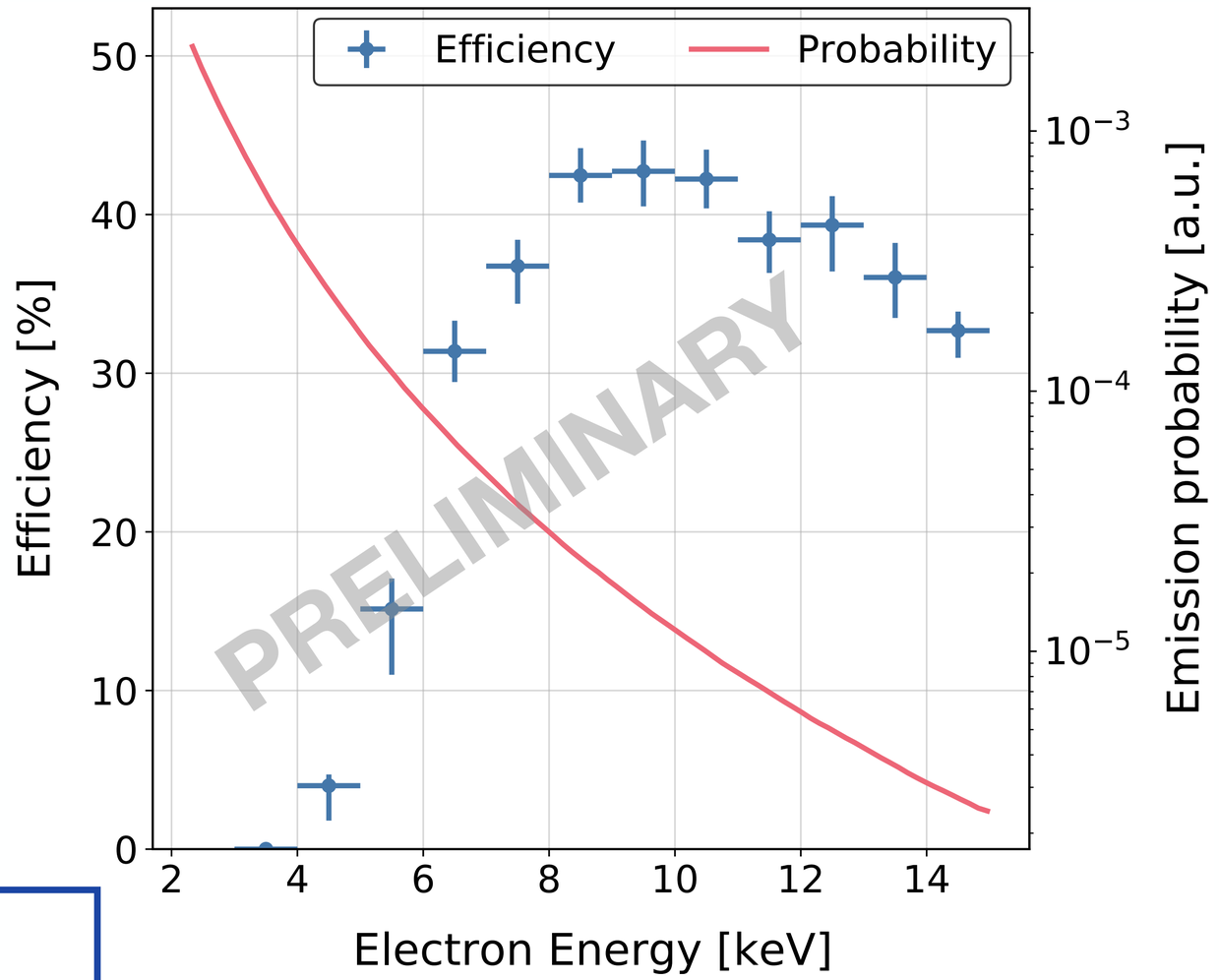

Results

- 0 events observed in signal region
  - Expected 0.45 ± 0.05 events from background
- Observed (Expected) 90% CL upper limit in multiples of theory cross section = 0.45 (0.65)

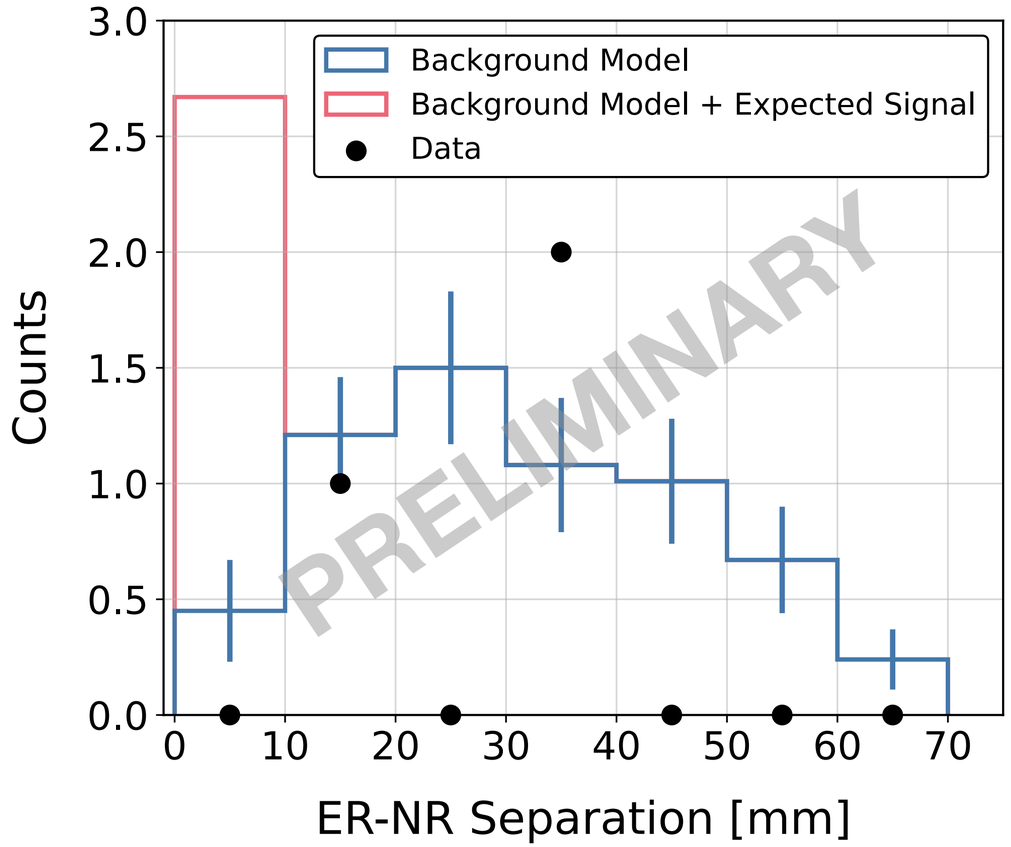

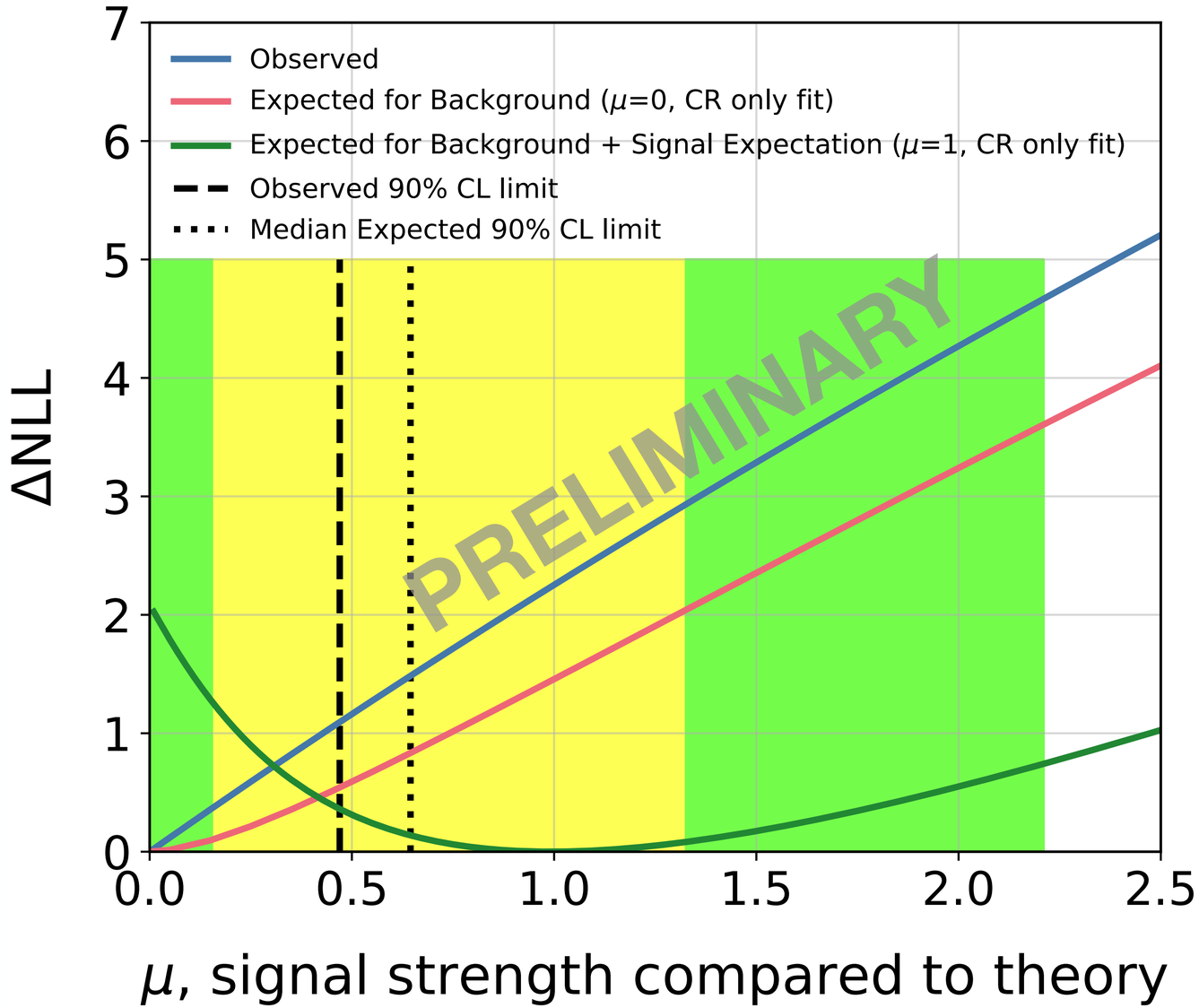

Summary

- The MIGDAL experiment aims to characterise the Migdal Effect in a range of species
- Performed the first search for the Migdal Effect in nuclear scattering of carbon and fluorine
- Observe 0 events in signal region
- We set a 90% CL limit of 0.45 times the theory cross section
- More science data planned this year with improved beam characteristics

Publications:

Overlap-aware segmentation for topological reconstruction of obscured objects
Preprint: 2510.06194 (2025)

Transforming a rare event search into a not-so-rare event search in real-time with deep learning-based object detection
Phys.Rev.D 111 (2025) 7, 072004

Commissioning of the MIGDAL detector with fast neutrons at NILE/ISIS
Nucl.Instrum.Meth.A 1069 (2024) 169971

3D track reconstruction of low-energy electrons in the MIGDAL low pressure optical time projection chamber
JINST 18 (2023) 07, C07013

The MIGDAL experiment: Measuring a rare atomic process to aid the search for dark matter
Astropart.Phys. 151 (2023) 102853

Backup

Nuclear Recoil Rate

- Collimator was designed for a D-D generator with an 8mm target spot size
- Generator actually has a 25mm target spot size
- Decrease in nuclear recoil rate by a factor of 4 compared to experiment design specifications
- Optimising collimator for next science run which will increase nuclear recoil rate

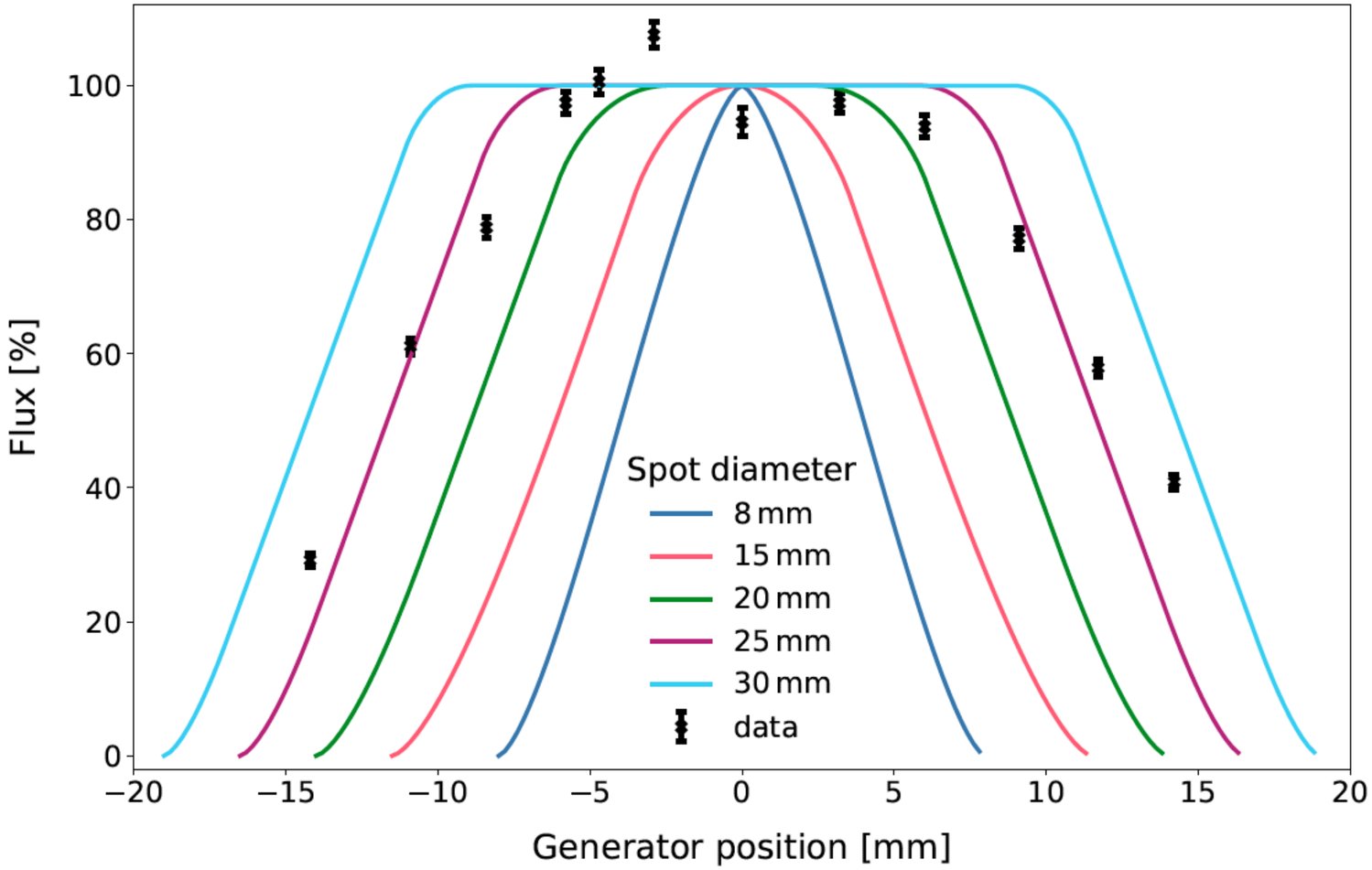

Simulation Framework

Particle interactions
Geant4

Track generation
Degrad
SRIM/TRIM

Electric fields
Gmsh/Elmer
ANSYS
COMSOL

Electron transport properties
Magboltz

Avalanche & signals
Garfield++

Camera read-out

ITO read-out

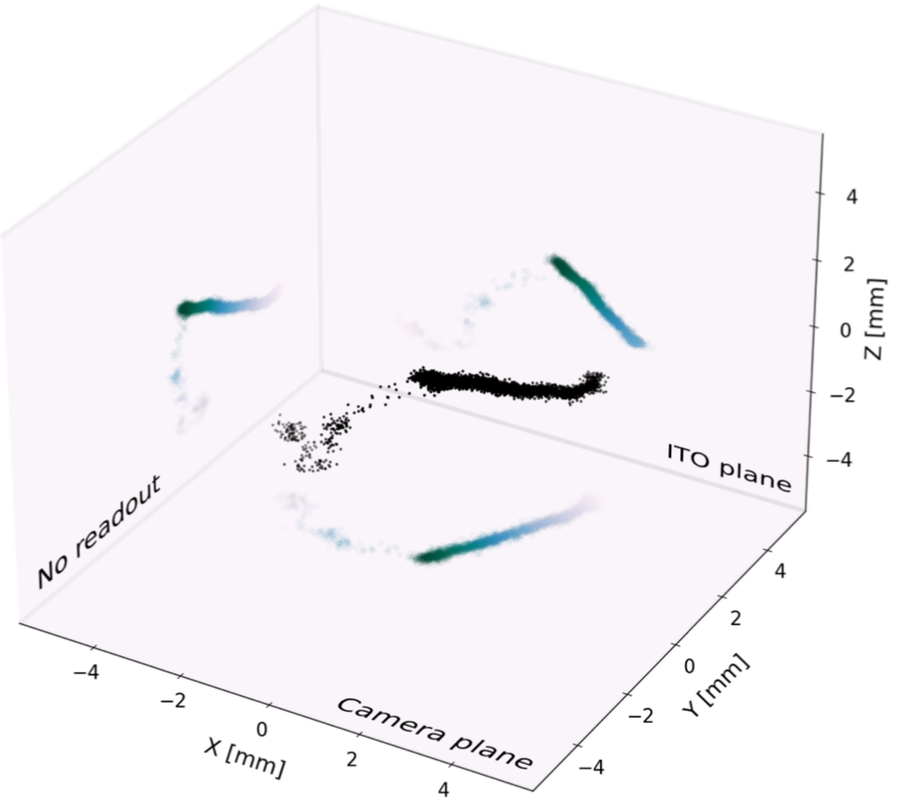

Simulating Electrons

- Ionisation of electron tracks from DEGRAD
- Plots show ^{55}Fe X-ray interaction producing Auger and photoelectron

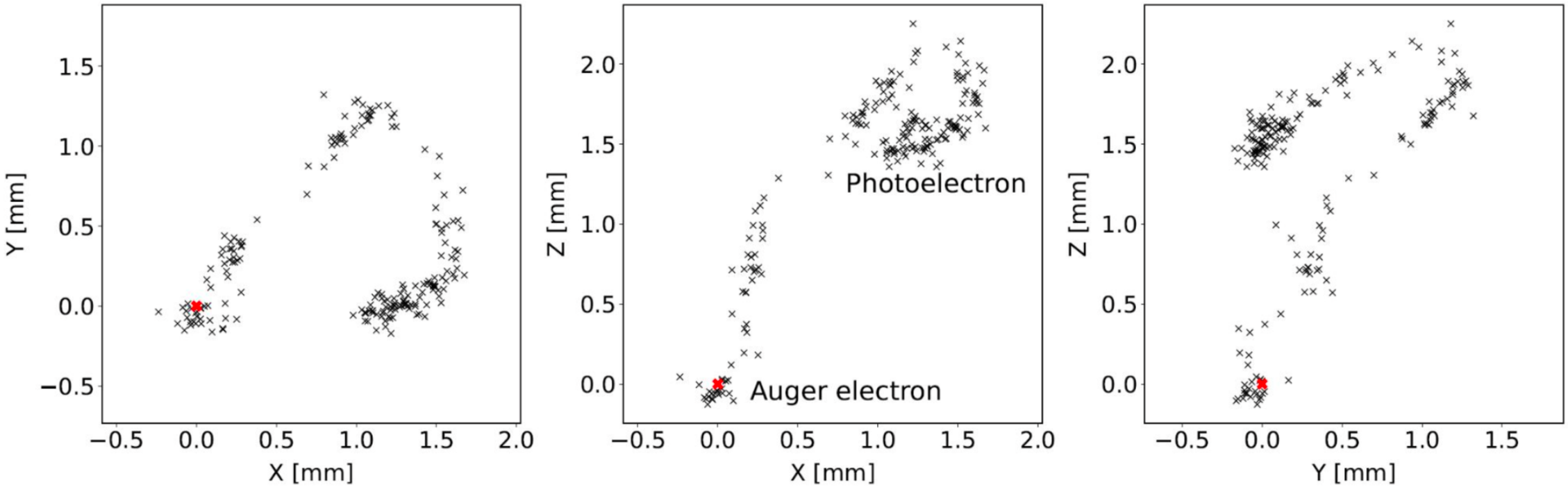

Simulating Nuclear Recoils

- Nuclear recoil tracks and atomic recoil cascades from TRIM with bespoke code for cascades
- Ionisation from Poisson distribution of energy losses

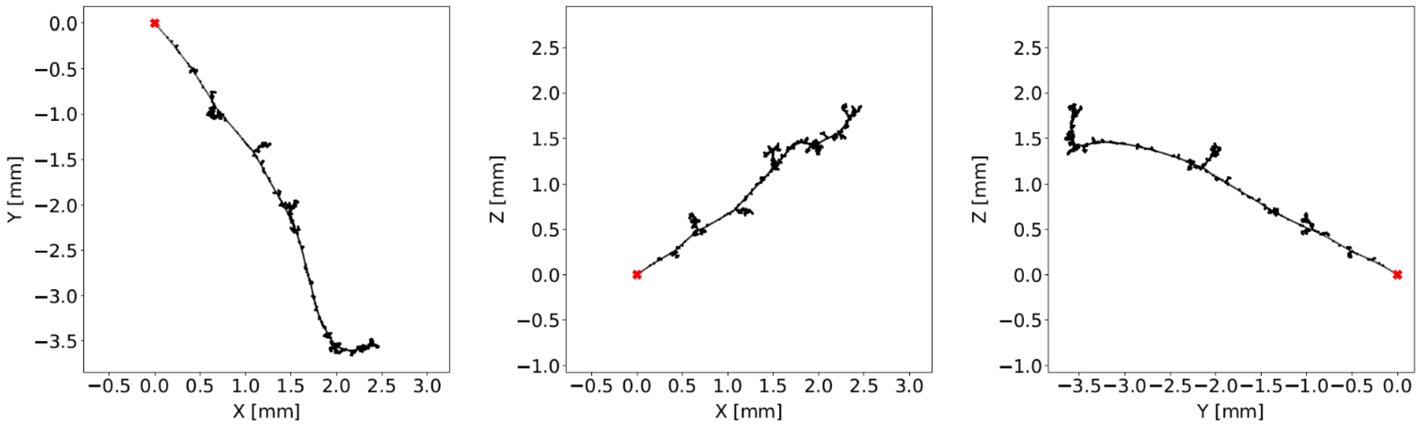

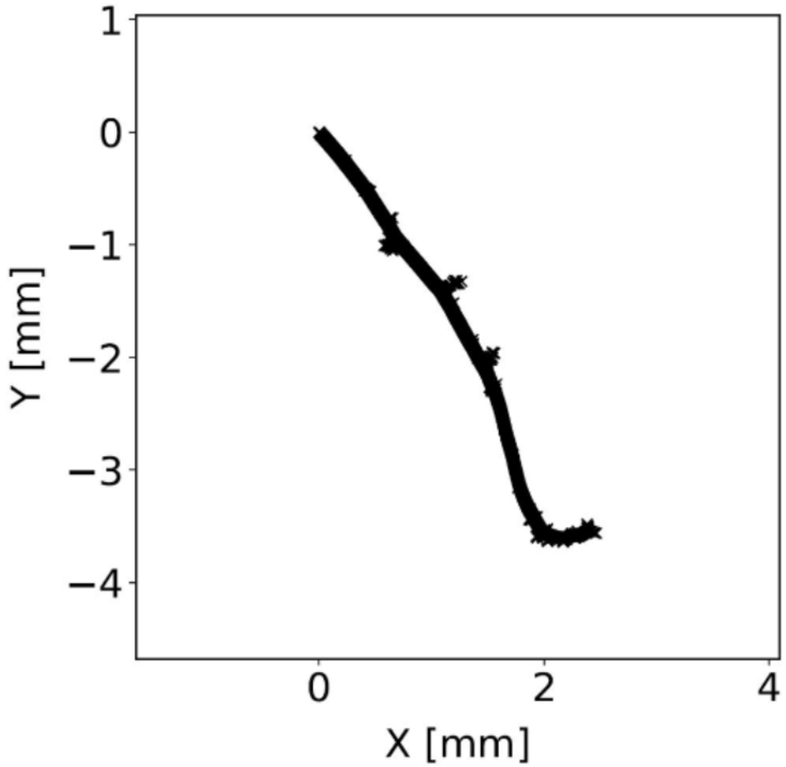

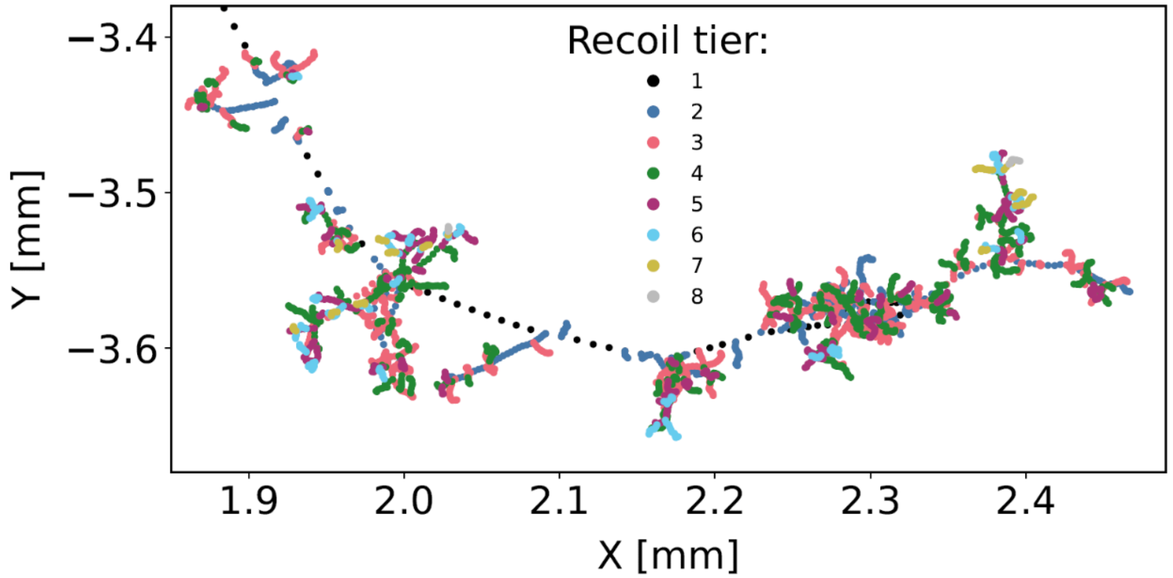

qCMOS Camera

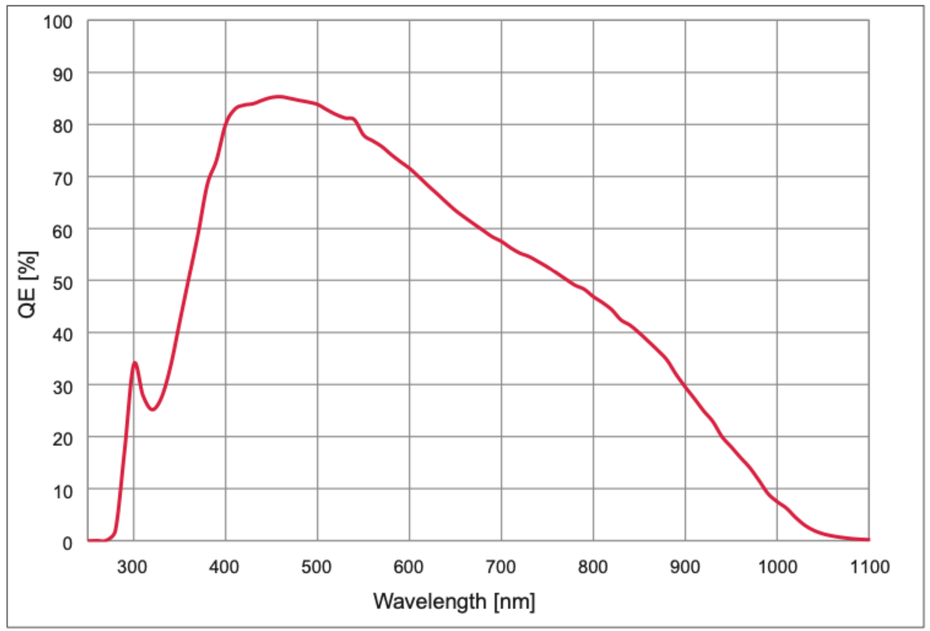

Hamamatsu Orca Quest

- Orca quest low noise CMOS camera
- Continuous 120 fps read-out with rolling shutter
- Synchronise offline using FPGA recorded timestamp information
- 39 μm pixel size (2x2 binning)
- EHD-25985 f/0.85 lens
- 0.43 electron RMS noise

Vignetting Corrections

- Vignetting correction applied to account for decrease in intensity at edges of frame

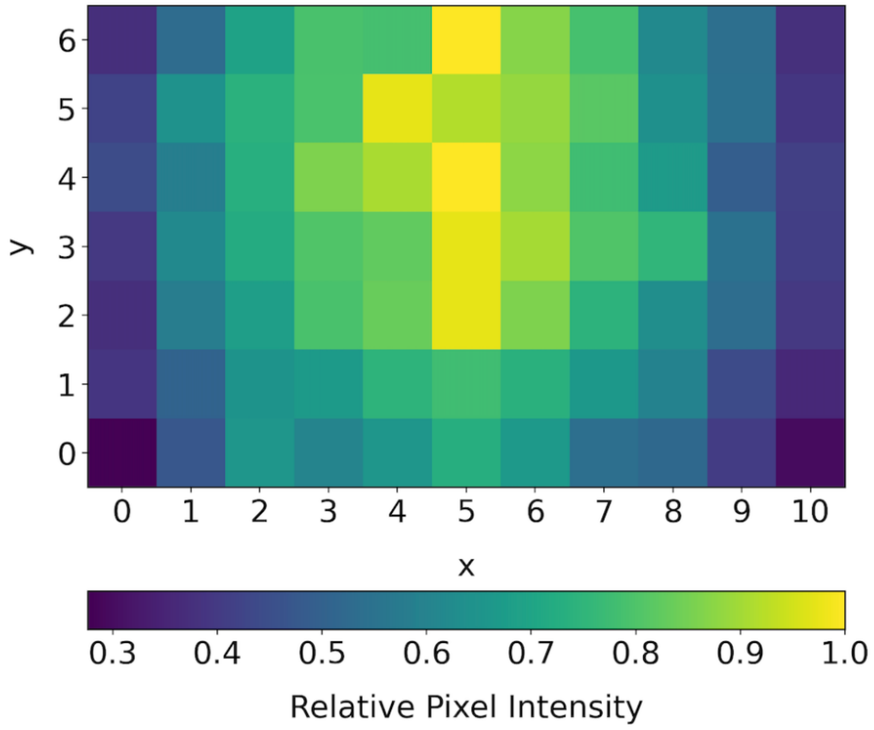

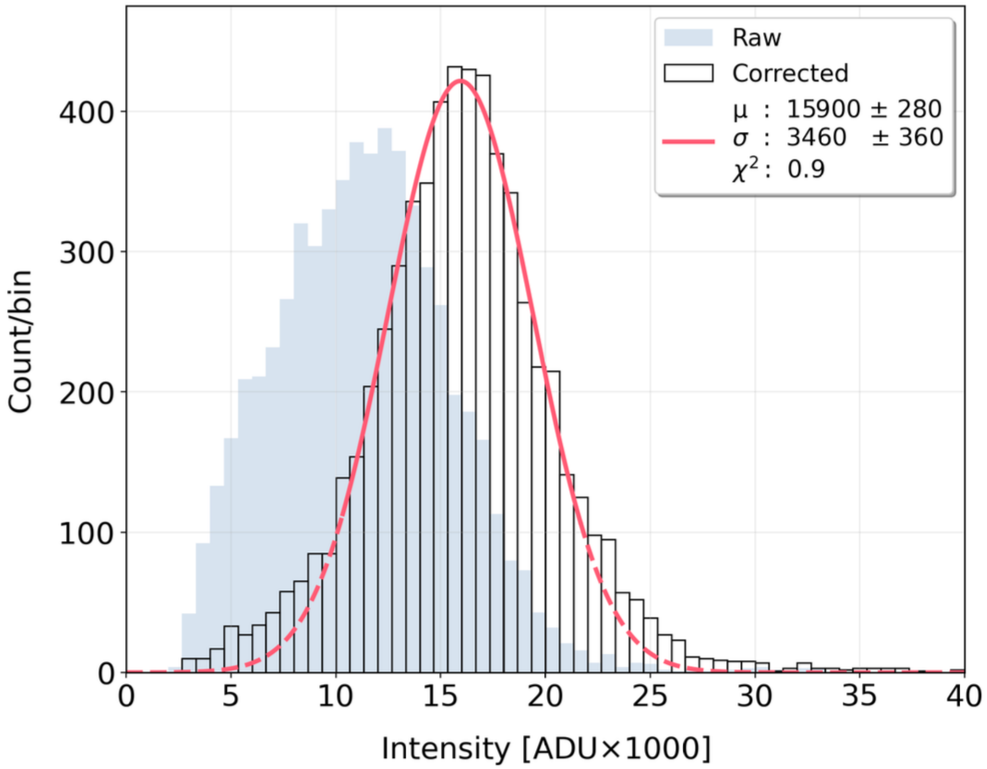

Electron Transport Properties

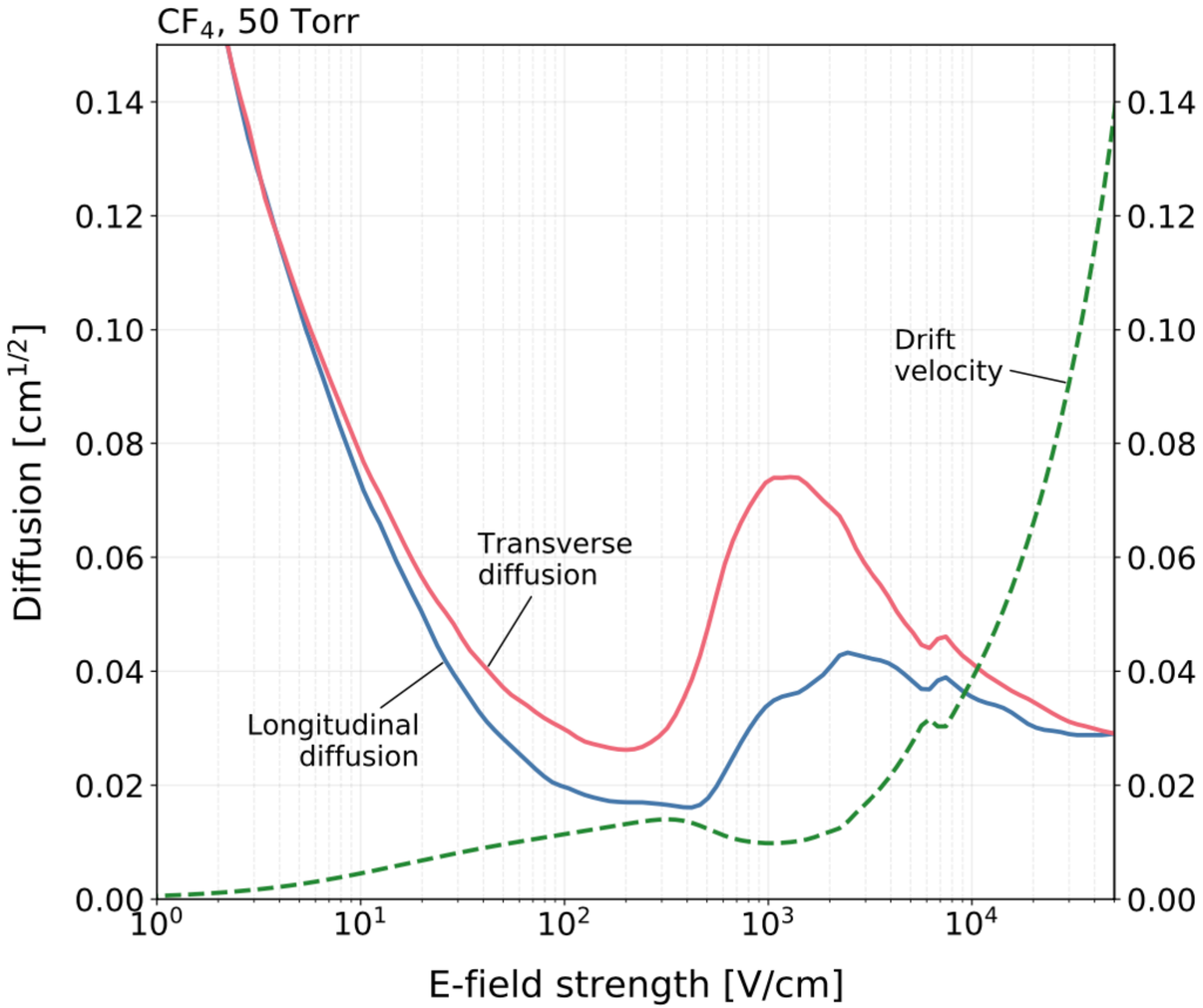

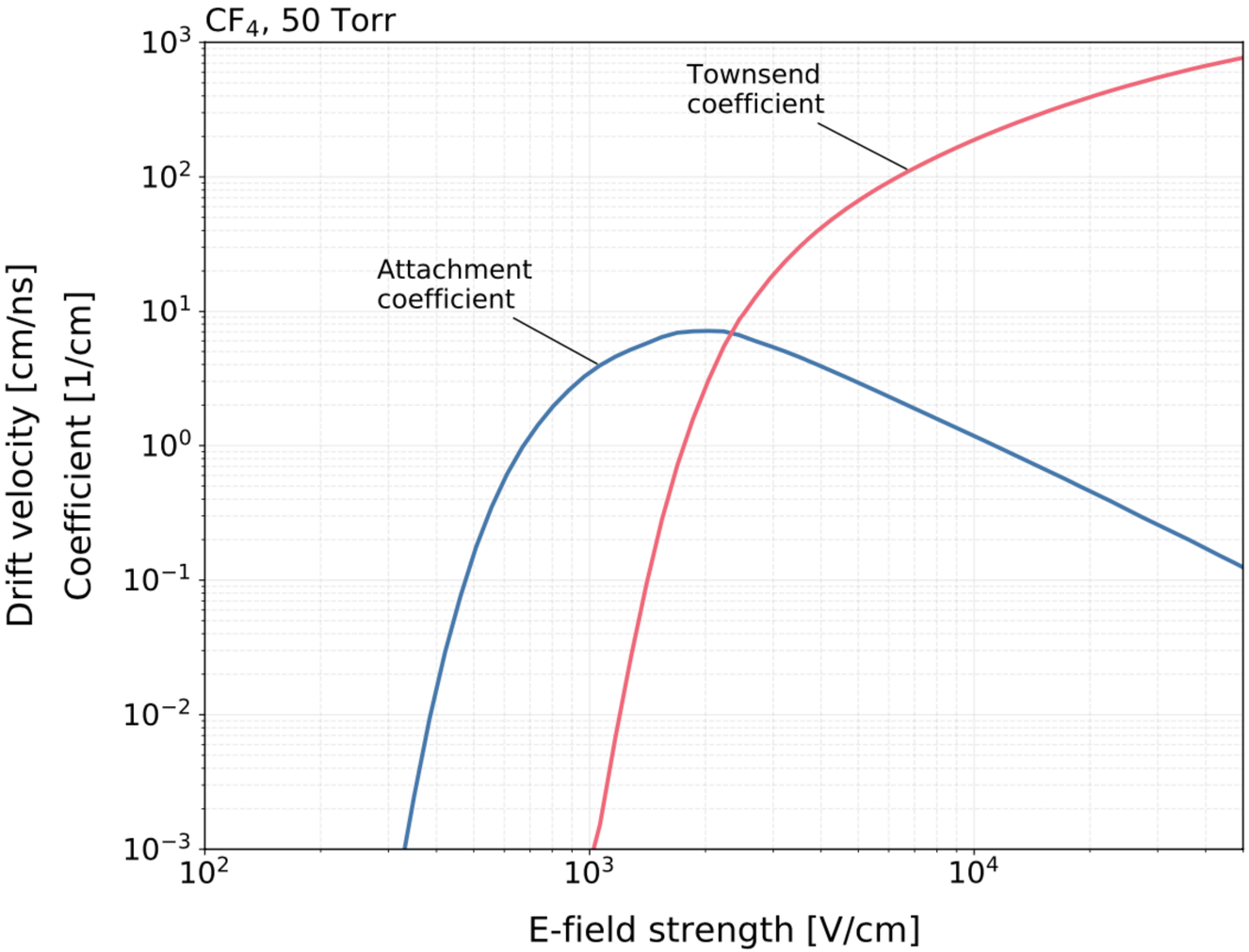

Energy Losses

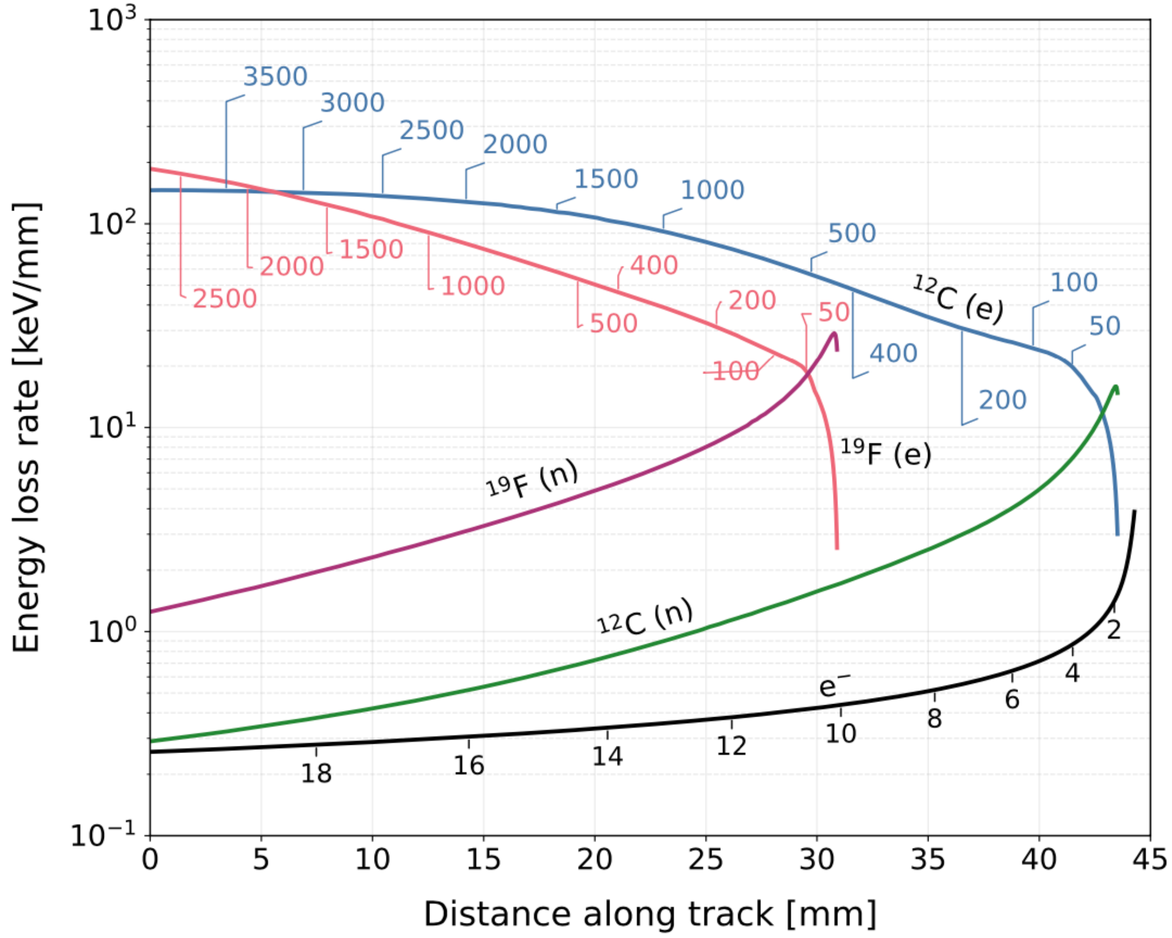

Event Displays

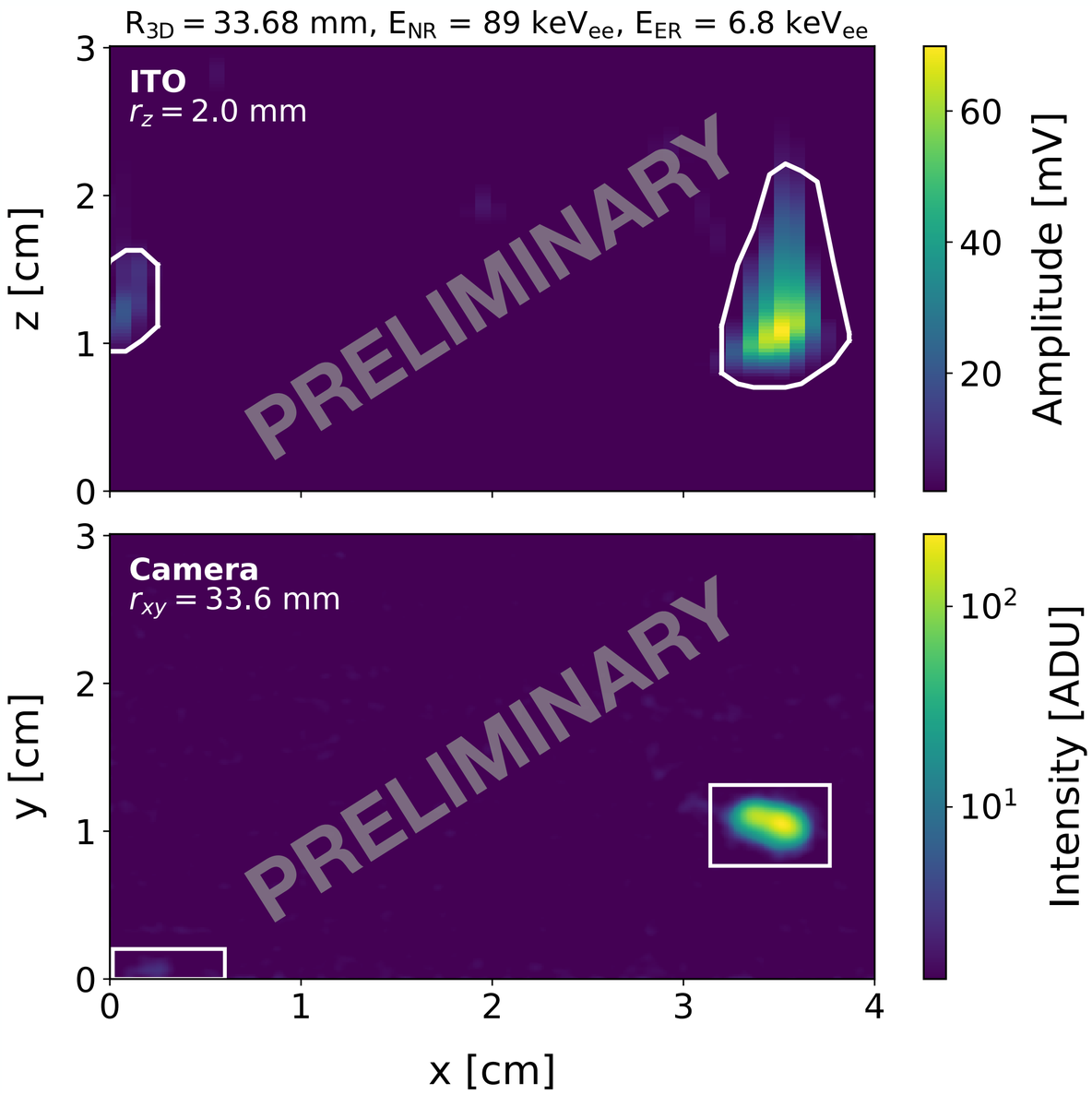

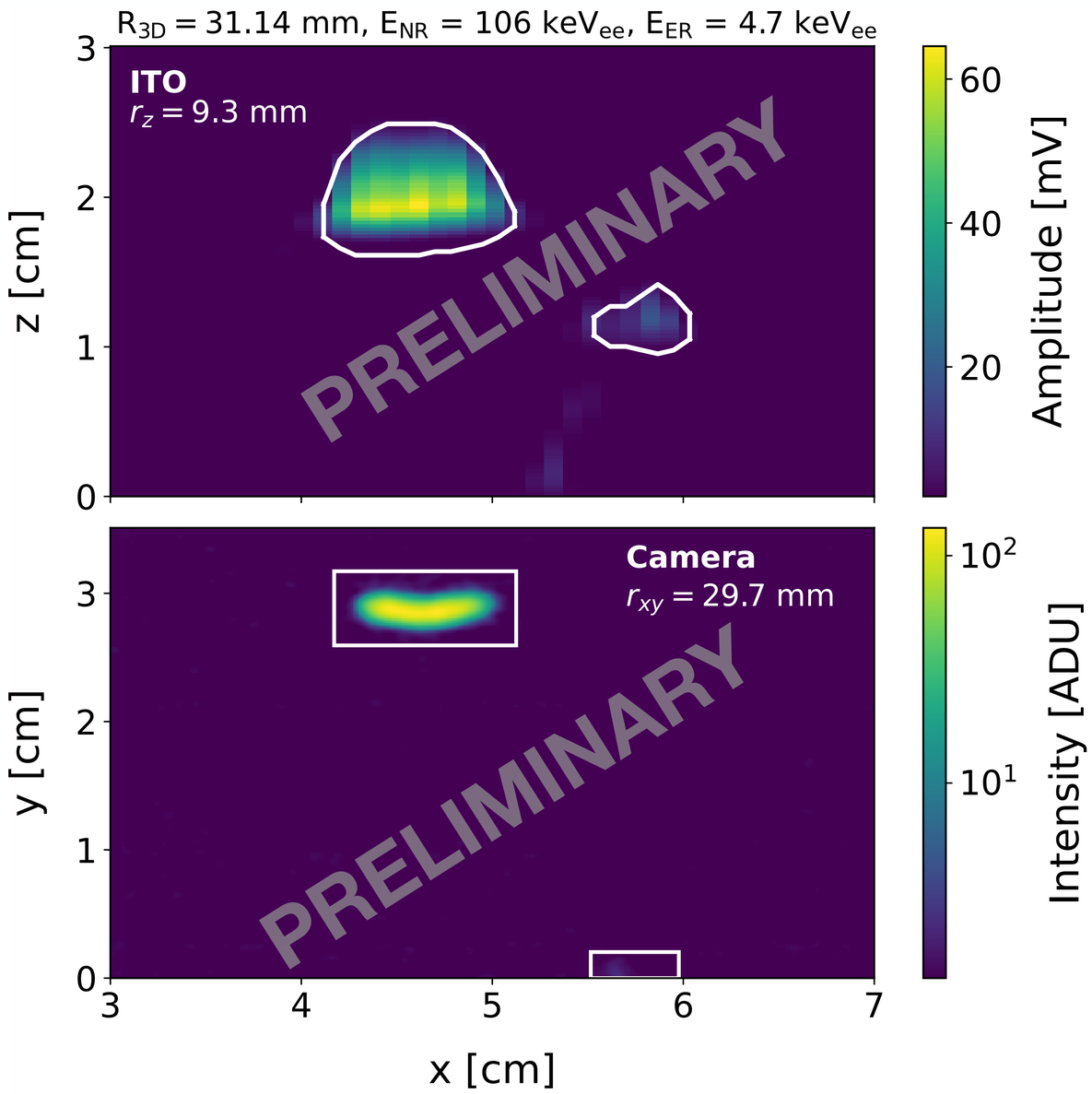

Statistical Analysis

Migdal probability per 10^6 NR wrt theory (theory prediction =1)

Efficiency

Background transfer factor

Expected number of inelastic events in CR

$$L = P(N_{SR}; \mu\epsilon N_{NR} + \tau N_{Bkg})$$

Number of events observed in SR

Number of NRs in millions

Expected number of inelastic events in CR

$$\times P(N_{CR}; N_{Bkg})$$

Number of events observed inCR

Central value

$$\times \prod^{i} G(\theta_i; \theta_{i,0}, \sigma_{\theta_i})$$

Nuisance parameter

Uncertainty

Signal Region

Control Region

Nuisance Parameters

	Relative Systematic Uncertainty	
Source	$+1\sigma$	-1σ
Efficiency	+6%	-6%
(x, y) vertex	+5.5%	-0.6%
z vertex	+2.4%	-1.6%
Theory uncertainty	+20%	-20%